Regulation of drebrin in dendritic spines by Egr-1 transcription factor

Chulmin Cho

Integrated Program in Neuroscience

McGill University

Montreal, Quebec, Canada

December 2015

A thesis submitted to McGill University in partial fulfillment of the requirements for the degree of Doctor of Philosophy

Dedication

This thesis is dedicated to my Father and Mother for their unceasing support and believing in me.

Acknowledgement

My heartfelt gratitude goes to my supervisory committee: Dr. Hemant Paudel, Dr. Lorraine Chalifour, Dr. Keith Murai, Dr. Anne McKinney and Dr. Josephine Nalbantoglu. Dr. Paudel granted me the opportunity to pursue graduate studies in his laboratory. Dr. Chalifour's intellectual and mental support, especially during the latter half of my studies, allowed me to become an independent researcher and confirm my volition to pursue research. Dr. Keith Murai was an essential part of my committee who was always available to answer questions and provide support by generously sharing his reagents, techniques and knowhow. I still cannot forget the anecdote Dr. McKinney shared with me regarding her experience as a graduate student. Her knowledgeable and helpful feedback was always sprinkled with smiles, encouraging me to push on. Dr. Nalbantoglu's unbiased frankness and kindness truly spurred me to always think positively and to face and overcome hardships instead of avoiding them.

I am also grateful for the prompt support, encouragement and confidence given me by Dr. Roderick McInnes. His heartfelt encouragement mixed with occasional jest truly brightened up my graduate life. I won't forget his belief in my "neat" confidence and the encouragement he gave me to stay in research.

I would like to extend my appreciation to my colleagues: Ryen MacDonald, Moonjeong Cho, Kristen Marcellus, Dr. Qin Xike, Dr. Hamid Qureshi and Jijun Shang as well as the rest of fellow scientists on the 6th floor. Ryen has been my colleague who's been through the highs and lows with me from the beginning. Two really is better than

one. Special thanks goes to Jijun, our technician, who was much more that. He decided to help me finish my studies until the very end and his heartfelt support carried me through.

My sincere acknowledgement also goes to the Alzheimer Society of Canada that provided the financial support to allow me to focus on research.

To my sister, Moonjeong, I am grateful to her for believing in me to accomplish whatever I set out to do. It made me stay true to my course in life.

To my soon-to-be bride, Ines, you have been at my side through the thick and thin and I look forward to the life journey we will embark together.

Last but definitely not least, I would like express utmost gratitude to my parents, Jong Suh Cho and Junehee Kim for their unwavering love and trust.

"*I can do all things through Christ which strengtheneth me*."

- Philippians 4:13

Table of Contents

Abbreviations

3xTg-AD	Triple transgenic model of AD
ABP	Actin binding protein
Abp1	Actin-binding protein 1
ABS	Actin binding sequence
AD	Alzheimer's disease
ADF	Actin-depolymerizing factor
ADF-H	ADF homology domain
AMPA	α-amino-3-hydroxy-5-methy-4-isoxazolepropionic acid
AMPAR	AMPA receptor
APP	Amyloid precursor protein
Arp2/3	Actin-related proteins 2 and 3
bHLH-PAS	Basic helix-loop-helix-Per-Arnt-Sim
CamKIIα	Calcium/calmodulin-dependent protein kinase IIα
ChIP	Chromatin immunoprecipitation
Cos-7	CV-1 in origin with SV40 gene
DECODE	Decipherment of DNA elements
DMEM	Dulbecco's modified eagle medium
Dox	Doxycycline
Egr-1	Early growth response-1
Egr-1 -/-	Egr-1 knockout
Egr-1 Tg	Egr-1 transgenic
ERE	Egr-1 response element
FBS	Fetal bovine serum
FL	Full-length
GABA	γ-amino butyric acid
GnRH	Gonadotropin-releasing hormone
HEK-293	Human embryonic kidney 293
IEG	Immediate early gene
KO	Knockout
LH	Luteinizing hormone
LTD	Long-term depression
LTP	Long-term potentiation
MAGUK	Membrane-associated guanylate kinase
MCI	Mild cognitive impairment
NGF	Nerve growth factor
NMDA	N-methyl-D-aspartate
NMDAR	NMDA receptor
PAK/LIM-K	P21-activated kinase (PAK)/LIM-kinase (LIM-K) pathway
PBS	Phosphate buffered saline
PC12	Rat pheochromocytoma
PD	Proline-rich domain

PFA	Paraformaldehyde
PS-1	Presenilin-1
PSD	Post synaptic density
PSD-95	Post synaptic density-95
RA	Retinoic acid
SAHA	Suberoylanilide hydroxamic acid
TSS	Transcriptional start site
tTA	Tetracycline-controlled transactivator
vGluT1	Vesicular glutamate transporter 1
WT-1	Wilm's tumour gene-1

List of Tables

List of Figures

Abstract

Dendritic spines are the actin-enriched protrusions on dendritic shafts that encase the postsynaptic machinery. The basis for morphological plasticity of dendritic spines is formed by changes in the actin cytoskeleton, which in turn, is orchestrated by actin binding proteins. A dynamic actin cytoskeleton allows the dendritic spines to rapidly and accordingly respond to various stimuli by changing their morphology, and this morphological plasticity ultimately leads to synaptic plasticity. In neurodegenerative diseases such as Alzheimer's disease (AD), this dynamicity inside dendritic spines is disrupted. Consequently, the dendritic spines are lost, which causes the loss of synapses. These findings highlight the importance of understanding the regulators of actin dynamics and the mechanisms leading to loss of dendritic spines. Drebrin is a F-actin binding protein that localizes to dendritic spines in the brain. Drebrin is required for synapse formation and structural plasticity during development as well as the process of learning and memory formation. Precipitous loss of drebrin has been observed in AD and other neurodegenerative diseases with synaptic pathology. However, the regulatory factor causing loss of drebrin in AD-related synaptic pathology remains elusive. Early growth response-1 (Egr-1) is an inducible zinc-finger transcription factor expressed in the brain that binds to the GC-rich consensus sequences on target promoters to regulate expression. Upregulation of Egr-1 has been found in AD brain. Herein, we hypothesized that Egr-1 downregulates drebrin expression and leads to synaptic dysfunction. We demonstrate that Egr-1 transcription factor binds to drebrin promoter. *In silico* analysis was performed to identify putative Egr-1 response elements (EREs) on drebrin promoter. To substantiate this, luciferase promoter assay and chromatin immunoprecipitation assay was used and

confirmed Egr-1 binding to drebrin promoter both *in vitro* and *in vivo*. Further, we demonstrate that Egr-1 negatively regulates drebrin mRNA and protein level. In primary hippocampal neurons and an inducible mouse model of Egr-1 overexpression, drebrin was downregulated upon Egr-1 upregulation. Conversely, an increase in drebrin mRNA and protein level was observed in Egr-1 -/- mouse. Furthermore, it was shown that Egr-1-mediated loss of drebrin parallels decrease in dendritic spine density. Immunocytochemical analysis revealed reduction in the density of dendritic protrusions upon Egr-1 upregulation. Reduction in spine density was observed in the CA1 region of the hippocampus in Egr-1 Tg mouse while an increase was observed in samples from Egr-1 -/- mouse. Immunocytochemical colocalization study also showed concurrent loss of vGLUT1 and PSD-95, suggesting a loss of putative functional synapses. We also demonstrate that Egr-1 upregulation mediates changes in other synaptic proteins in primary hippocampal neurons. In summary our data show that 1) Egr-1 downregulates drebrin by binding to drebrin promoter, 2) Egr-1 is inversely correlated with dendritic spine density and 3) Egr-1 mediates decrease in postsynaptic proteins and putative synaptic contacts. Therefore, we conclude that Egr-1 is a key regulator of drebrin and consequently, chronic upregulation of Egr-1 may exacerbate synaptic pathology in AD and AD-related disorders.

A. Abrégé

Les épines dendritiques protubérantes sont enrichies d'actines sur les arbres dendritiques qui encadrent la machinerie post-synaptique. La base de la plasticité morphologique est formée par la dynamique des épines dendritiques qui à leur tour sont dirigé par les protéines qui s'attachent aux actines. La dynamité de l'actine permet aux épines dendritiques de répondre rapidement et adéquatement à différent stimuli en changeant leur morphologies. De plus, cette plasticité morphologique guide la plasticité synaptique. Dans le cas de la maladie neurodégénératif telle que la maladie d'Alzheimer (MA), la dynamité des actines dans les épines dendritiques ont été perturbés. Conséquemment, les épines dendritiques perdues causent les pertes des synapses. Ces observations surlignent l'importance de comprendre les régulateurs de la dynamité de l'actine et les mécanismes guidant la perte des épines dendritiques. Drebrin est une protéine qui s'attache à l'actine F qui est localisée dans les épines dendritiques, dans le cerveau. Drebrin est nécessaire pour la formation de la synapse et pour la plasticité structurale durant le développement et aussi durant l'apprentissage ou la formation de la mémoire. La perte brutale du drebrin était observée chez MA et dans divers maladies neurodégénératives qui montrent une pathologie synaptique. Cependant, le facteur régulateur causant la perte du drebrin chez la pathologie synaptique liée à MA reste obscur. Le gène de réponse de croissance précoce (Egr-1) est un facteur de transcription exprimé dans le cerveau qui s'attache aux séquences consensus riche de GC sur le promoteur de la cible pour réguler son expression. Une surexpression de Egr-1 a été trouvé dans le cerveau de MA. Ci-inclus, nous émettons l'hypothèse que Egr-1 sous-régule l'expression du drebrin et induit la dysfonction de la synapse. Nous démontrons que la transcription du facteur Egr-1 attache au promoteur du

drebrin. L'analyse *in silico* est effectuée là où les éléments répondant à l'Egr-1 (EREs) sont trouvés sur le promoteur du drebrin. Pour soutenir cette découverte, l'évaluation du promoteur luciférase et l'immunoprécipitation de la chromatine sont utilisées pour confirmer l'attachement d'Egr-1 au promoteur drebrin à la fois *in vitro* et *in vivo*. Nous démontrons aussi que l'Egr-1 régule négativement le niveau de drebrin au niveau de l'ARNm et de la protéine. Dans les neurones primaires d'hippocampe et le model de souris inductible d'Egr-1, le souris Egr-1 Tg, le drebrin est sous-exprimé tandis que l'Egr-1 est surexprimé. Par ailleurs, l'augmentation du niveau de drebrin est observée dans le souris Egr-1 -/-. De plus, il est montré que la perte de drebrin médié par Egr-1 est en corrélation avec la diminution de la densité des épines dendritiques. L'analyse d'immunocytochimie montre une réduction de la densité de la protubérance dendritique quand l'Egr-1 est sur-régulée. Une réduction similaire dans la densité des épines est observée dans la région CA1 de l'hippocampe chez la souris Egr-1 Tg tandis qu'une augmentation est observée dans le cas de la souris Egr-1 -/-. Une étude d'immunocytochimie de la co-localisation montre des pertes simultanées de vGLUT1 et PSD-95, suggérant une potentielle perte fonctionnelle des synapses. Nous démontrons aussi que la surexpression d'Egr-1 a un rôle médiateur des changements des autres protéines synaptiques des neurones primaires d'hippocampique. En conclusion nos données montrent que 1) Egr-1 sous-exprime le drebrin en s'attachant au promoteur du drebrin, 2) Egr-1 est inversement en corrélation avec la densité de l'épine dendritique et 3) Egr-1 a un rôle médiateur de la diminution des protéines post-synaptique et des contacts synaptique putative. Donc nous concluons que l'Egr-1 est la clé régulatrice de drebrin et

conséquemment, la surexpression chronique d'Egr-1 peut exacerber la pathologie synaptique dans la MA et les maladies liées à la MA.

Preface & Author Contributions

The present thesis is organized in the traditional monograph format in compliance with the guidelines of McGill University for thesis preparation. This thesis presents original findings by Chulmin Cho in Chapter IV that are distinct contributions to knowledge.

Chapter 1 comprises the introduction, which presents the rationale and objectives of the research organized and written by C. Cho. Chapter 2 presents literature reviews that are relevant to the presented research and C. Cho organized and wrote the chapter. Current knowledge regarding dendritic spines, synaptic pathology, drebrin and Egr-1 are described in this chapter. Chapter 3 describes the materials and methods used in this research and was organized and written by C. Cho. Jijun Shang (Lady Davis Institute) is credited with generation of Egr-1 lentivirus and Egr-1 Tg mice.

Chapter 4 presents the original findings from this research. This chapter is divided into three sections. For all three sections, C. Cho designed and executed the experiments in their entirety, analyzed and interpreted the data, generated the figures and wrote the section. The first section is entitled "Egr-1 binds to Egr-1 response elements on drebrin promoter" where for the first time, Egr-1 is demonstrated to interact with drebrin promoter both *in vitro* and *in vivo*. This section was supervised by Dr. H. Paudel. The second section is entitled "Egr-1 negatively regulates drebrin *in vitro* and *in vivo*" where for the first time, Egr-1 is demonstrated to be negatively regulate drebrin mRNA and protein level *in vitro* and *in vivo*. This section was also supervised by Dr. H. Paudel. The third section is entitled "Loss of drebrin in response to Egr-1 upregulation results in loss of dendritic spines" where for the first time, Egr-1-mediated loss of dendritic spines as

well as putative synaptic contacts are demonstrated *in vitro* and *in vivo*. This section was supervised by Dr. H. Paudel, Dr. L. Chalifour, Dr. K. Murai, Dr. A. McKinney and Dr. J. Nalbantoglu.

Chapter 5 comprises the discussion section where the results are interpreted and explained by C. Cho. Lastly, Chapter 6 presents the final conclusion and summary organized and written by C. Cho.

Chapter 1. Introduction

1.1 Research rationale and hypothesis

The brain is at the heart of the nervous system. It receives and processes information from within and outside the body. The brain is a complex biological structure. It embodies all aspects of cognition ranging from the ones that occurs unconsciously to the decisions we make consciously. Despite the vastness in cognitive processes, each and every aspect of cognition is carried out by communication between 100 billion neurons in the brain. The communication between neurons occurs at specialized junctions known as synapses between the presynaptic axon and the postsynaptic dendrites that are formed and arranged in a precise manner for accurate neuronal activity and brain function. Furthermore, information is stored and changed by altering postsynaptic structure in addition to synapse formation and elimination [1].

Dendritic spines are protrusive boutons on dendrites that encase the postsynaptic elements of the mammalian forebrain. These spines form synapses by individually pairing up with a corresponding axon. In response to synaptic activity, dendritic spines change their structure due to the dynamics of actin cytoskeleton. The dynamics of actin cytoskeleton, in turn, are regulated by actin binding proteins (ABPs), which orchestrate the polymerization and depolymerization of actin filaments. This phenomenon gives rise to the structural plasticity [2,3] that is closely correlated with synaptic function. The structural plasticity of dendritic spines forms the basis of learning and memory.

Neurological and psychiatric diseases including AD [4], Schizophrenia [5] and mental retardation [6] display structural alterations of dendritic spines that leads to loss of the spines. As current treatment options for AD and AD-related disorders are limited and

often ineffective, preventing loss of synaptic homeostasis or its re-establishment offers a potential therapeutic target. In order to develop effective treatment, it is important to understand the underlying regulator and mechanisms of dendritic spine loss, which remains largely elusive. More fundamentally, identification of ABPs and their regulators that underlies dendritic spine loss is imperative.

Drebrin, an ABP expressed highly in neurons, specifically localizes to dendritic spines. Drebrin binds to actin, provides stability, and also regulates the interaction between F-actin and other ABPs in response to synaptic activity [7]. Drebrin is necessary for spine morphogenesis and maturation as it is required for recruitment of Post Synaptic Density-95 (PSD-95) and N-methyl-D-aspartate (NMDA) receptors (NMDARs) that are crucial components of a functional dendritic spine [8,9]. The interaction between F-actin and ABPs in conjunction with signaling receptors is important for maintenance of long-term potentiation (LTP) and morphological plasticity [10]. Furthermore, downregulation of drebrin expression suppresses F-actin accumulation within dendritic spines and prevents formation of the spines [11], highlighting the structural importance of drebrin in dendritic spines.

In AD and related disorders where dendritic spine loss occurs, drebrin is precipitously and greatly lost when compared with the loss of other ABPs [10,12-14]. Drebrin is also lost in animal models of AD [15-18]. Therefore, loss of drebrin may disrupt the actin dynamics and structural balance leading to loss of synaptic plasticity and cognitive function. However, the regulatory factor causing the loss of drebrin remains elusive.

Early Growth Response-1 (Egr-1), is a zinc finger transcription factor, is rapidly induced by a broad spectrum of stimuli such as shear stress [19], oxygen deprivation [20,21] and (brain) injury [22-25]. Egr-1 activates the expression of genes including those involved in cell death and injury [26]. In AD, Egr-1 mRNA was found to be upregulated approximately 4-fold in degenerating hippocampal pyramidal neurons [27]. Also, a microarray analysis of hippocampal gene expression from AD patients revealed significant upregulation of Egr-1 correlating with progression of AD [28]. Additionally, high density microarrays using Egr-1 transfected rat pheochromocytoma neuronal cell line (PC12) showed altered expression of many genes, including 23% reduction in drebrin [29]. These data suggests that Egr-1 may regulate drebrin loss observed in AD.

Herein, we sought to investigate the relationship between Egr-1 and drebrin. Based on the described data, we hypothesized that Egr-1 binds to drebrin promoter to negatively regulate drebrin expression and that Egr-1 upregulation results in loss of drebrin level. We further conjectured that Egr-1-mediated loss in drebrin would correlate with loss of dendritic spine density such as was observed during synaptic pathology.

Chapter 2. Literature Review

2.1 Dendritic spine: the thorns covering dendrites

Dendritic spines are micro-protuberances (0.5 to 2μm in length) emerging from dendrites [30] (Figure 1). They are the postsynaptic structure that receives the majority of excitatory glutamatergic axonal input in the mature mammalian brain to form the synapses [31]. Dendritic spines were first discovered in the vertebrate nervous system by Ramón y Cajal [32,33]. At the time of his discovery, dendritic spines were described as "thorns" or "short spines", but soon Cajal recognized them as possible axon targets [34] and used the term "synapse" to describe this connection [35]. However, it would not be until the advent of electron microscopy that dendritic spines were confirmed to be postsynaptic structure [36,37].

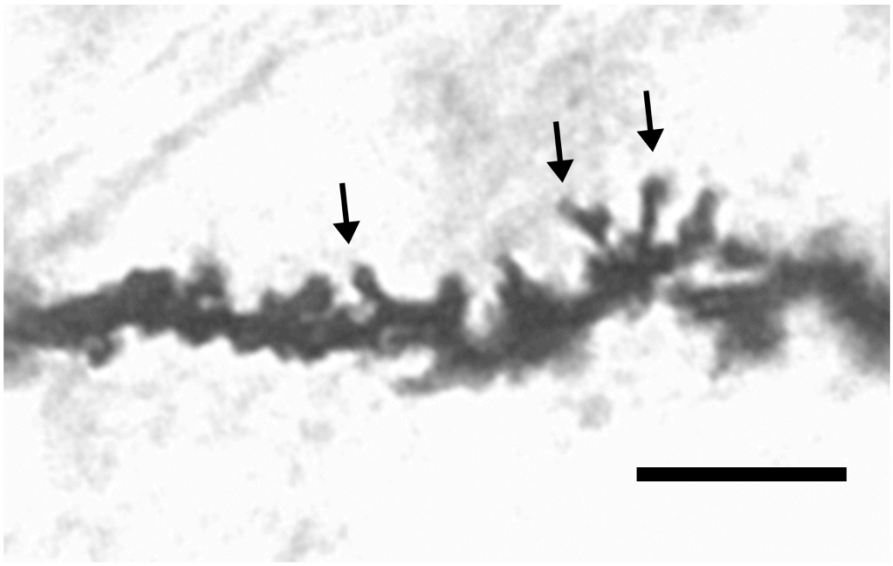

Figure 1. A micrograph showing dendritic spines on a segment of dendrite. Golgi staining was performed to visualize dendritic spines (examples indicated by arrows) present on hippocampal neurons. Scale bar, 5μm.

2.1.1 Microanatomy of dendritic spine

Glutamatergic synapses are defined by the presence of a presynaptic terminal and postsynaptic density (PSD) located on the head of a dendritic spine [36,38] (Figure 2A). PSD is a scaffold for glutamate receptors and associated signaling molecules. PSD is present as an electron-dense thickened postsynaptic membrane. Another essential component of dendritic spine is the actin cytoskeleton [11].

Actin, as the major cytoskeletal component, provides structural support to dendritic spines. A typical dendritic spine has a bulbous head connected to the parent dendrite by a thin neck (Figure 2A). The actin cytoskeleton is organized in network of branches while the neck is composed of short branched and longitudinal actin filaments [39]. Within a spine head, actin is organized into stable and dynamic pool [40,41]. The stable pool is located throughout the head and provides structural support. The dynamic pool is located below the surface and allows rapid morphological changes in response to synaptic stimulus.

These spines undergo dynamic morphological changes and are classified into: 1) thin spine with a small bulbous head and slender neck (<0.6μm in diameter); 2) stubby spine with no neck (head and neck widths are similar); and 3) mushroom spine with a short neck and a larger bulbous head (>0.6μm in diameter) [42] (Figure 2B). Despite the classification, these spine shapes reflect a continuum rather than separate classes as the shapes are interchangeable [43]. Many studies suggest the morphology of spines correlates with developmental stages and strength of synapses [1,44,45]. Specifically, imaging experiments indicated that spine head size correlates with synaptic strength as large heads are more stable and strengthens synaptic activity by expressing larger numbers of AMPA

(α-amino-3-hydroxy-5-methy-4-isoxazolepropionic acid) receptor (AMPARs) [44,46]. Based on these data, the mushroom spine is functionally classified as a mature spine while thin and stubby spines are classified as an immature spine [47].

Overall, dendritic spines possess the ability to change their shape and number accordingly and rapidly to stimulus, which makes them morphologically plastic. The morphological plasticity of dendritic spines is functionally important as it strongly correlates with learning and memory [48].

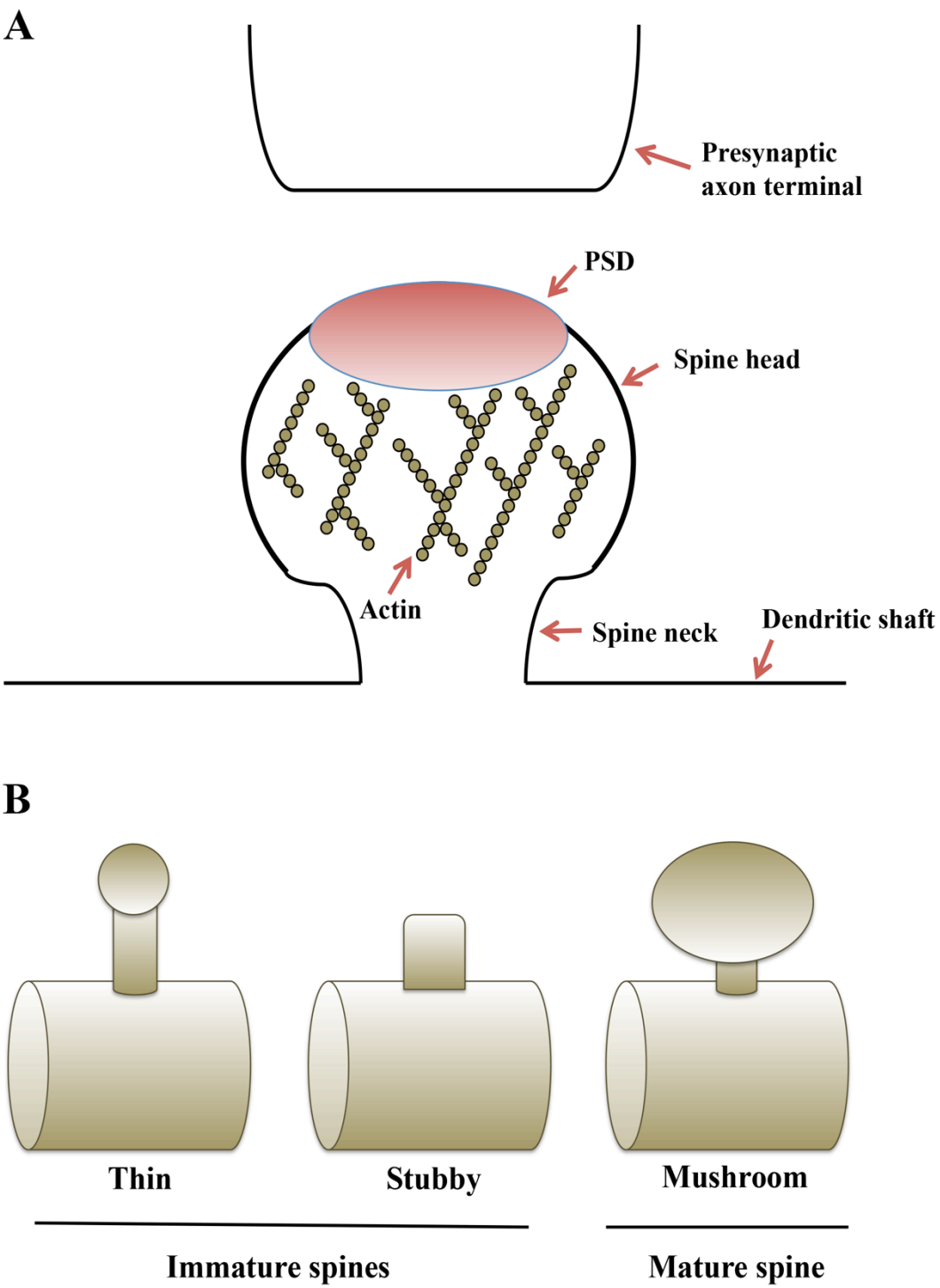

Figure 2. Schematic of a dendritic spine and its various morphologies. **A**, PSD and actin cytoskeleton constitutes major components of a dendritic spine. **B**, Dendritic spines are broadly categorized into thin, stubby or mushroom spines based on their morphology.

2.1.2 Morphogenesis of dendritic spine

So how does a dendritic spine emerge from the parent dendrite? The rules governing the development of dendritic spines remain unresolved and there are two main hypotheses (Figure 3). The first hypothesis posits that many headless thin projections called filopodia on dendrites are the precursors to dendritic spines (Figure 3A). These filopodia actively search for presynaptic terminals. Once synaptic contacts are made, the actin clusters within filopodia undergo structural changes to convert thin filopodia into mature dendritic spines [11]. In support of this, young brains display few spines and numerous filopodia that disappear once maturity is reached [49,50]. Furthermore, filopodia increase in number when synaptic activity or action potentials are blocked using tetradotoxin (TTX), suggesting a role in the formation of synaptic contacts [51]. Evidences against the filopodia being the precursor also exist. For example, most synapses in the young brain are formed on dendritic shaft [52]. Also, filopodia is rare in mature neurons and cannot explain the continuous emergence and disappearance of spines in adult brains [53-55]. Therefore, the second hypothesis postulates that filopodia are not precursors, but sensors to detect glutamate release from an axon [56] (Figure 3B). Once detected, shaft synapse forms and the dendritic spine emerges from it. Despite the controversy, both hypotheses converge on acknowledging the importance of filopodia in the formation of dendritic spines.

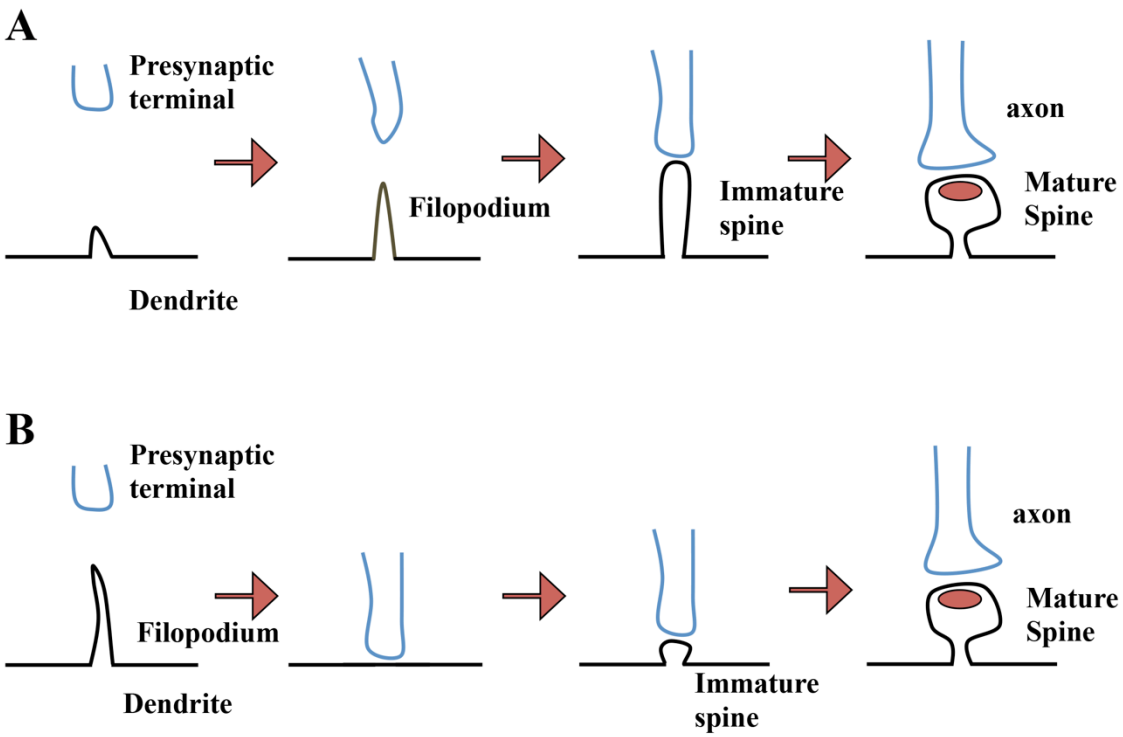

Figure 3. Two models of spine formation. **A**, Filopodia is thought to precede spine formation or **B**, act as a sensor for finding presynaptic terminals.

2.1.3 Maturation of dendritic spine

Maturation of a dendritic spine is marked by increases in head size and the number of AMPARs in conjunction with the formation of PSD at the distal tip of the spine head [57]. Dynamic reorganization of actin cytoskeleton increases the head size. Head size is proportional to the number of AMPARs recruited to the postsynaptic membrane [58,59]. AMPARs allow influx of Na^+ ions and propagate depolarizations of the postsynaptic neuron. Therefore, the number of AMPARs contributes directly to synaptic strength [60,61].

The AMPARs are a component of the PSD, which is a disk-shaped protein complex comprised of membrane-associated proteins involved in synaptic signaling and plasticity [44,62-64]. Other constituents of the PSD include receptor tyrosine kinases, ion channels, G-protein-coupled receptors, cell adhesion molecules, scaffold proteins, such as PSD-95 (please refer to Figure 5), signaling enzymes and cytoskeletal elements [65,66]. Therefore a mature dendritic spine contains the PSD that allows the postsynaptic neuron to receive, process and transmit the information received from the presynaptic neuron.

2.1.4 Plasticity of dendritic spine

Dendritic spines undergo structural remodeling throughout life [67] due to the underlying actin dynamics. The ability to change their size, number and shape in response to developmental [68-70], environmental [71-74] and behavioural cues makes the spines highly plastic [1,45,61,75,76]. The plasticity of dendritic spines, consequently, allows synapses to be formed and eliminated within minutes to hours thereby facilitating various cognitive processes including memory and learning [66,77,78]. This responsiveness of synapses to input is called synaptic plasticity.

Two well-characterized forms of synaptic plasticity that bring about enduring changes in synaptic strength are long-term potentiation (LTP) and long-term depression (LTD). LTP and LTD are complementary processes that are thought to be basis of encoding information for memory [79]. LTP represents a long term strengthening in synaptic transmission between two neurons resulting from strong and/or synchronous stimulation. Experimentally, LTP can be induced by brief (≤2s) and high frequency stimulus (50 to 200Hz and 100Hz for tetanic stimulation) [80,81]. LTD, on the other hand, represents a long term reduction in synaptic transmission that can be induced experimentally by lasting (≥30s) low-frequency stimulation (<10Hz) [82,83]. Synaptic strengthening by LTP is linked with spine enlargement and increase in spine density [42,84,85-88]. In contrast, synaptic weakening by LTD is linked with spine shrinkage and decrease in spine density. As LTP and LTD both derive from morphological changes of dendritic spines, it is important to understand the actin dynamics that enables these processes.

2.1.5 Actin cytoskeleton in dendritic spine

Dendritic spines are enriched with actin cytoskeleton proteins [89,90]. Inside a dendritic spine, actin can quickly polymerize from monomeric G-actin to filamentous F-actin and vice versa. The non-covalent interactions of G-actin monomers allow rapid assembly and disassembly of F-actin. Thus, the degree of actin polymerization, G-actin/F-actin ratio, determines the dendritic spine morphology [91].

Actin cytoskeleton proteins control the formation and dissociation of dendritic spines, and thus, the postsynaptic machinery [92]. In a mature spine, actin assembles and

positions the PSD; anchors and stabilizes postsynaptic receptors; and positions the translational machinery [93]. Also, synaptic plasticity is coupled with actin dynamics inside dendritic spines that respond to presynaptic input by modulating head morphology [94,95]. In relation, LTP induces spine enlargement accompanied by an increase in F-actin level while LTD is accompanied by depolymerization of F-actin [40] (Figure 4).

The importance of actin cytoskeleton proteins in spine formation, morphology and synaptic function raises the question about the regulatory factors responsible for the reorganization of actin. The actin dynamics, in turn, are regulated by actin binding proteins (ABPs). It is believed that disruption of actin dynamics lead to alterations in spine morphology, maturation and density which correlate with neurological disorders [96]. This points to the central role ABPs play in synaptic function, and the importance of understanding their function inside the spines.

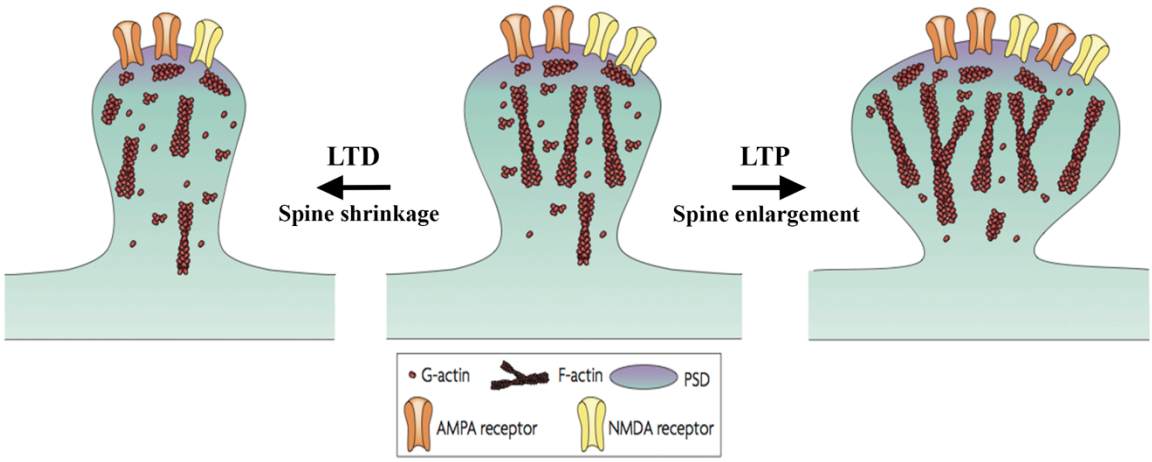

Figure 4. Schematic model of dendritic spine plasticity (Illustrations adapted from Cingolani and Goda. 2008 [97]). Synaptic activity-dependent change in spine morphology depends on actin dynamics.

2.1.6 Dendritic spine loss in synaptic pathology

As spine morphology and density are closely linked with synaptic function, even subtle changes in dendritic spines have the potential to significantly affect synaptic function and connectivity in the brain. In healthy individuals, dendritic spine density is decreased during normal aging in correlation with cognitive decline [98]. As disruption in spine morphology and density leads to aberrant changes in synapse function, dendritic spine loss is common in many neurological disorders. Neurological disorders such as mental retardation [10,99], schizophrenia [100-102] and AD are characterized by loss of dendritic spines and synaptic plasticity, which are reflected in corresponding deterioration of cognition and information processing [100,101,103,104].

AD is the most prevalent neurodegenerative disease, which in majority of cases, affect elderly individuals over 65 years of age [41]. AD is pathologically characterized by the presence of senile plaques, neurofibrillary tangles and neuronal loss [105]. In AD, synaptic dysfunction caused by dendritic spine loss precedes neuronal death [4]. Indeed, human studies have shown that the loss of dendritic spine and synapse occurs early and correlate robustly with cognitive decline whereas other pathological hallmarks including senile plaques and neurofibrillary tangles do not [106,107]. Supporting the idea that loss of dendritic spine is an early event, loss of dendritic spines was also evident early in animal models of AD before the onset of Aβ plaque formation [108,109]. Therefore, it would be of benefit to understand the underlying mechanism that mediates the spine loss in order to develop both the diagnostic markers of synapse loss and therapeutics against cognitive decline.

2.1.7 Actin binding proteins in dendritic spine

Actin is highly enriched in a dendritic spine compared with the parent dendrite. Although the role of actin cytoskeleton with regards to dendritic spine structure and function is well recognized, our understanding of the ABPs that regulate actin reorganization is limited. ABPs cooperatively orchestrate the actin dynamics as each ABP serves a specific role in polymerizing/depolymerizing, cross-linking, or side-binding F-actin. Each ABP serves its role via inducing changes in helical structure of actin filaments and affect binding of other ABPs to the actin [110].

The function of ABP is closely related to activities of small Rho GTPases such as Rac1, RhoA and Cdc42. Rho GTPases were found to participate in formation, branching and elimination of dendritic spines [111-113]. Furthermore, RhoA was found to be required for LTP-mediated changes in spine morphology whose downstream effector proteins include LIM-kinase (LIM-K) that directly regulates cofilin ABP by phosphorylation [114,115].

ABPs such as profilin and gelsolin polymerize and depolymerize actin respectively. Profilin binds to G-actin and accelerates the exchange of ADP to ATP on actin, which leads to F-actin polymerization [116,117]. Gelsolin, on the other hand, is the most potent actin severing ABP whose role in dendritic spines remains yet to be clarified [96]. It is thought that gelsolin increases the amount of G-actin that becomes available for additional actin polymerization during LTD [94]. Cofilin, similar to gelsolin, enhances actin depolymerization and is regulated during synaptic plasticity to modulate spine enlargement and shrinkage during LTP and LTD respectively [86,88,118].

Actin-related proteins 2 and 3 (Arp2/3) is an ABP that leads to actin cross-linking. Arp2/3 nucleates actin to form actin filaments at fixed angles allowing branched actin networks to form within dendritic spine [119,120]. Knockdown of Arp2/3 results in loss of dendritic spines without affecting the density of dendritic filopodia, suggesting the importance of Arp2/3 for enlargement and maturation of the spines [93,121].

Drebrin is an actin side-binding protein that stabilizes actin filaments and promotes actin polymerization [92,122]. Unlike other ABPs, drebrin is markedly reduced in the brains of patients with AD and animal models of AD [12,15] as well as people with Down's syndrome [10]. Therefore drebrin may be the target in AD and AD-related disorders whose disruption causes disorganization of actin filaments and leads to loss of dendritic spines.

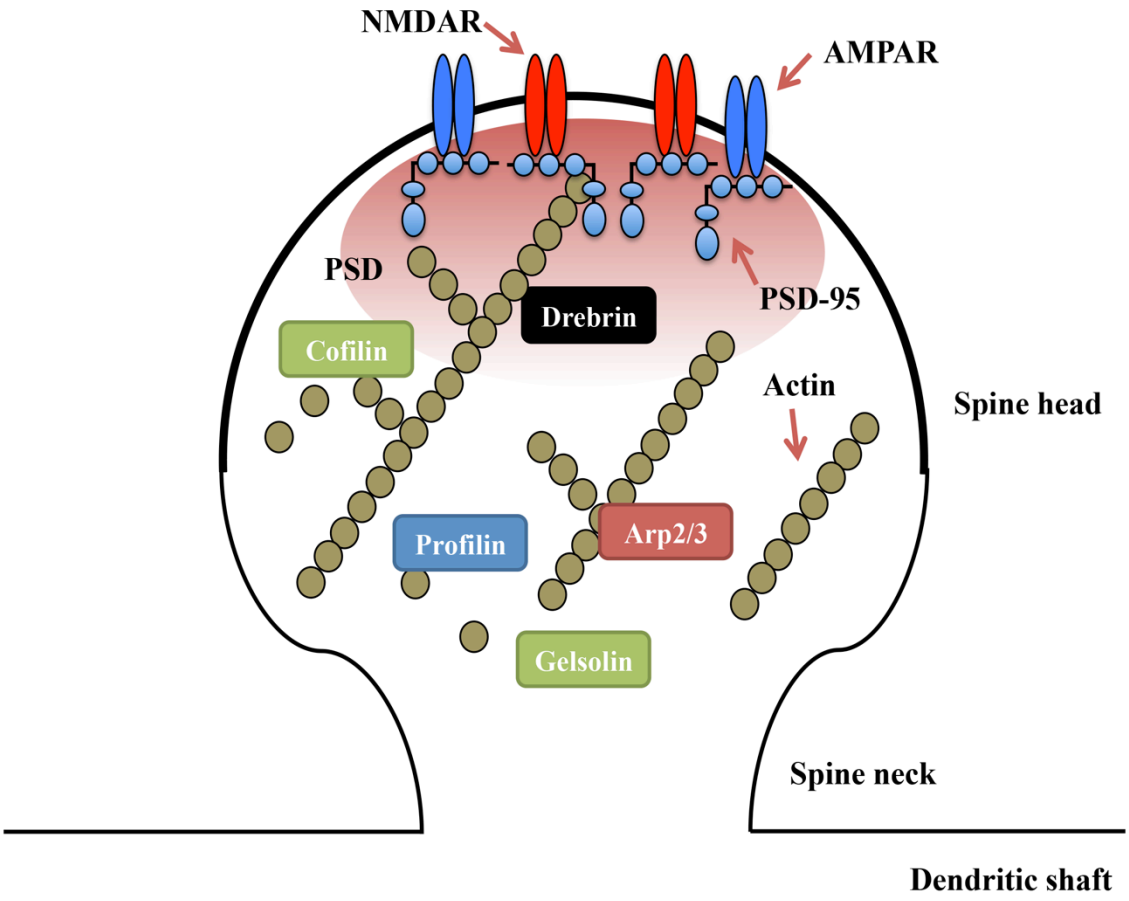

Figure 5. Schematic illustration of ABPs and other components of the PSD (not drawn to scale). Some examples of ABPs that regulate actin dynamics by promoting polymerization (blue box), depolymerization (green box), cross-linking (Arp2/3) or side-binding (black box). Other component of the PSD that is noteworthy for the purposes of this study is PSD-95, a scaffolding protein on which AMPARs and NMDARs dock.

2.2 Drebrin: More than just a developmentally regulated brain protein

Drebrin, **d**evelopmentally **re**gulated **br**ain prote**in**, was first discovered in the optic tectum of chick embryos while studying changes in composition of 54 proteins using two-dimensional electrophoresis [123]. Initially marked as spots 5 (S5), 6 (S6) and 54 (S54), the name drebrin was given due to the changes in the expression pattern during the course of development from the fourth day of incubation to hatching. Later studies would identify S5, S6 and S54 as corresponding to different isoforms of drebrin; E1, E2 and A isoform respectively [124]. It would soon be revealed that drebrin is a major ABP involved in regulating dendritic spine morphology and synaptic pathology.

2.2.1 Isoforms of drebrin and its phylogenetic conservation

Drebrin consists of two major isoforms: embryonic (E) and adult (A) forms (Figure 6). Each isoform is a product of alternative mRNA splicing from a single gene [125]. In the chicken, Drebrin E isoform is further classified into E1 and E2 forms. In other species including human, rat and cat [126,127], a single isoform of E that lacks Ins2, and an A isoform exist. In chicken, cloning of drebrin cDNA showed amino acid sequence for E1 and E2 were identical except for that the E1 isoform has a 43 amino acid (129-bp) insertion (Ins 1) in the middle [128]. Drebrin A contains an additional 46 amino acid (138-bp) insertion (Ins 2) upstream of the Ins 1 [129]. The Ins1 and In2 are found on separate exons [129]. Although Ins 1 and Ins 2 define drebrin E and A isoforms, their function remains elusive. Both drebrin E and A isoforms do not have membrane spanning domains, according to hydrophobicity analysis [130].

Immunohistochemistry and immunoblotting studies found variability in the molecular weights of drebrin between different isoforms and species while their

isoelectric points were comparable at 4.5. The apparent molecular weight of drebrin E and A are considerably greater than the deduced molecular weight due to the acidic nature of drebrin. For example, the deduced molecular weights of chick drebrin E1, E2 and A are 62.2kDa, 66.6kDa and 71.5kDa respectively. However, the apparent molecular weight of chicken drebrin E1, E2 and A are 95kDa, 100kDa and 110kDa respectively [129]. For rat drebrin A, the deduced molecular weight is 77.5kDa while the apparent molecular weight is 140kDa [130].

Drebrin E and A isoforms share high homology and are conserved across species [128,129,131-133,126]. Mouse *dbn*1 is located in chromosome 13 [134] and rat *dbn1* is on chromosome 17. In human, *DBN1* has been mapped to chromosome 5 [132]. The deduced amino acid sequence of the human drebrin cDNA is 92% identical to the rat and mouse [133]. A conservation of 80% was observed for the rat and chicken as well as human in the amino-terminal half (domain C1, residues 1-361 in rat) that includes the actin binding domain and two short regions in the carboxyl-terminal region (domain C2, residues 521-539, and C3, residues 596-653). The phylogenetic conservation for Ins2 is especially high with 100% among mammals [129]. While mouse and rat contains a single transcriptional start site (TSS), human drebrin gene contains two TSSs separated by approximately 1 kbs (Figure 12A). The upstream TSS is the predominant TSS that expresses the E and A isoforms via alternative splicing [132]. The downstream TSS transcribes the minor transcript variant with a different 5' untranslated region (UTR) and 5' coding sequence when compared with the predominant transcript variant. Specifically, the first 31 amino acids of the minor transcript variant differ from the first 29 amino acids of the predominant

transcript variant. However, the functional difference between the two TSSs as well as the determining factor leading to transcription from either TSSs remains elusive.

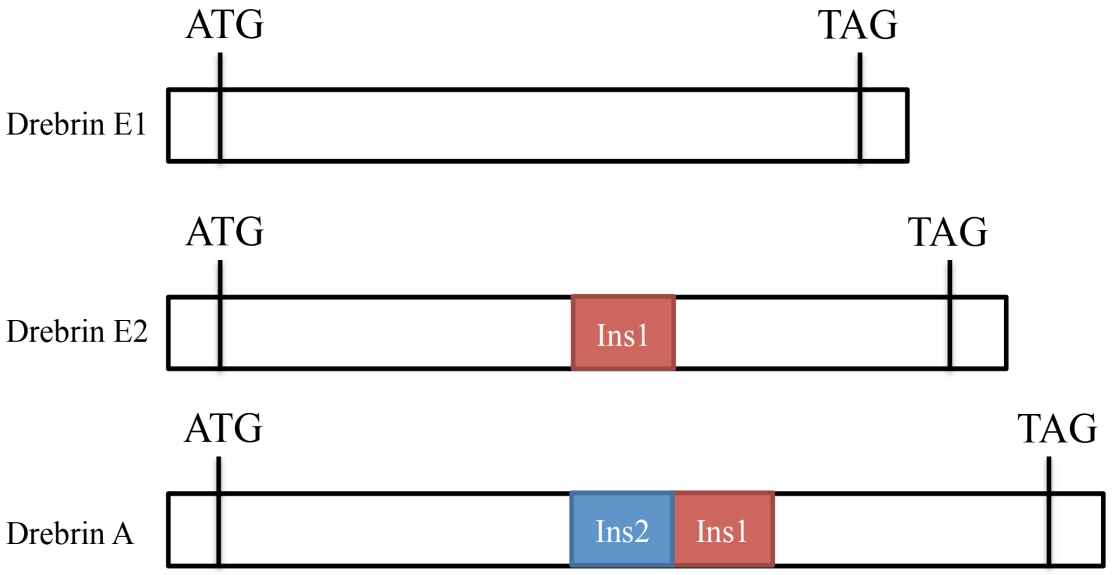

Figure 6. Schematic representation of drebrin isoforms in chicken. Unlike other mammals, chicken expresses an additional drebrin E isoform, E1, without Ins1. The physiological role of Ins1 and Ins2 remains to be elucidated.

2.2.2 Domain structure of drebrin

Four binding domains exist on drebrin (Figure 7): an N-terminal actin-depolymerizing factor (ADF) homology domain (amino acid residue 8-134 of rat drebrin E)[135], an actin binding domain (amino acid residue 135-355), a proline-rich domain (amino acid residue 410-419) and C-terminal Homer binding domain [136]. The ADF homology domain is able to interact with actin, but is not required for the F-actin binding activity as the N-terminal high-affinity actin binding domains (amino acid residue 233-355) alone is sufficient to bind and remodel F-actin [122,137]. Most likely, ADF homology domain acts as a functional building block, which is found in other ABPs including cofilin [135]. A 43 amino acid sequence (residue 173-227) is responsible for the submembranous localization of drebrin [138]. The proline-rich domain on drebrin is used to bind profilin, which leads to actin polymerization [139]. Drebrin is also able to interact with Homer, a postsynaptic scaffold protein that anchors signaling proteins including glutamate receptor subunits, via its homer binding domain [140].

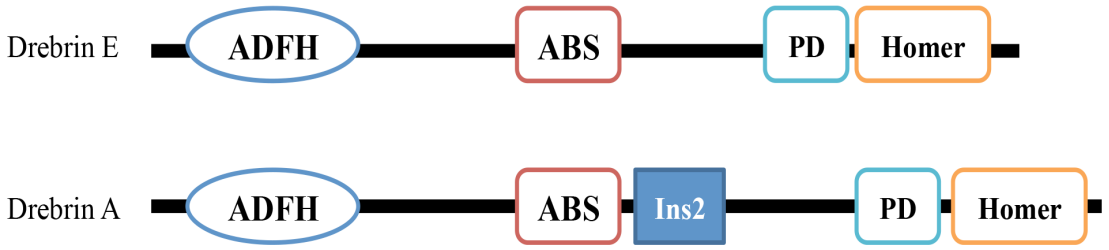

Figure 7. Schematic illustration of drebrin domain structure. ADFH: ADF homology domain; ABS: Actin binding sequence; PD: Proline-rich domain; Homer: Homer binding domain

2.2.3 Temporal regulation of drebrin expression

Expression of drebrin E and A isoforms are spatiotemporally regulated in the brain which includes the optic tectum of chicken and the occipital cortex of rat [124,125]. Temporally, drebrin E expression predominates during embryonic stages while drebrin A expression is dominant in the adulthood [123]. Immunoblotting and Northern blot analysis of chick optic tectum revealed that drebrin E expression is increased beginning from neuroblast migration and final mitosis of neuronal cells. Elevated expression of drebrin E persists until neurite formation and synaptogenesis. As neurons mature, drebrin A expression begins to increase while drebrin E expression declines by 80% and remains low into the adulthood [131]. Drebrin A isoform is predominant expressed in mature neurons for the remainder of life [122]. Similar temporal expression of drebrin E and A isoforms was observed in rats [126]. Based on these observations, similar temporal expression pattern is expected in mouse and human where in adults, drebrin A expression is high while drebrin E expression remains low [141].

2.2.4 Spatial regulation of drebrin

Drebrin expression is regulated spatially at cellular and subcellular level. Immunohistochemical analysis of rat brains showed drebrin immunoreactivity in the gray matter [92]. Approximately 75% of the cerebral cortex in rat is immunolabelled for drebrin E and A [142]. Drebrin E is expressed throughout the adult brain at low levels, with the exception of olfactory bulb where it is abundantly expressed [125]. Drebrin A is highly expressed when compared with drebrin E in the forebrain where spine plasticity is high, but it is expressed at lower levels in other regions that have less plasticity [92]. Strong

drebrin A expression was observed in the cerebral cortex and hippocampus, but minimal expression was observed in cerebellar cortex, pons, medulla and spinal cord.

During development, drebrin E is observed in neuronal cell bodies as well as developing axons and dendrites [124]. However, in adulthood, drebrin E is localized mainly to neuronal cell bodies. Drebrin A, on the other hand, specifically localizes to the postsynaptic dendritic spines. In support, transfection of mature cultured neurons with drebrin A showed spontaneous accumulation of drebrin A in dendritic spines [122]. These data indicate both cellular and subcellular specificity of drebrin E and A.

2.2.5 Drebrin-actin interaction

Drebrin is an actin side-binding protein that provides F-actin stability and promote polymerization by interacting with profilin and α-actinin. The precise mechanism by which drebrin interact with actin is unknown. However, the association between drebrin and actin has been found *in vitro* in neuroblastoma and primary neurons [143]. Furthermore, drebrin and actin were found to be bound *in vivo* in dendritic spines using immunoelectron microscopy [92]

Drebrin does not bind G-actin. Drebrin binds F-actin at the molar ratio of 5 actin: 1 drebrin with a dissociation constant (K_d) of $1.2x10^{-7}$M, thus making drebrin a strong competitors to other ABPs that share the actin binding site such as tropomyosin [144]. In order to bind to actin, drebrin utilizes its ABS in the N-terminal half of the protein, which contains a coiled-coil domain and a helical domain that can independently bind F-actin [137]

Drebrin binds and stabilizes F-actin by interacting with myosin and prevents actomyosin from interacting with F-actin, which results in inhibition of spine retraction [122]. Furthermore, drebrin stabilizes F-actin by inhibiting cofilin, an actin severing protein, from binding to F-actin [145]. Drebrin-bound actin is resistant to the actin depolymerizing agent Cytochalasin D that blocks actin filament elongation [146,147]. However, drebrin-bound actin becomes vulnerable to another actin-destabilizing ABP, gelsolin [144]. In addition to providing stability, drebrin can bind to actin to change kinky F-actin configuration to straight filaments [144,148]. Drebrin was also shown to have actin bundling activity [137]. These data indicate the various roles drebrin plays in actin reorganization and stability within dendritic spines.

2.2.6 Drebrin in dendritic spines

Drebrin plays a pivotal role in dendritic spine formation, maturation and morphology. Drebrin expression is increased in parallel with neurite outgrowth and is found in the basal region of growth cones of differentiating human neuroblastoma cells (SH-SY5Y) and rat pheochromocytoma (PC12) cells [149,150]. In developing hippocampal neurons, drebrin localizes to filopodia that becomes the spines [11]. Drebrin was shown to be required for clustering of F-actin to these filopodia as antisense oligonucleotides against drebrin led to decrease in the density of the filopodia. Filopodia containing drebrin co-localized with the presynaptic vesicle protein, synapsin I, whereas filopodia devoid of drebrin did not. Thus, drebrin appears to be precursor of postsynaptic structure that leads to synapse formation.

Drebrin is also required for recruitment of PSD constituents during spine maturation. Drebrin recruits PSD-95, the major glutamate receptor scaffolding component of the PSD, to the spines (refer to Figure 5) [11]. Drebrin also is required for glutamate receptor function as drebrin co-localizes with AMPAR GluR1 and GluR2 [151,152]. Furthermore, homeostatic accumulation of a glutamate receptor, NMDARs, at synapse requires drebrin A where NR2A subunit of NMDARs is prominent in drebrin-immunopositive spines [8]. Downregulation of drebrin led to decreases in glutamatergic synaptic activity [153].

As an ABP, drebrin provides stability to dendritic spines. Drebrin is required to maintain the width of dendritic spines where the inhibition of drebrin led to decrease in spine width. When drebrin is overexpressed, it led to spine elongation and enlarged megapodia formation in mature neurons [122] and immature neurons [9] respectively. Thus, drebrin stabilizes F-actin by facilitating actin polymerization. In addition, drebrin increases the spine density via its interaction with a transcriptional co-activator spikar that directly mediates the increase in spine density [154]. Consequently, inhibition of drebrin by antisense oligonucleotide leads to a decrease in the spine density, which is also evident in a drebrin knockout model [8,155]. Drebrin also utilizes its proline-rich c-terminus to bind to Homer, which is a postsynaptic scaffold protein used to link signaling proteins such as Shank and Cdc42, and facilitate the growth of dendritic spines [140,156-160]. Overall, drebrin is an essential ABP for dendritic spine function whose absence would lead to disruption of spine formation, maturation and morphology.

2.2.7 Drebrin in synaptic plasticity and brain function

Drebrin expression correlates with synaptic plasticity. Increases in drebrin expression correlates with the sensitive period of the visual cortex where cortical plasticity is high [161,162]. Furthermore, drebrin expression remains elevated in brain regions that undergo life-long synaptic plasticity [141]. Drebrin was shown to regulate dendritic spine plasticity and synapse function by increasing the spine density [153]. This, in turn, increases glutamatergic transmission in the form of increased frequency and amplitude of miniature excitatory postsynaptic currents (mEPSCs) in hippocampal neurons. Therefore, drebrin is able to modulate synaptic plasticity by regulating the actin dynamics inside dendritic spines.

Drebrin is functionally implicated in memory, learning and cognition. Knockdown of drebrin A in whole rat brain causes deficits in memory formation, sensorimotor gating and cognitive function [163]. Similar memory deficits are observed when drebrin is depleted, which is thought to occur partly due to reduced levels of dopamine receptor D1 and D2 that is known to facilitate the formation of dendritic spines and is a regulator of memory formation and maintenance[155,164-167]. Furthermore, electrophysiological study demonstrated hippocampal slices from drebrin KO mouse having inhibited memory-related high-frequency-induced synaptic strengthening [155]. These data indicate the necessity of drebrin in higher brain function and propose a possible mechanism by which drebrin loss leads to cognitive deficits in brain disorders.

2.2.8 Loss of drebrin during synaptic pathology

Gradual decline of drebrin E and A in concordance with the decrease in spine density occurs during normal aging[13]. Even greater and marked loss of drebrin is

observed in AD and AD-related disorders where dendritic spines are lost with disease progression [10,12-14,168-170]. In humans, drebrin was found to be significantly decreased in the frontal cortex and temporal cortex upon the analysis of postmortem human frontal cortex, temporal cortex and cerebellum of patients with AD and Down syndrome [10]. When quantified, greater than 80% of drebrin protein was found to be lost in the hippocampus and cerebral cortex of AD patients [13]. In AD, postsynaptic sites degenerate more extensively than presynaptic ones where greater loss of drebrin occurs compared to the presynaptic synaptophysin [12]. Furthermore, loss of drebrin occurs early in the pathogenesis of AD that the loss is observed in mild cognitive impairment (MCI), which precedes AD [171]. According to ante mortem analysis using the Mini-Mental State Examination in combination with postmortem brain analysis, drebrin loss also correlates with progression of cognitive impairment [14].

Loss of drebrin is also observed in the animal models of AD where drebrin is linked to AD pathogenesis [15-18]. In old 16-18-mo Tg2576 transgenic mouse, 50% drebrin loss is observed in parallel with Aβ accumulation while the presynaptic synaptophysin remains stable [15]. Thus, the postsynaptic protein drebrin may be a more sensitive marker of synapse loss than the presynaptic protein synaptophysin. Similarly, $APP^{NLh/NLh}$/$PS\text{-}1^{P264L/P264L}$ double-knockin (2xKI) mouse shows loss of drebrin-containing spines and AMPAR activity in the CA1 region of hippocampus at 6 months of age [16,172]. Also, 2-mo presenilin conditional double knockout (PScDKO) mouse show loss of both synaptic and nonsynaptic drebrin A [173]. Therefore, drebrin appears to be a pathological target that is affected early and progressively in the pathogenesis of AD. Additionally, these data

suggest drebrin loss results in loss of functional dendritic spines that may be implicated in cognitive decline.

2.2.9 Regulation of drebrin

Despite the significance of drebrin loss in neurological disorders, the regulatory factors controlling drebrin expression and information regarding drebrin promoter are unexplored. Thus, the mechanism of drebrin loss in AD and related disorders also remains to be found. There are two transcription factors (TFs) known to bind to drebrin promoter to regulate its expression, NXF and Sim2. NXF and Sim2 belong to the basic helix-loop-helix-Per-Arnt-Sim (bHLH-PAS) protein family that is known to be related to Down's syndrome pathology [174]. Sim2, especially, is expressed abundantly in Down's syndrome due to the Sim2 locus trisomic state [175]. NXF and Sim2 both form heterodimers with the Arnt subclass of bHLH-PAS factors and compete with each other to bind to multiple binding sites on drebrin promoter and regulate drebrin gene expression as NXF-Arnt2 and Sim2-Arnt2. NXF activates drebrin promoter according to reporter gene assays with luciferase reporter construct, DNA array technology and ChiP assay. Sim2, on the other hand, represses drebrin transcription according to reporter gene assays. Excessive Sim2 in Down's syndrome is thought to downregulate drebrin, although functional studies are required to assess whether this is the case [176]. In AD, however, linear regression analysis demonstrated weak positive correlation between Sim2 and drebrin [168]. Also no significant change in Sim2 was found between AD and control patients [177]. Therefore Sim2-mediated regulation of drebrin appears specific to Down's syndrome. These data suggest that the regulatory factor responsible for drebrin loss in AD and related disorders remains to be determined.

At the posttranslational level, drebrin was found to be regulated in several ways. First, drebrin is a substrate of proteases such as caspase-6 induced during AD [178,179]. In support, close association of caspase-6 accumulation and loss of drebrin was found in animal models of AD [15,180]. Furthermore, drebrin is also degraded by calpain, a protrease which is activated in response to glutamatergic NMDAR activation [181]. Excitotoxicity due to the overactivation of NMDARs was found to induce neuronal death in neurodegeneration [182-184]. The NMDA-induced excitotoxicity induces calpain activity and lead to degradation of drebrin in primary neurons and an *in vivo* experimental model of cerebral ischemia [181]. Additionally, decreases in drebrin clusters in response to application of amyloid beta (Aβ) oligomers, which is the protein thought to be responsible for AD pathology, was found to be mediated by histone deacetylase [185]. However, since loss of drebrin mRNA and protein is observed in AD, translation alone does not sufficiently explain the loss of drebrin. Therefore, the severity of drebrin loss and its detrimental effect on dendritic spines prompted us to study drebrin regulation in relation to AD.

2.3 Early growth response-1

Synaptic rearrangements induced by all cellular events including growth, memory formation and consolidation, learning, stress as well as pathological stimuli including neurodegeneration and cell death require changes in gene expression and *de novo* protein synthesis [186-190]. Egr-1 is induced rapidly in response to synaptic activity. By doing so, Egr-1 connects the cell surface events to the orchestrated and persistent changes in gene expression, thereby altering neuronal function [191-193]. Egr-1 regulates genes involved in cellular events including brain injury, ischemia and AD [25,194,195]. Therefore, understanding the underlying molecular and biochemical mechanisms of Egr-1-mediated regulation in brain is a crucial in order to comprehend the synaptic modification that occurs during normal cellular process and pathology.

2.3.1 Egr-1: A gene with many names

Egr-1 constitutes a member of immediate early genes (IEGs)-encoded transcription factor. Egr-1 belongs to the Egr family of proteins that comprise of five members: Egr-1, Egr-2, Egr-3, Egr-4 and WT-1 (the product of the Wilms' tumour gene) [25]. Egr-1 was first discovered as a nerve growth factor (NGF)-induced factor in NGF-treated PC12 cells [196]. The term Egr-1 is synonymous with Krox-24, NGF1-A, TIS8 and Zenk due to its discovery in five independent discoveries.

Egr-1 protein is comprised of functionally independent domains (Figure 8) [197-199]. The N-terminal region contains a strong activation domain with serine and threonine motif and corresponds to the activator domain, while the C-terminal region contains weak activation domain with proline, serine and threonine motif. Egr-1 activator domain is required for Egr-1 to regulate target gene expression [200]. Additionally, Egr-1 has a

repressor domain where Egr-1-mediated actions can be regulated. For repression, nuclear co-repressors called NGFI-A binding proteins (NABs) bind to the repressor domain and suppress transcriptional activity of Egr-1 [201]. The DNA binding domain consists of three Cys2His2 zinc finger protein motifs, which are structured as antiparallel beta-pleated sheets followed by alpha helix [202,203]. Egr-1 also has a bipartite nuclear localization sequence (NLS) located near and within the DNA binding domain [204,205]. Thus, Egr-1 is able to translocate from the cytoplasm into the nucleus to function as a TF by binding to its target DNA sequences.

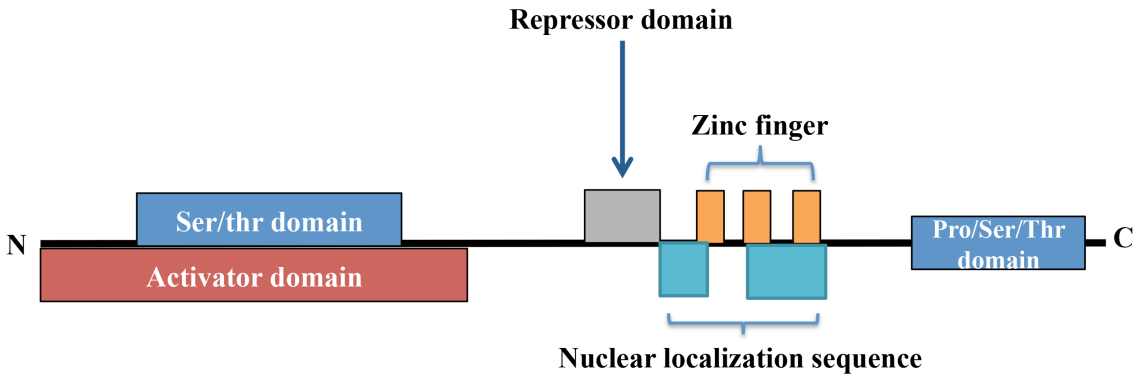

Figure 8. Schematic illustration of Egr-1 domain structure

2.3.2 Egr-1 expression in the brain

Egr-1 is present as a single-copy gene and it is conserved between species [206]. Depending on the initiation sequence, either a 82 or 88kDa protein is produced [207]. Egr-1 is highly expressed in the brain and shows regional differences [208,209]. The basal expression of Egr-1 is high in the cerebral cortex, primary olfactory structures, hippocampus, amygdala and striatum. In the hippocampus it is most highly expressed in CA1 and followed by CA2 to CA4 with negligible level in the dentate gyrus [25]. Egr-1 protein is not detected in white matter [210]. Therefore, Egr-1 is expressed highly in regions that display continuous and high levels of synaptic plasticity similar to drebrin.

Initially, Egr-1 expression is absent in the embryo, but begins to increase post-natally and into adulthood. Egr-1 expression reflects neuronal activity. Egr-1 expression was found to correlate with c-Fos induction, which is expressed in parallel with neuronal firing of action potentials [211,212]. The induced expression of Egr-1 mRNA and protein are tightly linked with dopamine D1 receptor and glutamatergic AMPA and NMDA receptors [213,214], suggesting Egr-1's involvement in synaptic activity.

2.3.3 Egr-1 as a transcription factor

Egr-1, as a member of IEG, is thought to constitute the initial step in transcriptional regulation by binding to its target promoters [215]. Egr-1 uses its three zinc finger protein motifs that recognize and bind to a GC-rich 9 base pair EREs (GCG(G/T)GGGCG) on the promoters of its target genes [202,203]. However, non-consensus EREs also exist in CpG islands, which are regions of DNA that have cytosine nucleotide and guanine nucleotide in linear sequence near the transcription start site (TSS) [215].

Therefore, Egr-1 is able to regulate the transcription of a wide range of genes by binding to a 9 base pair GC-rich sequences.

In the brain, Egr-1 is induced during normal physiological process such as synaptic plasticity as well as during pathological process such as AD. Egr-1 can either induce or repress expression of its target genes [25,29]. Interestingly, Egr-1 was found to downregulate the majority of its target genes in the brain [29]. Despite a large number of genes already being identified as the targets of Egr-1 in various cells and tissues, only a few genes are known to be targets of Egr-1 in neurons. Specifically, Egr-1 was found to regulate the expression of synapsin I [216], acetylcholinesterase [217], Arc/ARg3.1 [218] and $GABA_A$ receptor subunits $\alpha 2$, $\alpha 4$ and θ [219] using either *in vitro* assays or *in vivo* ChIP and Egr-1 overexpression experiments. According to high-density microarrays using PC12 neuronal cell line, Egr-1 overexpression alters the expression of signaling molecules, synaptic proteins, proteasome-related proteins, metabolic proteins, transcription factors and vesicle trafficking protein [29]. When NMDARs were stimulated in rat hippocampal neurons to create a model of synaptic plasticity, Egr-1 was further found to downregulate genes that are involved in synaptic plasticity including the amyloid pathology-related protein cystatin C and the vesicular Ca^{2+} sensor protein synaptotagmin [29]. In response to Egr-1 overexpression, one of the Egr-1 target genes identified was drebrin where 23% downward change was observed [29]. Therefore, Egr-1 may downregulate drebrin under pathological conditions.

2.3.4 Induction of Egr-1 expression

Egr-1 expression is regulated and maintained by synaptic plasticity as it can be induced via NMDARs, AMPARs and dopamine D_1 receptors. The expression of Egr-1

mRNA and protein correlate closely with activation of NMDARs. *In vivo* administration of NMDA was shown to elevate Egr-1 level dose-dependently in the rat brain including cerebral cortex and hippocampus [220]. Inhibition of NMDAR by antagonists abolished basal and visual input-induced mRNA and protein expression of Egr-1 [213]. Similar effects were also observed in the cortex, hippocampus and striatum [221]. Furthermore, activity of AMPARs was shown to be implicated in regulation of Egr-1 in the sensorimotor cortex [214]. Other studies additionally linked Egr-1 expression with L-type voltage-sensitive calcium channels [222] and dopamine D_1 receptor activation in response to dopamine [223,224]. Furthermore, inhibition of γ-amino butyric acid (GABA) receptor, a major inhibitory receptor, induced Egr-1 expression in the hippocampus and cerebral cortex [225]. Therefore, Egr-1 is induced in response to activation of glutamatergic receptors that are involved in synaptic plasticity.

2.3.5 Egr-1 in synaptic plasticity and higher brain function

Under physiological conditions, Egr-1 is required for maintenance of hippocampal LTP and the consolidation of several forms of memories [226,227]. Hippocampal LTP is temporally comprised of: induction phase that requires elevation in postsynaptic Ca^{2+}; early maintenance phase that requires protein kinases; late phase that requires gene transcription and protein synthesis [228-232]. Egr-1 mRNA is transiently upregulated in response to LTP-inducing stimulation after ten minutes to two hours in the dentate gyrus of hippocampus [233-235]. Therefore Egr-1 is not involved in the immediate phase following LTP induction, but is involved in the transition from LTP induction to protein synthesis-dependent late phase [236]. Furthermore, targeted inactivation of Egr-1 in mice led to the absence of late phase LTP in the dentate gyrus, a brain region where basal

expression of Egr-1 remains low but is induced in response to LTP, suggesting Egr-1-mediated synthesis of downstream effector proteins is necessary [226]. Consistent with this idea, Egr-1 gain-of-function in mice enhanced LTP in the dentate gyrus and increased the expression of downstream effector genes synapsin II and the proteasome 20S β-subunit PSMB9 [227].

Synaptic plasticity including LTP and LTD is presumed to form the neural basis for learning and memory formation. Consequently, Egr-1 expression has been implicated in learning and memory formation. In support, Egr-1 induction was observed following exposure to a learning paradigm in the hippocampus and the inferior gyrus of rats and monkeys, respectively [237,238]. In Egr-1 deficient mice, deficits in hippocampal-dependent spatial learning and long-term memory was observed when the mice were tested using the open-field water maze, conditioned taste aversion and novel object recognition [226]. Egr-1 inactivation did not affect short-term memory, as expected. Furthermore, Egr-1 deficient mice showed impairment in forming stable hippocampal place cell representations when exposed to novel environment [239]. On the other hand, Egr-1 gain-of-function in mice increased the resistance to extinction of conditioned taste aversion suggesting a stronger memory formation [240]. In line with this, Egr-1 gain-of-function also led to increased capacity to form a long-term spatial memory, which was assessed by the novel object recognition test [227]. These data indicate the importance of Egr-1 in learning and memory formation under physiological conditions. However, the role of Egr-1 in brain pathologies remains to be determined.

2.3.6 Egr-1 in pathology

Egr-1 is involved in various pathologies of the brain although its role remains largely elusive. Egr-1 is increased in response to focal brain injury induced by intracerebral saline injection [241]. Also, Egr-1 mRNA is observed in the cerebral cortex upon induction of transient focal ischemia [242]. The degree of Egr-1 induction correlates with the severity of unilateral hypoxia-ischemia, which produces seizures and infarctions in severe cases [243].

Interestingly, studies indicate an involvement for Egr-1 in neurodegenerative diseases, such as AD, where loss of dendritic spines is prevalent [27,28,195]. Egr-1 was identified as significantly upregulated, and correlated with the progression of the disease, in a microarray analysis of hippocampal genes from AD patients [28]. Furthermore, Egr-1 mRNA was elevated by 4-fold in degenerating hippocampal pyramidal neurons of AD brain [27]. Significantly, increased Egr-1 protein level was found in both temporal cortex and hippocampus of AD brain[195]. Therefore, Egr-1 appears to be chronically upregulated as AD progresses in brain regions that normally display high synaptic plasticity. This raises the need to examine the role chronically upregulated Egr-1 plays in AD and related pathologies.

2.4 Specific Aims and Goals

Based on these data, we hypothesized the following:

1) Egr-1 binds to drebrin promoter to regulate drebrin expression
2) Egr-1 negatively regulate drebrin expression
3) Egr-1 upregulation leads to decrease in drebrin mRNA and protein levels
4) Egr-1-mediated loss of drebrin correlates with decrease in dendritic spine density

Based on our hypotheses, the objectives of the thesis were:

Aim I. Identify Egr-1 response elements on drebrin promoter.

Egr-1 transcription factor regulates target gene expression by binding to GC-rich Egr-1 response elements (EREs) on the target's promoter. We hypothesize Egr-1 regulates drebrin transcriptionally by binding to EREs present on drebrin promoter.

Aim II. Examine Egr-1-mediated regulation of drebrin *in vitro* and *in vivo*.

Drebrin is lost in brain disorders with synaptic pathology including AD [10]. On the contrary, Egr-1 was found to be upregulated in AD [27,28]. We hypothesize Egr-1 upregulation leads to loss of drebrin. Consistent with this hypothesis, Egr-1 deficit may results in increased drebrin expression.

Aim III. Examine Egr-1-mediated changes in dendritic spines *in vitro* and *in vivo*.

We hypothesize Egr-1-mediated loss of drebrin leads to loss of dendritic spine density. The Egr-1-mediated loss of spine density may result in loss of putative synaptic

contacts. Consistent with this hypothesis, Egr-1 deficit would lead to increased drebrin expression, which would be reflected in increased spine density.

Chapter 3. Materials and Methods

3.1 Antibodies

The following antibodies were used as primary antibodies: mouse monoclonal anti-drebrin (1:1,000 – 1,500 for both immunoblotting and immunofluorescence) (Abcam), rabbit polyclonal anti-drebrin (1:1,000 – 1,500 for both immunoblotting and immunofluorescence) (Abcam), rabbit monoclonal anti-PSD-95 (1:1,000 for immunoblotting and 1:250 for immunofluorescence) (Cell Signaling Inc.), mouse monoclonal anti-GAPDH (1:30,000) (Milipore), rabbit polyclonal anti-Egr-1 (1:1,000 for immunoblotting and 1:250 for immunofluorescence) (Santa Cruz), mouse monoclonal anti-vGluT1 (1:1,000 for immunoblotting and 1:150 for immunofluorescence) (NeuroMab), mouse monoclonal anti-Myc tag (1:1,000 for immunoblotting) (Cell Signaling Inc.), rabbit polyclonal anti-tubulin (1:1,000 – 3,000) (Sigma-Aldrich), mouse monoclonal anti-β-actin (1:2,500) (Sigma-Aldrich), mouse monoclonal anti-synaptophysin (1:1,000) (Sigma-Aldrich), rabbit polyclonal anti-cofilin (1:1,000) (Abcam), rabbit polyclonal anti-GluA1 (1:2,000) (Millipore), and rabbit polyclonal anti-profilin 1 (1:1,000) (Abcam) antibodies. For immunoblotting, horseradish peroxidase-conjugated goat anti-mouse IgG (Promega) and anti-rabbit IgG antibodies were used (1:2,500). For immunocytochemistry, the following goat anti-mouse or anti-rabbit IgG (H+L) secondary antibodies with following flurophores were used: Alexa Fluor® 488, 555, 594 and 647 (1:250) (ThermoFisher Scientific). Acti-stain 488 phalloidin (1:300) (Cytoskeleton) was used to stain F-actin.

3.2 Mouse strains

All procedures were approved by the Lady Davis Institute/Jewish General Hospital Animal Care Committee and were performed according to the guidelines of the Canadian Council on Animal Care. All mice were kept under a normal 12h light/dark cycle, and had access to food and water *ad libitum*. For experiments, mice were anesthetized using isofluorane before euthanasia with CO_2.

3.2.1 Triple transgenic model of AD (3xTg-AD)

3xTg-AD mice (obtained from Jackson laboratory #004807) that were 3-, 9- and 15-mo were used for the study. Generation of 3xTg-AD mouse was described previously [244]. Briefly, these mice express the Thy1.2 expression cassette containing human APP (695 isoform) with Swedish double mutation (KM670/671NL) and human four-repeat tau with P301L mutation was co-microinjected into the pronuclei of single-cell embryos harvested from homozygous $PS1_{M146V}$ knockin mouse. 3xTg-AD mouse develop both neurofibrillary tangles and amyloid plaques with age similar to AD in correlation with cognitive and behavioural changes [245]. Nontransgenic control mice with same genetic background (a hybrid 129/C57BL6) were used.

3.2.2 Egr-1 knockout (-/-) mouse

For the study, 12-mo Egr-1 -/-, +/- and +/+ mouse with C57BL6 background were used [246]. The originating parental Egr-1 -/- mice were a gift from Dr.Jeffrey Milbrandt (University of St.Louis). In brief, LacZ-neomycin cassette was integrated into Nde1 restriction site upstream of the first zinc finger of Egr-1 under the control the murine phosphoglycerate kinase-1 (Figure 9A). As a result, Egr-1 gene was rendered non-

functional. The Egr-1 -/- females are infertile due to the loss of Egr-1-mediated expression of luteinizing hormone (LH) in the gonadotropin-releasing hormone (GnRH)-LH axis [247]. Therefore, Egr-1 -/- mice were generated by mating Egr-1 -/- males with Egr-1 +/- females. Egr-1 -/- mice were genotyped by PCR using the following gene-specific primers [248]: neo-929 (5'-CTCGTGCTTTACGGTATCGC-3'), Egr-1 - 1263 (5'-AACCGGCCCAGCAAGACACC-3') and Egr-1 - 1677 (5'-GGGCACAGGGGATGGGAATG-3'). Egr-1 -/- yielded a 520bp DNA fragment from neo-929 + Egr-1 – 1677 primers while no DNA fragment was amplified using the Egr-1 – 1263 + Egr-1 – 1677 primers (Figure 9B). Conversely, the Egr-1 +/+ mouse yielded a 414bp DNA fragment from Egr-1 – 1263 + Egr-1 – 1677 primers while no DNA fragment was amplified from neo-929 + Egr-1 – 1677. For Egr-1 +/-, both 520bp and 414bp DNA fragments were amplified. Cyclophilin, a housekeeping gene, was used as a PCR control.

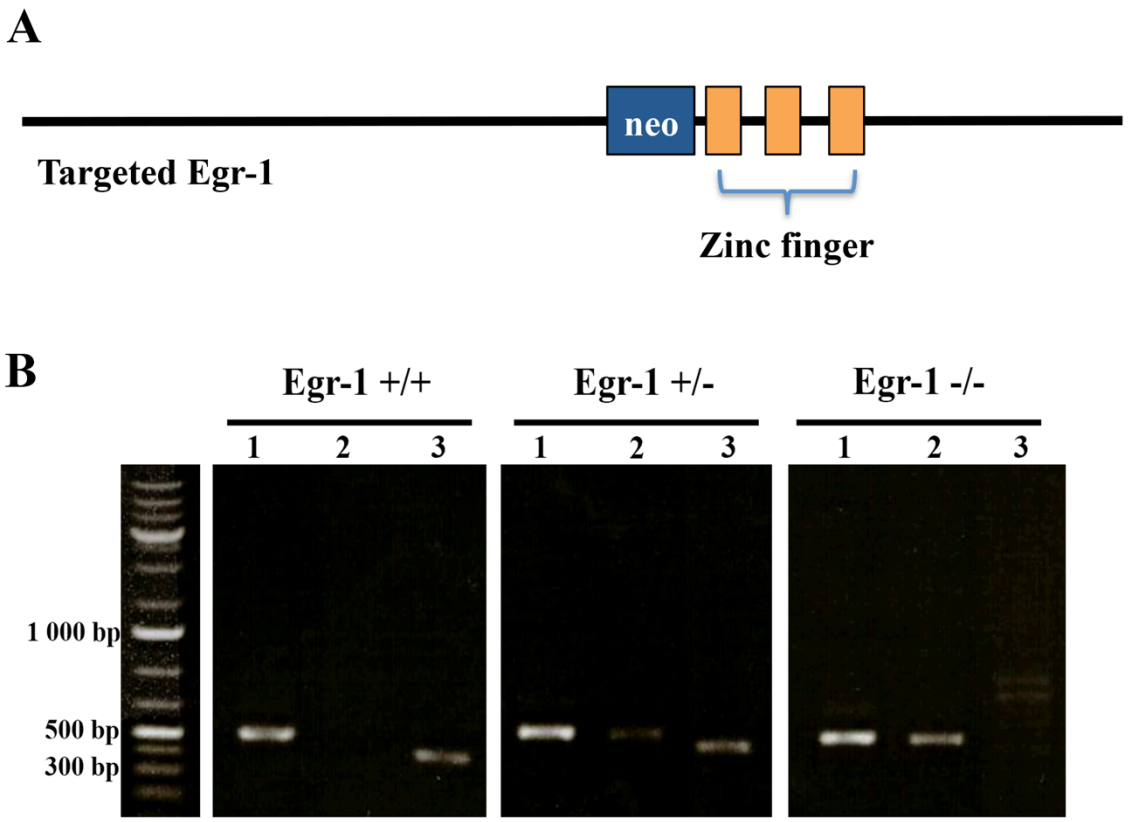

Figure 9. Egr-1 -/- mouse. **A**, Neomycin cassette (neo) was inserted upstream of the first zinc finger. **B**, Egr-1 -/- mouse was identified by the presence of cyclophilin band (Lane 1) and neomycin band (Lane 2) but not Egr-1 band (Lane 3). Egr-1 +/- mouse expressed all three bands while Egr-1 +/+ mouse did not have the neomycin band.

3.2.3 Egr-1 transgenic (Tg) mouse

Egr-1 overexpressing transgenic (Tg) mice were generated. Here, Egr-1 Tg mice were created using the tetracycline (tet)-off system to complement the Egr-1 -/- mouse model. The tet-off system allows control of target gene expression spatiotemporally (Figure 16A).

Human Egr-1 cDNA was cloned and inserted into the vector pBI (Clontech Laboratories). The transgene construct was microinjected into fertilized eggs of C57BL6 and surgically transferred to recipients by IRIC Transgenic Core Facility (University of Montreal, Montreal, QC). By screening genomic DNA from tail biopsies for the presence of the transgene using PCR, potential six founder (F_0) mice were identified. F_0 mice were crossbred with transgenic mice expressing the tetracycline-controlled transactivator protein (tTA) that are under the control of the forebrain specific calcium/calmodulin-depdent protein kinase IIα (CamKIIα) promoter (Jackson Laboratory). The camKIIα promoter specifies Egr-1 upregulation to be localized to the forebrain including hippocampus, prefrontal cortex and striatum. As a result, offspring containing both the CamKIIα-driven Egr-1 and tTA, here called Egr-1 Tg mice, was generated. F_1 offspring were genotyped by PCR and analyzed with immunoblotting. Egr-1 Tg mice showed normal fertility.

The Egr-1 upregulation in Egr-1 Tg mice can also be temporally controlled by oral administration of doxycycline (Dox), a tetracycline derivative. Therefore, dox suppresses Egr-1 expression and prevents the binding of tTA, a fusion protein composed of the Tet repressor and the activation domain of herpes simplex virus protein VP16, to the Tet operator. Only the Egr-1 Tg mice expressed both Egr-1 and tTA, allowing

spatiotemporal expression of Egr-1 in the forebrain. Taken together, the CamKIIα-driven and tTA-regulated expression of Egr-1 was induced in the forebrain upon removal of dox from their diet. For our experiments, Egr-1 upregulation was induced by withdrawing dox from the diet at 2-mo and 15-mo. Egr-1 Tg mice were analyzed after 3 months of Egr-1 upregulation. Littermates that were single positive for either Egr-1 or tTA were used as the control.

3.3 Cell culture

All cells were maintained at 37°C in a 95% humidified incubator with 5% CO_2. The human neuroblastoma cell line clone from the SK-N-Be(2) neuroblastoma cell line known as M17 cells (Sigma-Aldrich) were maintained in a 1:1 mixture of Minimum Essential Medium (MEM) and F12 medium containing 10% fetal bovine serum (Life Technologies) and 1% (v/v) penicillin/streptomycin (Life Technologies). Human Embryonic kidney 293 (HEK293) cells as well as the monkey kidney tissue-derived cos-7 (CV-1 in Origin with SV40 genes) cell line were maintained in Dulbecco's Modified Eagle Medium (DMEM) supplemented with 10% fetal bovine serum and 1% (v/v) penicillin/streptomycin (Life Technologies). To passage the cells, the cells were rinsed with warm phosphate buffered saline (PBS) (Life Technologies) and incubated with 0.05% trypsin-EDTA for 3-5 min. The cell suspension was then centrifuged at 1000 to 1500rpm for 5 min, and re-suspended in appropriate media and seeded accordingly.

3.4 Primary hippocampal neuron culture

Primary hippocampal cultures were prepared according to previously described methods with minor modifications [249]. Briefly, hippocampi were dissected from postnatal

day 0 Spraque Dawley rats, dissocated by 1% papain treatment and sequentially titurated using Pasteur pipettes. The neurons were plated on either poly-L-lysine-coated coverslips or 6-well plates in Neurobasal-A medium (Life Technologies) supplemented with 2% B-27, 0.2% GlutaMAX-1 and 1% penicillin-streptomycin (Life Technologies). 3-4x10^5 cells were plated per well of a 24-well plate for immunocytochemistry and 5-6x10^6 cells were plated per well of a 6-well plate for immunoblot and qRT-PCR. After neurons attached onto the coverslips, the coverslips were transferred into a plate containing a hippocampal astrocyte feeder layer maintained in the same media as described above. 3μM Cytosine β-D-arabinofuranoside (Sigma-Aldrich) was added to the cultures 4 days after plating to inhibit glial proliferation.

3.5 Lentiviral vector production and administration

Lentiviral transduction was used to upregulate Egr-1 in hippocampal neurons as lentiviral vectors can transduce non-dividing neurons, express transgene for long-term studies and have low toxicity [250,251]. Here, human Egr-1 cDNA (Origene) with a myc tag added to the C-terminus was subcloned into the bicistronic lentiviral expression vector pLVX-IRES-ZsGreen1 using Lenti-X™ HTX Packaging system (Clontech Laboratories Inc.) (Figure 10). A lentivirus expressing ZsGreen1 (Ln-vector) was created as a control. To calculate the titer, HEK293 cells were transduced with different dilutions of either Egr-1 lentivirus (Ln-Egr-1) or Ln-vector with 8μg/ml polybrene (Sigma-Aldrich). 72hr post transduction, HEK293 cells were collected and fixed with 2% paraformaldehyde (PFA) (Bioshop). The titre was calculated by quantitating the percentage of GFP-positive population identified using flow cytometry. Titers for Ln-Egr-1 and Ln-vector ranged from 1x10^7 to 3x10^8 IU/ml and 1x10^7 to 2x10^9 IU/ml, respectively. Primary neurons were

infected on the day of plating with multiplicity of infection (MOI) ranging from 5 to 25. Purified lentivirus was added directly into the wells and medium was replaced with conditioned medium after 12 to 24hr of incubation.

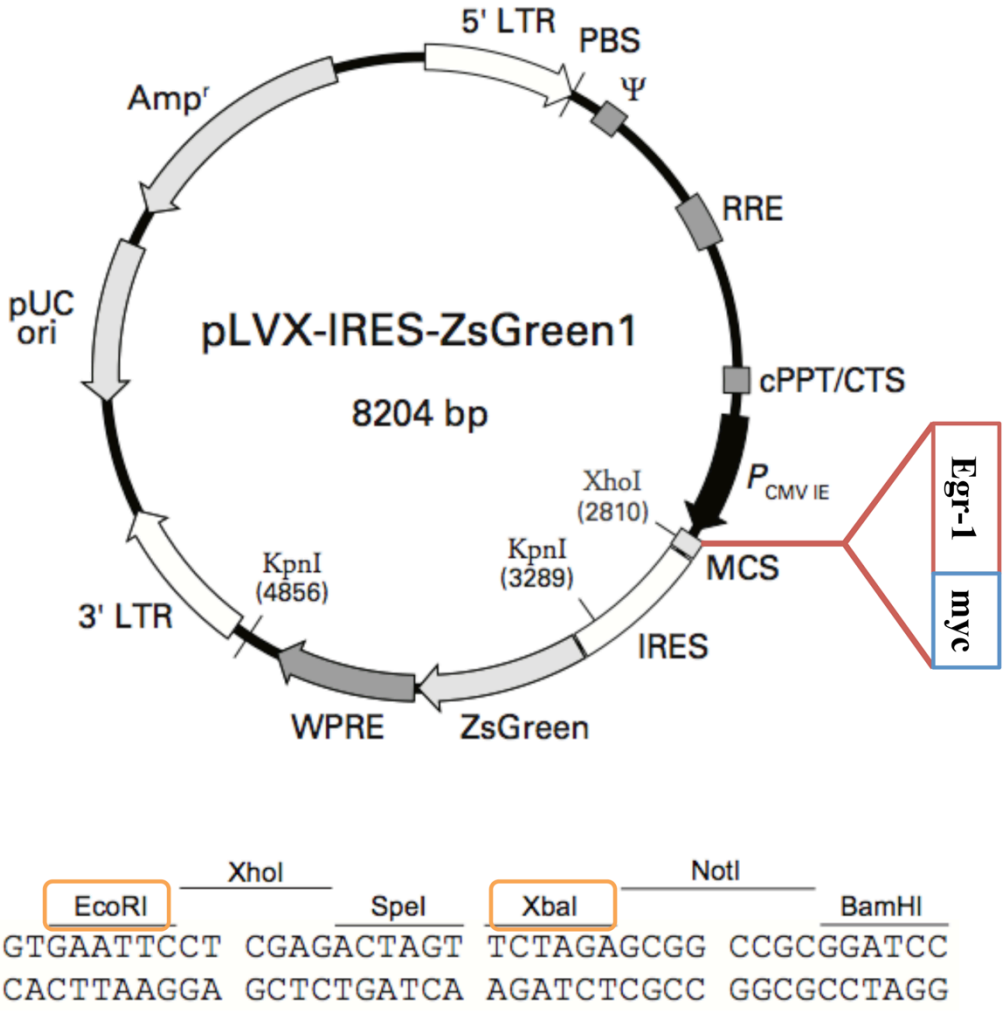

Figure 10. (adapted from Clontech) pLVX-IRES-ZsGreen1 vector map with multiple cloning site (MCS). Myc-tagged Egr-1 was inserted using EcoR1 and XbaI restriction enzymes into the MCS.

3.6 Luciferase promoter assay

3.6.1 Drebrin-luciferase constructs

The human drebrin promoter region from -624bp to +1386bp relative to the predominant transcriptional start site was synthesized (GenScript) and subcloned into the pGL4.23[luc2/minP] vector (Promega) using KpnI and SacI restriction sites in MCS (Figure 11,12A) using the following primers: forward; 5'-ATAGGTACCAGCAACTGGGGTGGATTTGAG-3', reverse; 5'-TATCTCGAGAGCTTGTCTCTCGCGTCC-3'. The various 5' deletion constructs were created as KpnI-SacI fragments (Figure 11) using the following forward primers: -347 construct; 5'-ATAGGTACCCGGACGGGGCAGGTGAGGGTT-3', -2 construct; 5'-ATAGGTACCGCATGGCCGGCGTCAGCTTCA-3', +454 construct; 5'-ATAGGTACCCGCCACCTTCGAGCGGGCGAG-3', +1052 construct; 5'-ATAGGTACCGGAAACCGAGGGGTTCCTCAC-3'. The same reverse primer used for the full length construct was used for the deletion constructs.

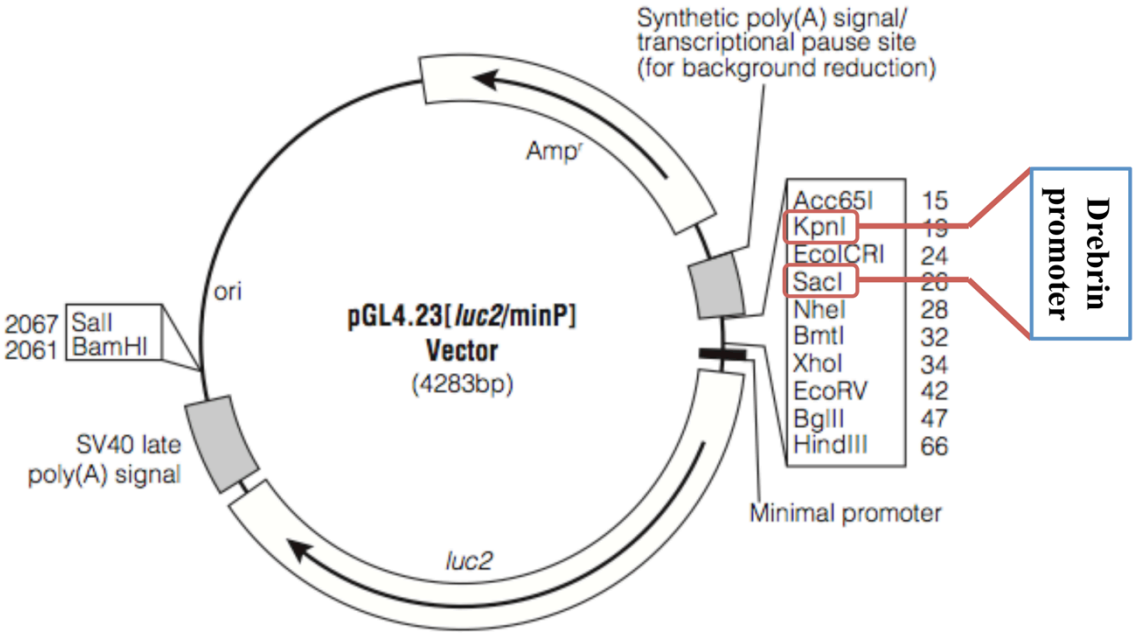

Figure 11. (adapted from Promega) pGL4.23 [luc2/minP] vector map. A fragment of drebrin promoter was inserted into pGL4.23 luciferase vector using KpnI and SacI restriction enzyme sites into the MCS.

3.6.2 Transient transfection and luciferase assays

Cos-7, HEK293 and primary hippocampal neurons were transfected using Lipofectamine 2000 (Life Technologies) at 70% confluency in 12-well plates. Cells were transfected with 200ng of pCMV6-XL5-Egr-1 (Egr-1 plasmid), 100ng of either pGL4.23-Dbn (or deletion constructs) or pGL4.23-vector, and 5ng of Renilla control plasmid pRL-CMV (Promega). 24hr after transfection, luciferase and Renilla expression was measured using Dual-Luciferase® Reporter Assay System (Promega) according to a manufacturer's instructions using GloMax® 20/20 luminometer (Promega).

3.7 Chromatin immunoprecipitation

Chromatin immunoprecipitation (ChIP) was performed using EZ-Magna ChIP™ (Millipore), according to the manufacturer's instructions. Briefly, M17 cells were transfected with pCMV6-XL5-Egr-1 for 48hr prior to cross-linking with 1% formaldehyde. Cells were washed twice with phosphate-buffered saline, incubated in cell lysis buffer for 15min, and sonicated in nuclear lysis buffer to an average chromatin length of 500bp. Sheared cross-linked chromatin was then subjected to immunoprecipitation for 16hr at 4°C using anti-Egr-1 antibody (Santa Cruz Biotechnology). Normal rabbit IgG was added as a negative control for the immunoprecipitation. Immunoprecipitated DNA fragments were amplified and quantitated by real-time PCR with PCR primers specific to the human drebrin promoter or a distant region on chromosome 5. Primer optimization was performed using standard curves and the following primer sets with a slope between -3.1 and -3.4 were used: 5'-AAGGGGCAATCTGTGTGTGTGCT-3' and 5'-GGTTTTAGGGCTGAGGGGAGGC-3' for the region -2851 ~ -2736 from the transcription start site on drebrin promoter, 5'-

TCCCTCCATGGCTCTCCCCA-3' and 5'-GCACCCAGGCAGGGACACAG-3' (-1586 ~ -1450), 5'-GGGTGGGGTGTTGTGTGAGCTG-3' and 5'-TGGTGCGTCCCACCTCATGTT-3' (-529 ~ -465), 5'-CTGGAGCTGCTGGCGGCTTA-3' and 5'-CCAGTCGGCCGCGCTCT-3' (+27 ~ +84), and 5'-AGGGTGACCATCGGGATGAGGAG-3' and 5'-TGGGCCAGGCAAGCTGAGATAG-3' for 123bp region on chromosome 5 where no known ERE was found in the proximity of 500bp.

3.8 Immunoblotting

Primary neurons or brain tissue were lysed in RIPA buffer composed of 10mM Tris at pH7.2, 150mM NaCl, 5mM EDTA, 0.1% Triton X-100, 0.1% SDS, 1% deoxycholate, protease inhibitor cocktail and PhosSTOP (Roche) and solubilized in sample buffer composed of 2% SDS, 0.1M dithiothreitol, 10% glycerol, 1mM EDTA, 62.5mM Tris at pH6.8, and 0.01% bromophenol blue. Five to 80μg of protein was loaded and electrophoresed through SDS-PAGE gel (10% acrylamide) and transferred onto Immobilon-P transfer membrane (Millipore). The membranes were blocked in either 5% nonfat milk or BSA in TBST, immunostained overnight at 4°C with appropriate primary antibodies, incubated with secondary antibodies for an hour at room temperature, and visualized with Pierce ECL Western Blotting Substrate (Thermo Scientific). The chemiluminescent signals were collected on x-ray film, digitally scanned and quantitated using ImageJ.

3.9 Quantitative real-time PCR

Total RNA was prepared from cells and brain tissues using RNeasy® Mini Kit and RNeasy® Lipid Tissue Kit (Qiagen) according to the manufacturer's instructions. One μg of total RNA was converted into cDNA using qScript™ cDNA SuperMix (Quanta Biosciences) according to manufacturer's instructions. cDNA was then used as a template for real-time PCR using ABI 7500 (Applied Biosystems). Quantitect SYBR® Green PCR Mastermix (Qiagen) was used according to the manufacturer's instructions. The sequences of primers are as follows: for mouse drebrin, 5'-ATAACCCACGGGAGTTCTTC-3' (Forward) and 5'-TGGCAGGTGATATAGGGAAA-3' (Reverse) or 5'-CTGACCAATGGAGAGACCAC-3' (Forward) and 5'-GGTGATGTCGATTTCTGGAG-3' (Reverse); for rat drebrin, 5'-ATAACCCACGGGAGTTCTTC-3' (Forward) and 5'-TGGCAGGTGATATAGGGAAA-3' (Reverse) or 5'-CCTCCAGAAATCGACATCAC-3' (Forward) and 5'-TGGGTAGAGAAGCAGACAGG-3' (Reverse); for mouse Egr-1, 5'AGCGAACAACCCTATGAGCACC-3' (Forward) and 5'-ATGGGAGGCAACCGAGTCGTTT-3' (Reverse); for human Egr-1, 5'-AGCAGCACCTTCAACCCTCAGG-3' (Forward) and 5'-GAGTGGTTTGGCTGGGGTAACT-3' (Reverse); for mouse GAPDH, 5'-CATCACTGCCACCCAGAAGACTG-3' (Forward) and 5'-ATGCCAGTGAGCTTCCCGTTCAG-3' (Reverse); for rat GAPDH, 5'-AGACAGCCGCATCTTCTTGT-3' (Forward) and 5'-CTTGCCGTGGGTAGAGTCAT-3' (Reverse). The mRNA levels were normalized to GAPDH mRNA levels as an internal control.

3.10 Immunocytochemistry

Hippocampal neurons transduced with either Ln-Egr-1 or Ln-vector were fixed with 4% paraformaldehyde and 4% sucrose in 0.1M PBS for 10min at 4°C. After rinsing with PBS, cells were permeabilized with 0.25% Triton X-100 for 5 min. Subsequently, cells were washed with PBS and incubated for 45 min with 2% BSA and goat serum in PBS to reduce non-specific staining. The cells were then incubated overnight at 4°C in primary antibodies or Acti-stain 488 followed by 1hr incubation with corresponding Alexa Fluor® 488-, 555- and 647-labelled secondary antibodies (Life Technologies). The coverslips were washed and mounted with ProLong® Gold antifade reagent (Life Technologies).

3.10.1 image acquisition and analysis

Z-stack confocal images (optical section thickness = 1μm) of immunolabelled primary hippocampal neurons were collected using Zeiss LSM5 Pascal microscope and a Zeiss 63x oil-immersion objective lens. Ten to 15 GFP-positive neurons were chosen at random from two to five coverslips from two to three independent experiments for each treatment. ImageJ was used for image processing and Reconstrct software was used for analysis. Only dendritic segments that were clearly visible were measured. All clear protrusions, regardless of their shape, that emanated laterally from the dendrite were quantified while those projecting above and below were not quantified. Dendritic protrusions were counted manually by scrolling through the Z-stacks at the same position. Dendritic protrusions next to each other were considered separate if they were >0.5μm apart. The widths and lengths of protrusions were measured and used for morphological classification (Table 1).

Table 1. Morphological classification of dendritic protrusions

Spine Type	Length (μm)	Width (μm)
Filopodium	Greater than 2	-
Mushroom	Shorter than 2	Greater than 0.6
Thin	Between 0.5 and 2	Less than 0.6
Stubby	Shorter than 0.5	Less than 0.6

3.11 Golgi staining

Golgi staining performed on sections prepared from 12-mo Egr-1 -/- and +/+ mice (n=3 mice/genotype) as well as 18-mo Egr-1 Tg and littermate control mice (n=3 mice/genotype), used the FD Rapid GolgiStain Kit (FD NeuroTechnologies) according to the manufacturer's instructions. Briefly, brains were isolated and cut into 2mm coronal sections using brain matrix (Ted Pella, Inc.). Brain sections were then impregnated with 1:1 mixture of FD Solution A:B for 2 weeks in the dark at room temperature. The sections were then immersed in FD Solution C for 48hr at 4°C in the dark. Tissue sections of 100μm were cut at -23°C using the cryostat Leica CM3050 S and mounted on 2% gelatin-coated glass slides. The mounted sections were allowed to dry at room temperature. Subsequently, the sections were stained in 1:1:2 mixture of FD Solution D:E:distilled water, dehydrated, cleared in xylene, and coverslipped using Permount mounting solution (Fisher) and allowed to dry before quantitative analysis.

3.11.1 Quantification of golgi staining

Z-stack confocal images (optical section thickness = 0.5μm) of pyramidal neurons in the CA1 of hippocampus were taken using Zeiss LSM5 Pascal microscope with a Zeiss 63x oil-immersion objective lens. Quantification was carried out using the rapid Golgi spine analysis method previously described [252]. Here, 10-15 neurons per animal were

used for quantification. Neurons obscured by neighbouring neurons or glia were excluded from analysis. For each neuron, straight branches longer than 10μm were used for analysis, and proximal (30~120μm from soma) and distal (220-340μm from soma) segments of dendrites were quantified using Reconstruct software. Spine densities were calculated as number of spines per 10 micrometer in individual mice group. Also, the width and length of spines were measured to categorize the dendritic spines according to their morphology (Table 2). The same criterion was used as in Table 1 with an additional morphological classification, branched. If more than one spine head was observed on a single neck, the dendritic spine was classified as branched.

Table 2. Morphological classification of dendritic spines

Spine Type	Length (μm)	Width (μm)
Filopodium	Greater than 2	-
Mushroom	Shorter than 2	Greater than 0.6
Thin	Between 0.5 and 2	Less than 0.6
Stubby	Shorter than 0.5	Less than 0.6
Branched	More than 1 spine head on a single neck	

3.12 Statistics

All data were averaged across animals and cell lines within each experimental group. The data were presented as means ± SEM. Statistical comparisons were conducted by Student's t test (paired, 2-tailed) and one-way ANOVA with post-hoc comparisons. Statistical significance was accepted at $P<0.05$.

Chapter 4. Results

4.1 Egr-1 binds to Egr-1 response elements on drebrin promoter

4.1.1 Egr-1 induces activity of drebrin promoter construct

Egr-1 binds to specific GC-rich target sequences, known as EREs, in genomic DNA to regulate transcriptional activity of target genes [196]. To test the hypothesis that Egr-1 binds to drebrin promoter to regulate drebrin expression, putative EREs on human drebrin promoter were identified using the Champion ChIP Transcription Factor Search Portal derived from Decipherment of DNA Elements (DECODE) database from SABiosciences (Figure 12). Human drebrin gene contains two transcriptional start site (TSS) separated by 1 308bps (Figure 12A). Transcription from the upstream TSS accounts for the predominant isoform of drebrin while the downstream TSS accounts for the minor transcript variant. *In silico* analysis identified two putative EREs on drebrin promoter within 3kb proximity of either TSS. One was 85bps upstream of the predominant TSS and a second was 735bps upstream of the minor TSS (574bps downstream of the predominant TSS).

Based on the location of putative binding sites, a 2,013bp fragment encompassing the region from -624 to +1,386bp relative to the predominant TSS was synthesized and cloned into the pGL4.23-luciferase reporter vector (Figure 12A). The promoter constructs pGL4.23-dbn was subsequently anlayzed for promoter activity by co-transfection with human Egr-1 cDNA (Figure 12B) into three different cell lines to test for variability among cell lines as well as species. The cell lines used were: cos-7 fibroblast-like cell line derived from monkey kidney, HEK293 human embryonic kidney cells and 7 DIV rat primary hippocampal neurons. Luciferase promoter assays yielded similar results in all

three cell lines. Activation in promoter activity was observed in response to the addition of Egr-1 (Figure 12C-E). In cos-7 cells, the increase in promoter activity was 28-fold compared to Egr-1+pGL4.23-vector control (Figure 12C). In HEK293 and primary hippocampal neurons, 80- and 6-fold increase in promoter activity were observed, respectively (Figure 12D,E). Comparatively, notable activation was not observed in the absence of Egr-1 for both pGL4.23-dbn and –vector. Therefore, an interaction between Egr-1 and drebrin promoter was recapitulated in different cell lines derived from human, monkey and rat, which suggests Egr-1-drebrin interaction may be conserved among species. Based on these results, Egr-1 evidently associates with drebrin promoter.

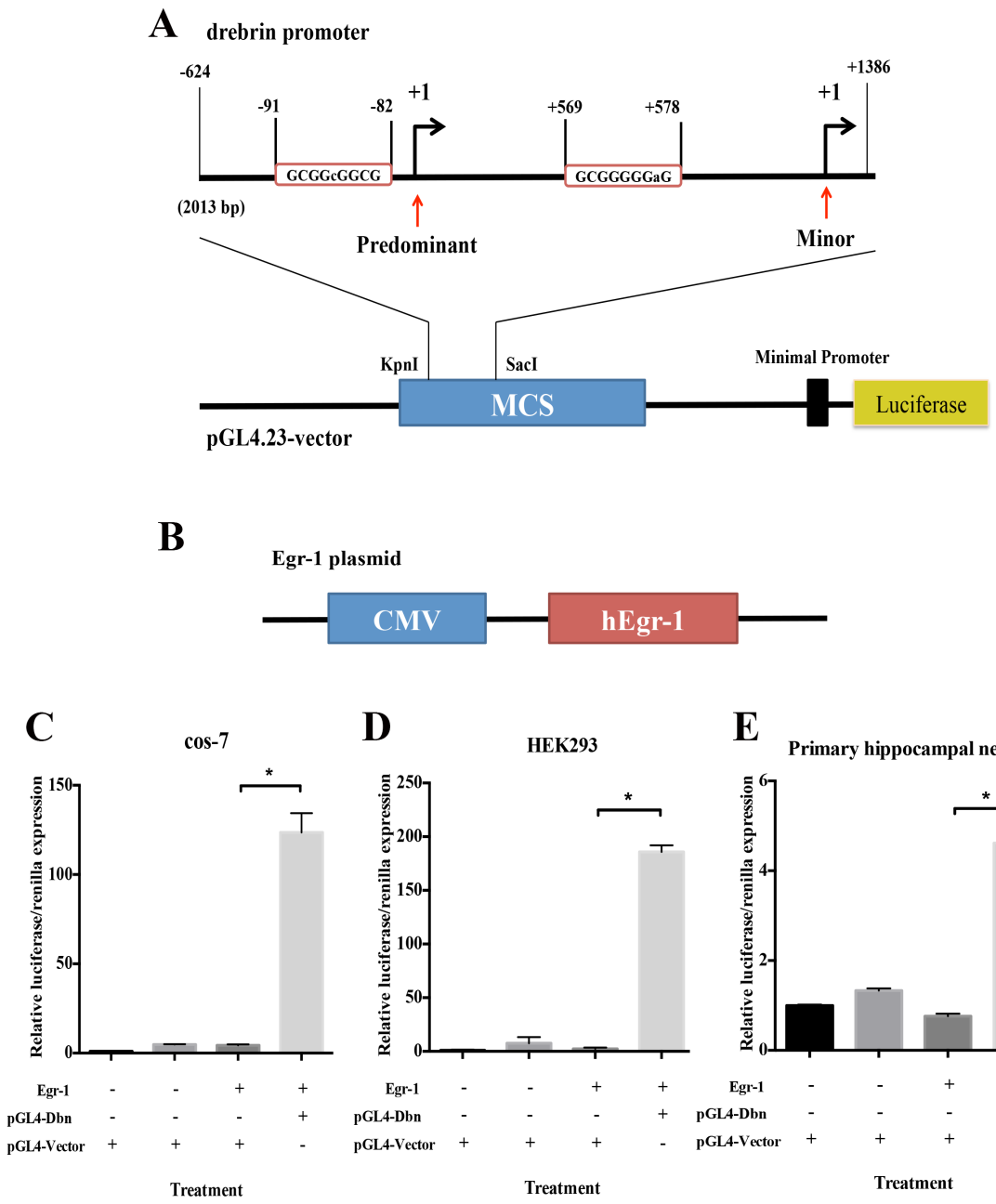
A
drebrin promoter
-624
-91
-82
+1
+569
+578
+1386
+1
GCGGcGGCG
GCGGGGGaG
(2013 bp)
Predominant
Minor
KpnI
SacI
Minimal Promoter
MCS
Luciferase
pGL4.23-vector
B
Egr-1 plasmid
CMV
hEgr-1
C
cos-7
D
HEK293
E
Primary hippocampal neuron
Relative luciferase/renilla expression
Egr-1
pGL4-Dbn
pGL4-Vector
Treatment

Figure 12. *In vitro* promoter assay to study the interaction between Egr-1 and drebrin promoter. pCMV6-XL5-Egr-1 and pGL4.23-drebrin or -vector were co-transfected with Renilla control vector into cos-7, HEK293 and primary hippocampal neurons to study Egr-1 interaction with drebrin promoter. **A**, Schematic illustration of the human Egr-1 plasmid and **B**, 2,013bp fragment of drebrin promoter that was subcloned into pGL4.23 luciferase vector with. Two putative EREs (red box) were identified on drebrin promoter. Luciferase assay shows significant increased activity when Egr-1 was co-transfected with drebrin promoter when compared with the empty luciferase vector in **C**, cos-7, **D**, HEK293, and **E**, primary hippocampal neurons. The luciferase activity of pGL4-vector alone was arbitrarily designated as 1 and was used to calculate relative luciferase activities of other treatments. *$p<0.0001$. Error bars indicate mean ± SEM.

4.1.2 Egr-1-induced activity of drebrin promoter is lost in the absence of EREs

The promoter assay revealed increased Egr-1 expression led to increased signaling from the drebrin promoter. To identify where Egr-1 binds on drebrin promoter, we prepared a series of 5'-deletion constructs (Figure 13A) of the full-length drebrin promoter and tested for promoter-derived luciferase activity in cos-7 cells and rat primary hippocampal neurons in the context of Egr-1 overexpression.

When the deletion construct -347bp (from the predominant TSS) that had both putative EREs intact was co-transfected with Egr-1, no significant difference was observed in luciferase activity when compared with the full length promoter although an increasing trend by 1.25- and 1.10-fold was observed for cos-7 and primary neurons, respectively (Figure 13B,C). However, a deletion of the upstream putative ERE (-2bp construct), significantly reduced luciferase activity by 47% and 57% compared with the full-length and -347bp deletion constructs, respectively. Further deletion of the promoter sequences in between two EREs to position +454bp with the downstream putative ERE preserved led to decrease in promoter activity by 31% and 30% compared with the deletion to -2bp for cos-7 and primary neurons, respectively. This suggests the possibility of non-consensus EREs being present other than the identified putative EREs. In terms of magnitude of change in promoter activity, a greater difference in luciferase activity was observed when a putative ERE was deleted compared with the deletion of promoter region without identified EREs. In fact, when compared to the full-length construct, the +454bp construct showed 16% and 15% from the -2bp deletion for cos-7 and primary neurons respectively. In comparison with pGL4-vector control in both cell lines, a reduction in promoter activity was seen upon removal of both putative EREs by

deleting position +1052bp. In cos-7 cells, promoter activity was reduced by 90% and 96% when compared with +454bp construct and full-length respectively. Similarly, in primary neurons, promoter activity was reduced by 54% and 87% when compared with +454bp and full-length respectively. Therefore an additional 49% and 42% decrease in promoter activity from +454bp compared to full-length was observed for cos-7 and primary neurons respectively.

In cell lines derived from monkey and rat, the luciferase activity displayed similar trends further supporting the hypothesis that the interaction between Egr-1 and drebrin promoter is conserved among different species. In conclusion, loss of putative EREs lead to significant decrease in promoter activity of drebrin. Therefore Egr-1 binds to the two identified EREs located at -85bp and +570bp as well as possibly other non-consensus EREs on drebrin promoter to regulate drebrin expression.

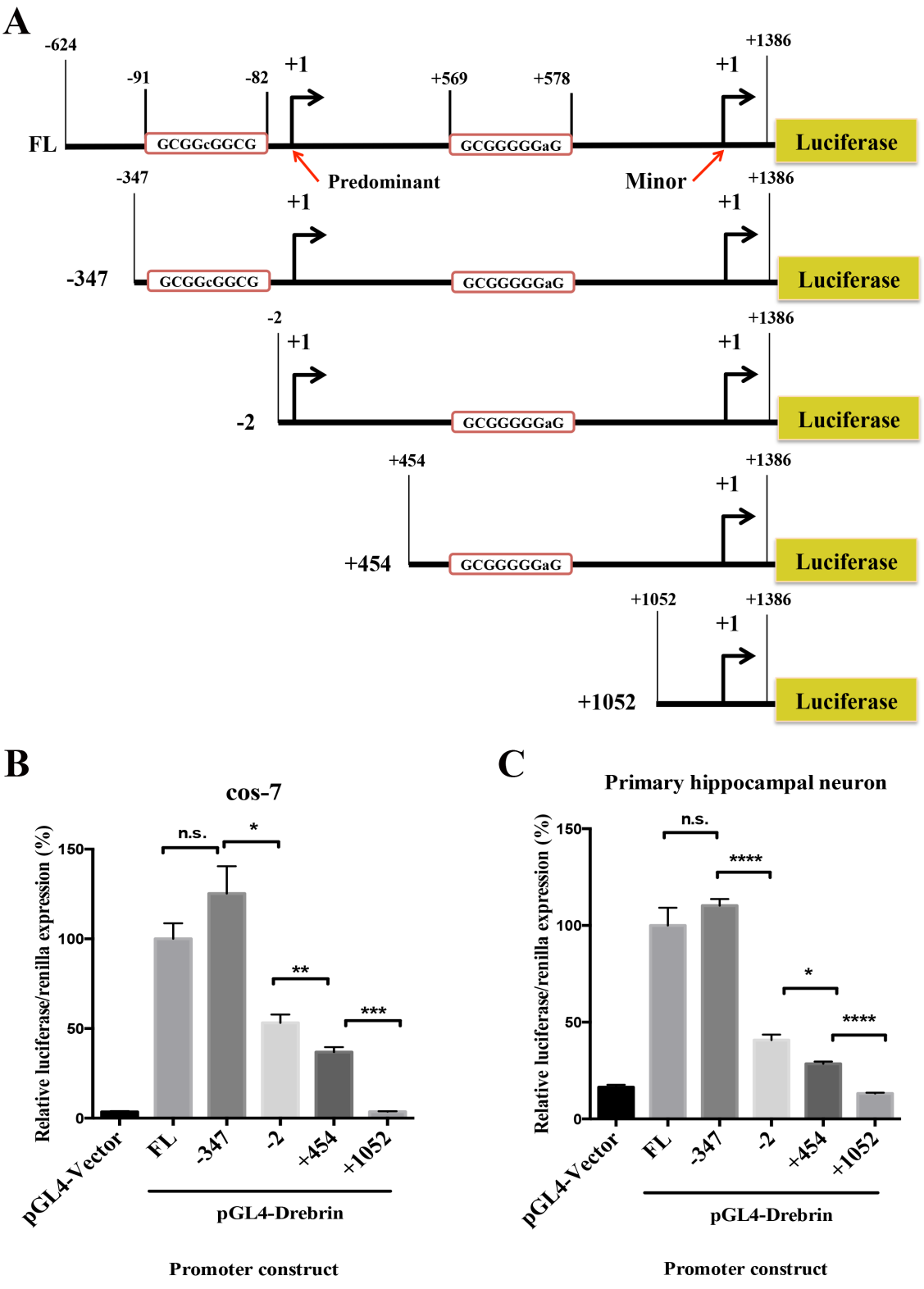
A
-624
-91
-82
+1
+569
+578
+1386
+1
FL
GCGGcGGCG
GCGGGGGaG
Luciferase
Predominant
Minor
-347
-347
+1
+1386
+1
GCGGcGGCG
GCGGGGGaG
Luciferase
-2
-2
+1
+1386
+1
GCGGGGGaG
Luciferase
+454
+454
+1386
+1
GCGGGGGaG
Luciferase
+1052
+1052
+1386
+1
Luciferase
B
cos-7
Relative luciferase/renilla expression (%)
150
100
50
0
n.s.
*
**
***
pGL4-Vector
FL
-347
-2
+454
+1052
pGL4-Drebrin
Promoter construct
C
Primary hippocampal neuron
Relative luciferase/renilla expression (%)
150
100
50
0
n.s.
****
*
****
pGL4-Vector
FL
-347
-2
+454
+1052
pGL4-Drebrin
Promoter construct

Figure 13. Luciferase promoter assay with deletion constructs of human drebrin promoter. **A**, Schematic illustration shows full-length (FL) drebrin promoter from which four deletion constructs were generated. Luciferase promoter assay of deletion constructs was performed in **B**, cos-7 cells and **C**, primary hippocampal neurons. Luciferase activity of pGL4-vector was arbitrarily designated as 1 and was used to calculate relative luciferase activity of the drebrin constructs. *$p<0.01$; **$p<0.05$; ***$p<0.0005$; ****$p<0.0001$. Error bars indicate mean ± SEM.

4.1.3 Egr-1 binds to EREs on drebrin promoter *in vivo*

Luciferase promoter assays have identified multiple EREs on drebrin promoter. In order to verify that the EREs identified *in vitro* using luciferase promoter assay are in fact *in vivo* EREs, we employed chromatin immunoprecipitation (ChIP) assay. Here, we focused on the upstream predominant TSS that expresses the E and A isoforms via alternative splicing. First, the *in silico* analysis performed using the Champion ChIP Transcription Factor Search Portal for the promoter assay (Figure 12A) was substantiated by Whole Genome RVista analysis (Figure 14A). Here, two additional putative EREs were located at -2,430bp and -245bp from TSS in addition to the putative ERE at -85bp. ChIP-seq data available on UCSC Genome Browser identified predicted EREs at regions -2,675bp to -2,740bp and -72bp to -347bp upstream of TSS using K562 leukemia cells, GM12878 B-lymphocytes and H1-hESC human embryonic stem cells (Figure 14C).

For ChIP assay, four sets of primers were designed along drebrin promoter to validate putative EREs (Figure 14B). Three of the four primer sets were designed upstream of TSS at -2,800bp, -1,500bp and -500bp. The remaining primer set was designed for +50bp downstream of TSS. GC-rich drebrin promoter proved difficult in designing precise primer sets at the proposed putative EREs. However, this discrepancy was accounted for the size of sheared DNA being between 500bps to 1,000bps in length. In addition to the four primer sets, a false positive primer set with a 123bp product was designed on same chromosome 5 as an off-target control where no known EREs are found within 500bp proximity.

To define EREs *in vivo* in a cell from neuronal origin, a human neuronal cell line – M-17 neuroblastoma – was used. M-17 cells were prepared for ChIP assay by being

cross-linked and immunoprecipitated with either rabbit anti-Egr-1 antibody or normal rabbit IgG for ChIP assay. qRT-PCR of the DNA immunoprecipitated with Egr-1 showed two regions with greater than 4-fold enrichment of Egr-1 compared with the off-target control: -2,800bp (4.2-fold) and -500bp (4.9-fold) (Figure 14D). Therefore Egr-1 most likely binds to the predicted EREs as these two regions are within 500bp proximity of the predicted EREs. Amongst two putative EREs close to the TSS (Figure 14A) at -245bps and -85bps, the ERE at -245bps is more likely to be the dominant *in vivo* ERE, because of the fold enrichment detected by the two primer sets designed around these two binding sites (Figure 14B). Greater enrichment was observed for the -500bp primer set than the +50bp, which supports the -245bp ERE as the Egr-1 binding site. However, this does not exclude the ERE at -85bps as Egr-1 was shown to interact with the ERE at -85bps using luciferase promoter assay (Figure 13). The other two primer sets also had significant enrichment of Egr-1 where 1.8- and 2.3-fold increase was observed for position -1,500bp and +50bp respectively. These results suggest that Egr-1 has multiple binding sites on drebrin promoter in the brain, predominantly at – 2,430bp and -245bp, where Egr-1 bind and may regulate transcription of drebrin.

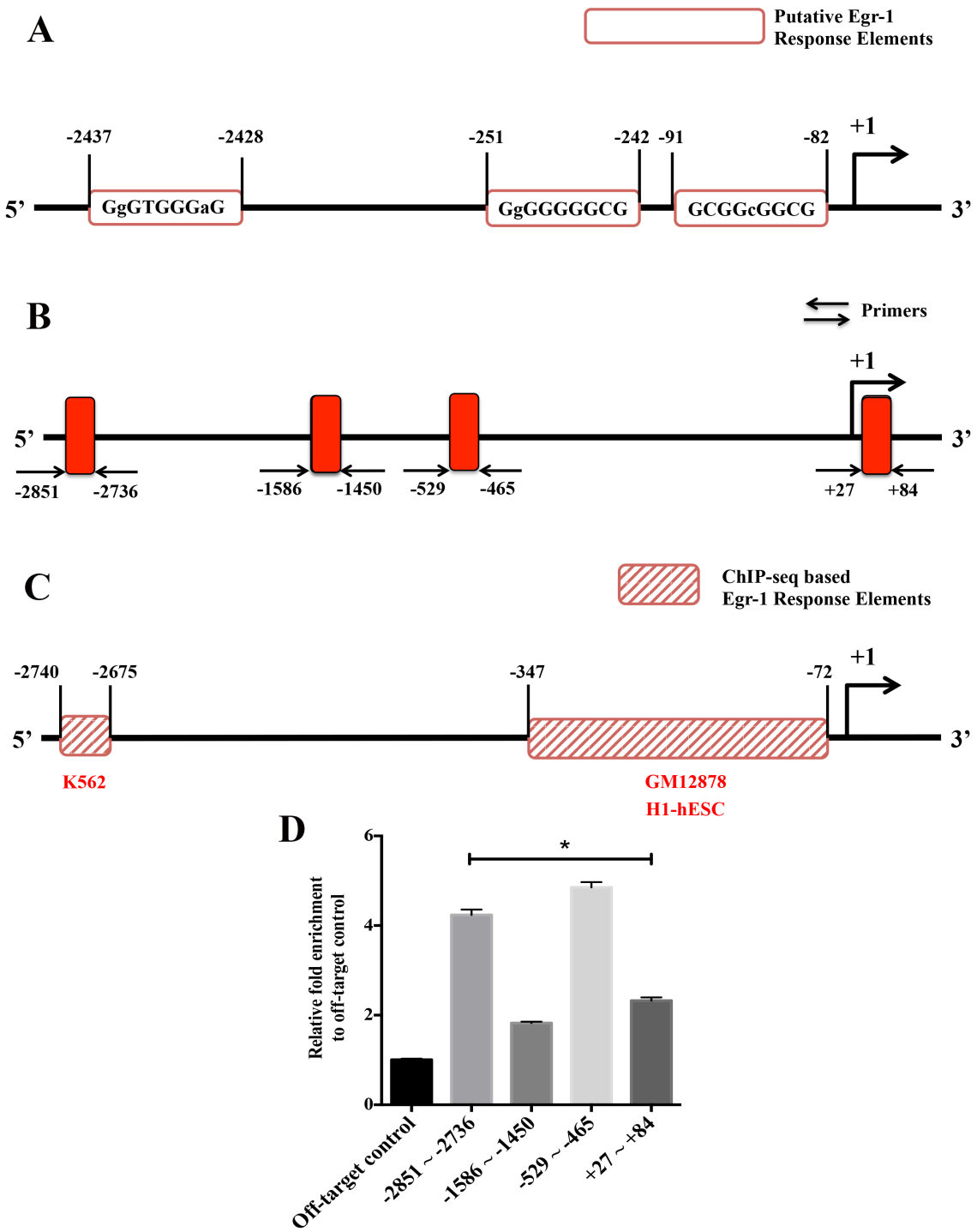
A
Putative Egr-1
Response Elements
-2437
-2428
-251
-242
-91
-82
+1
5'
GgGTGGGaG
GgGGGGGCG
GCGGcGGCG
3'
B
Primers
+1
5'
3'
-2851
-2736
-1586
-1450
-529
-465
+27
+84
C
ChIP-seq based
Egr-1 Response Elements
-2740
-2675
-347
-72
+1
5'
3'
K562
GM12878
H1-hESC
D
Relative fold enrichment
to off-target control
6
4
2
0
*
Off-target control
-2851 ~ -2736
-1586 ~ -1450
-529 ~ -465
+27 ~ +84

Figure 14. Identification of EREs on drebrin promoter *in vivo*. **A**, *In silico* analysis of EREs on drebrin promoter was performed using Whole Genome RVista. Three putative EREs were found within 3kb from the predominant TSS. Consensus Egr-1 binding sequences that are conserved are denoted in capital letters. **B**, ChIP-Seq data available on UCSC genome browser identified two EREs on drebrin promoter using non-neuronal cell lines K562 (leukemia cells), GM12878 (B-lymphocytes) and H1-hESC (human embryonic stem cells. **C**, Primer sets were designed along the 3kb span of drebrin promoter in close proximity to the putative EREs. **D**, qRT-PCR result following ChIP assay identified two regions, -2,851 to -2,736 and -529 to -465, where the mRNA fold enrichment exceeded 4-fold compared to the off-target control confirming the putative EREs as well as those provided by UCSC genome browser. *$p<0.0001$. Error bars indicate mean ± SEM.

4.2 Egr-1 negatively regulates drebrin *in vitro* and *in vivo*

4.2.1 Drebrin is lost in response to Egr-1 upregulation in primary hippocampal neurons

The luciferase promoter and ChIP data strongly suggest that Egr-1 binds to EREs on drebrin promoter leading to regulation of drebrin expression. To test whether Egr-1 alters drebrin expression in neurons, we used lentiviral transduction of the virus encoding Egr-1 *in vitro* in P-0 rat primary hippocampal neurons (Figure 15). The lentivirus allows long-term transgene expression in non-dividing cells such as neurons with minimal toxicity. Here, the human Egr-1 cDNA sequence was cloned with a myc peptide at the C-terminus. This construct was inserted into a lentiviral vector that simultaneously also expressed ZsGreen1 as the indicator of transduction efficiency (refer to Figure 10).

Primary hippocampal neurons were prepared and transduced with either Ln-Egr-1 or Ln-Vector on the day of plating and were allowed to upregulate Egr-1. After 9 DIV, total RNA and protein lysates were collected in triplicate from primary neurons for qRT-PCR and immunoblotting, respectively. Significant upregulation of Egr-1 was confirmed at both mRNA and protein level (Figure 15A-C). For immunoblotting, a 19.6-fold increase in Egr-1 protein was confirmed by probing for either the myc-tag or Egr-1 where the inserted human Egr-1 protein migrated at approximately 87kDa (Figure 15B,C). Long-term expression of ZsGreen1 was visually confirmed in hippocampal neurons at 18 days post transduction where the transduction efficiency remained at 40 to 50% (Figure 15D). The expression of ZsGreen1 in lentiviral vectors allowed visual confirmation of primary neurons transduced to upregulate Egr-1 by green fluorescence under a confocal

microscope (Figure 15E). Therefore, hippocampal neurons are successfully transduced with Ln-Egr-1 to upregulate Egr-1 expression.

We found downregulation of drebrin mRNA and protein level in response to Egr-1 upregulation in hippocampal neurons (Figure 15F-H). Drebrin mRNA, according qRT-PCR, was significantly reduced by 77% while immunoblotting showed significant 48% reduction in protein level. These data indicate that Egr-1 transcriptionally downregulate drebrin expression *in vitro*.

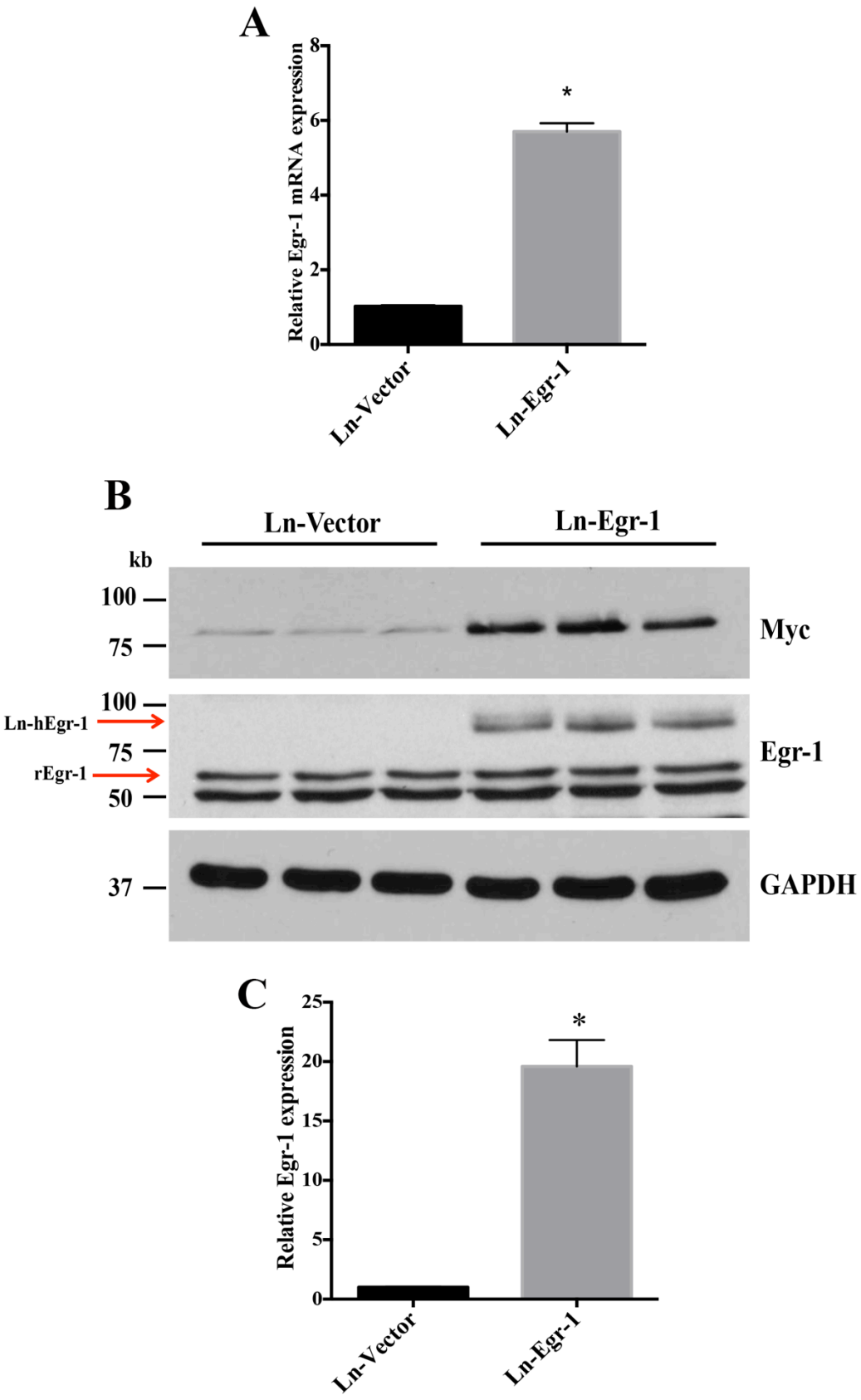
A
Relative Egr-1 mRNA expression
8
6
4
2
0
*
Ln-Vector
Ln-Egr-1
B
Ln-Vector
Ln-Egr-1
kb
100
75
Myc
100
Ln-hEgr-1
75
rEgr-1
50
Egr-1
37
GAPDH
C
Relative Egr-1 expression
25
20
15
10
5
0
*
Ln-Vector
Ln-Egr-1

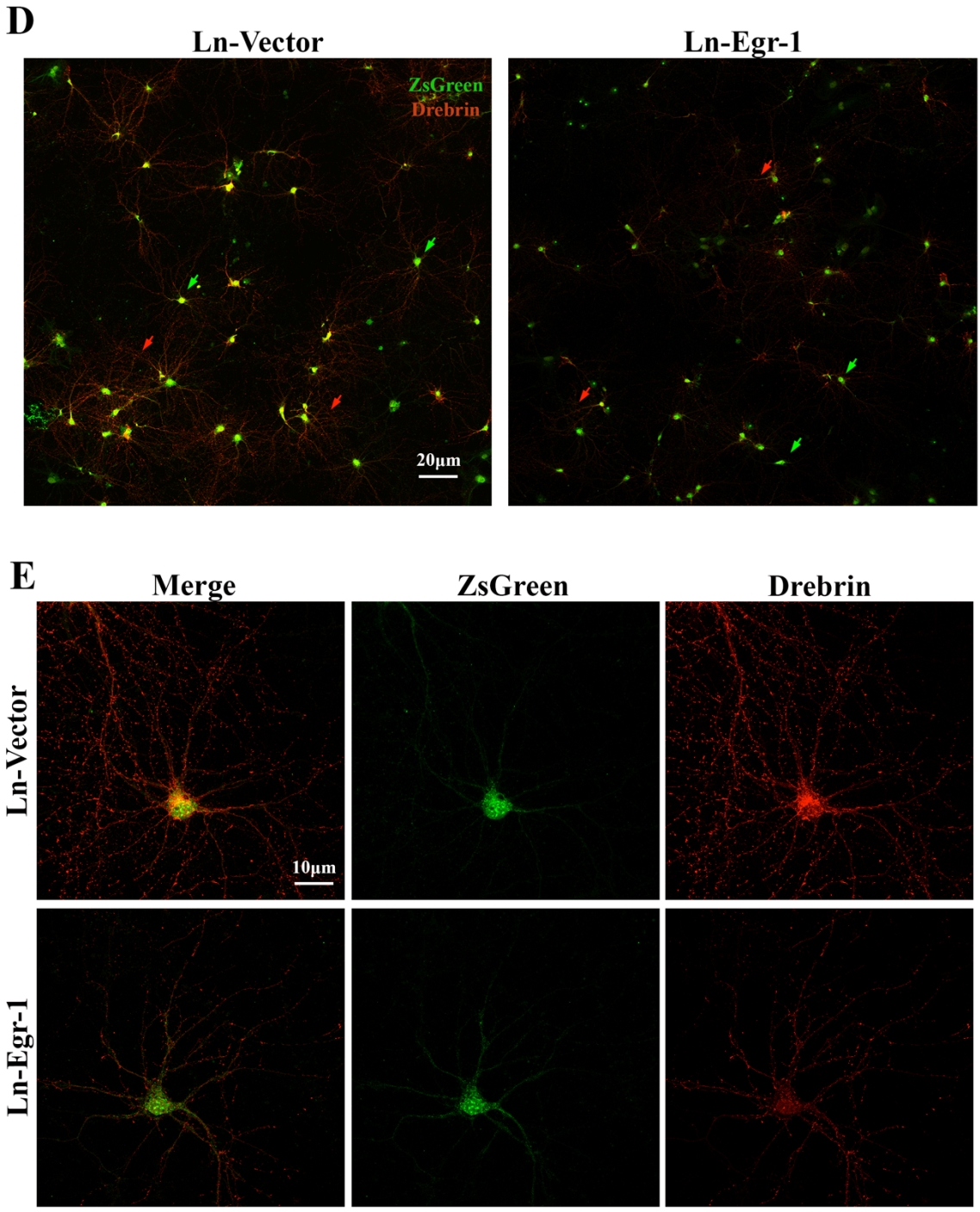
D
Ln-Vector
Ln-Egr-1
ZsGreen
Drebrin
20μm
E
Merge
ZsGreen
Drebrin
Ln-Vector
Ln-Egr-1
10μm

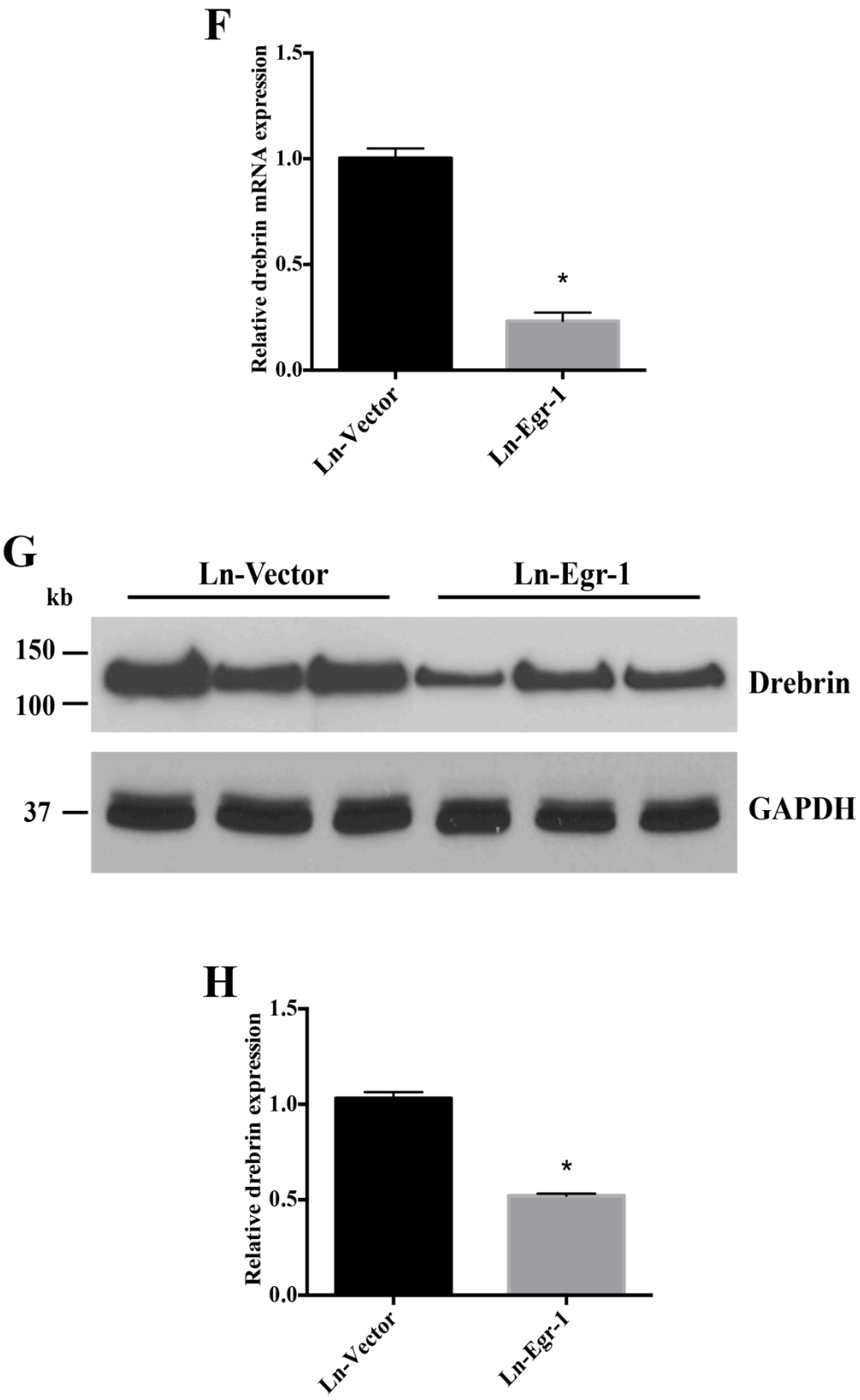
F
Relative drebrin mRNA expression
1.5
1.0
0.5
0.0
*
Ln-Vector
Ln-Egr-1
G
kb
Ln-Vector
Ln-Egr-1
150
100
Drebrin
37
GAPDH
H
Relative drebrin expression
1.5
1.0
0.5
0.0
*
Ln-Vector
Ln-Egr-1

Figure 15. Egr-1 upregulation and changes in drebrin level *in vitro*. Egr-1 was upregulated in primary hippocampal neurons at with Ln-Egr-1 and Ln-Vector. The primary neurons were transduced on the day of plating and Egr-1 upregulation was observed from 24hr after transduction to the end of the culture. For comparison between Ln-Egr-1 and Ln-Vector, the values for Ln-Vector were arbitrarily designed as 1. **A**, qRT-PCR analysis of Egr-1 mRNA level in transduced neurons. **B**, Immunoblotting for Egr-1 and myc proteins in transduced neurons. **C**, Densitometry analysis of the immunoblot for Egr-1 protein level. **D**, Transduction efficiency of 40-50% was determined under 10x objective. **E**, Transduced neurons expressed ZsGreen (green) and were immunolabelled for drebrin (red) at 18 DIV. **F**, qRT-PCR analysis of drebrin mRNA level in transduced neurons. **G**, Immunoblotting for drebrin protein in transduced neurons. H, Densitometry analysis of the immunoblot for drebrin protein level. *$p<0.0001$. Error bars indicate mean ± SEM.

4.2.2 Drebrin is lost in response to Egr-1 upregulation in Egr-1 Tg mouse

To further test the hypothesis that Egr-1 upregulation leads to loss of drebrin, an *in vivo* inducible model of Egr-1 was generated using the tet-off system (Figure 16A). In this model, here called Egr-1 Tg mice, the expression of Egr-1 is controlled spatiotemporally. Here, the use of Ca^{2+}/calmodulin-dependent protein kinase IIα (CamKIIα) promoter [253,254] directs Egr-1 expression to the excitatory glutamatergic neurons in the forebrain that includes hippocampus, prefrontal cortex and striatum allowing spatial control. Furthermore, Egr-1 expression can be temporally controlled by withdrawing/adding doxycycline (dox) from/to the diet.

To test whether Egr-1 upregulation was specific to the forebrain of Egr-1 Tg mice and could be controlled with doxycycline, 2-mo Egr-1 Tg mice were divided into two groups (n=3/genotype): dox-free diet group and dox diet group. Dox was removed from the diet of 2-mo mice for two weeks allowing Egr-1 upregulation. Age-matched littermate controls that carried either the tTA transgene or the Egr-1 transgene, but not both, were given dox-free diet for the same duration. At the end of two weeks, the mice were euthanized and Egr-1 protein level was measured (Figure 16B). We found that Egr-1 upregulation was specific to Egr-1 Tg mouse that received dox-free diet and was localized to hippocampus and prefrontal cortex that are part of the forebrain and not in cerebellum that is a part of the hindbrain. These data, therefore, confirmed the validity of our model.

To test our hypothesis that upregulation of Egr-1 leads to reduction in drebrin expression, we induced Egr-1 expression in 16-mo aged Egr-1 Tg mice (n=3) for 3 months by removing dox from their diet (Figure 17). Upregulation of Egr-1 in AD is

observed in aged individuals and corresponds with the progression of AD [28]. Therefore, we allowed Egr-1 Tg mice to develop normally until they reached an age comparable to the elderly in human counterpart. Furthermore, Egr-1 induction was directed to the forebrain, which includes hippocampus and prefrontal cortex that are severely affected in AD [101,255-257]. Hence, after 3 months, brain lysates from hippocampus, prefrontal cortex and cerebellum were prepared and changes in Egr-1 and drebrin level were quantified. Cerebellum represented a control brain region where Egr-1 upregulation was not observed. Significant upregulation of Egr-1 mRNA and protein was confirmed in hippocampus and prefrontal cortex of the aged Egr-1 Tg mouse (Figure 17A-D). We verified significant 36- and 22-fold increase of Egr-1 mRNA in the hippocampus and prefrontal cortex respectively but not in cerebellum. This increase in Egr-1 mRNA translated into significant increase in protein level in hippocampus and prefrontal cortex using immunoblotting by probing for the human Egr-1 or the myc tag attached to the C-terminus (Figure 17B,C).

We found Egr-1 induction in aged Egr-1 Tg mouse led to significant reductions in drebrin mRNA and protein level in the forebrain, but not in cerebellum (Figure 17B-F). Drebrin mRNA was reduced by 52% and 25% in the hippocampus and prefrontal cortex respectively, but only the reduction in the hippocampus was statistically significant (Figure 17E). We also found drebrin protein was significantly reduced by 16% and 25% in the hippocampus and prefrontal cortex respectively (Figure 17F). Therefore, these results support the hypothesis that Egr-1 upregulation leads to loss of drebrin *in vivo*.

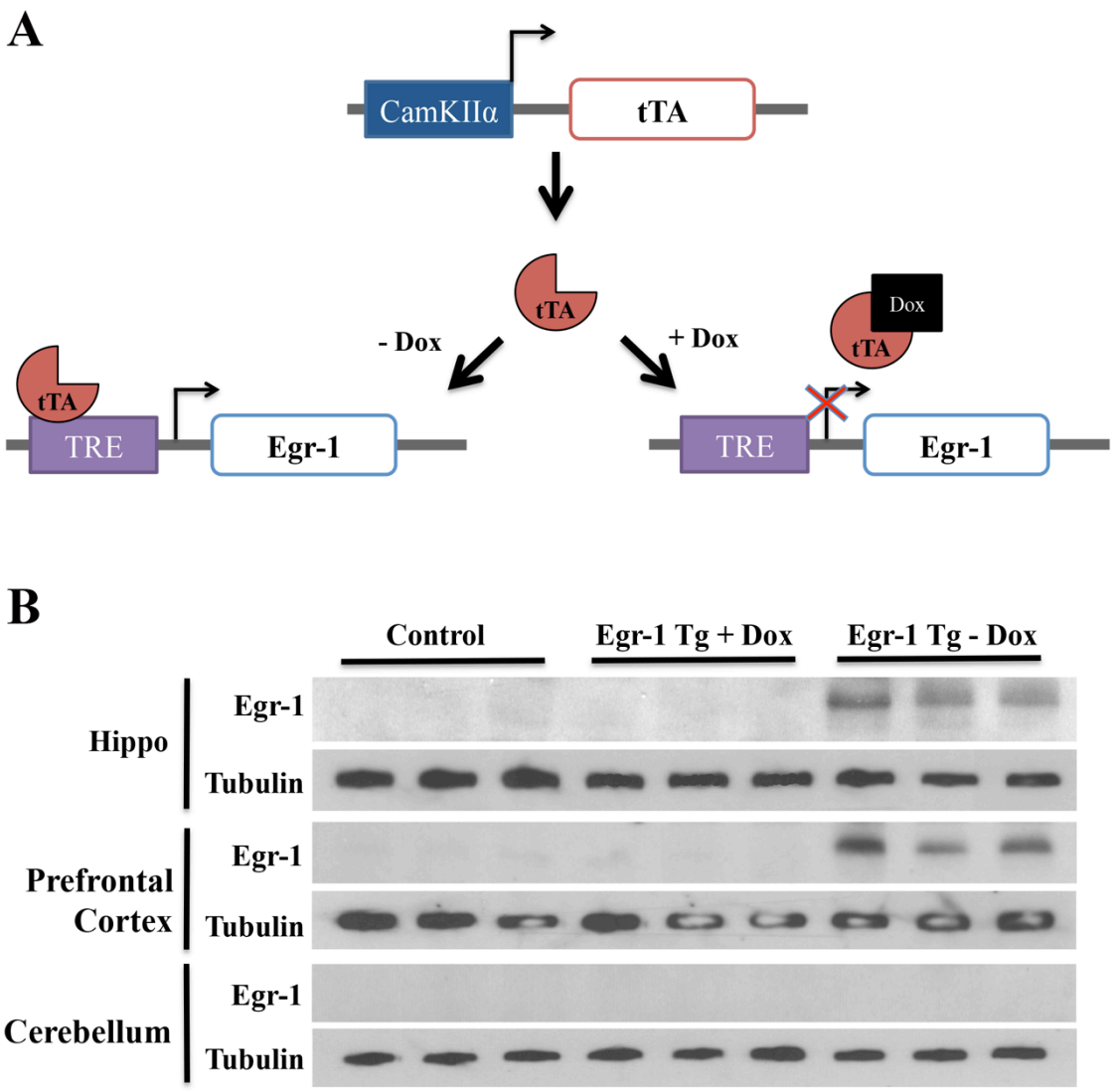

Figure 16. Generation of Egr-1 Tg mouse. **A**, Schematic diagram of tet-off system shows how spatiotemporal regulation of drebrin is achieved. Egr-1 Tg mouse express both the tTA and Egr-1 transgenes. CamKIIα-driven expression of tTA localizes to the forebrain where in the absence of dox, binds and drives the upregulation of Egr-1. **B**, Egr-1 upregulation was specific to the hippocampus and prefrontal cortex of Egr-1 Tg mice that were fed dox-free diet. Egr-1 upregulation was not observed in Egr-1 Tg mouse fed with dox-free diet and in littermate controls.

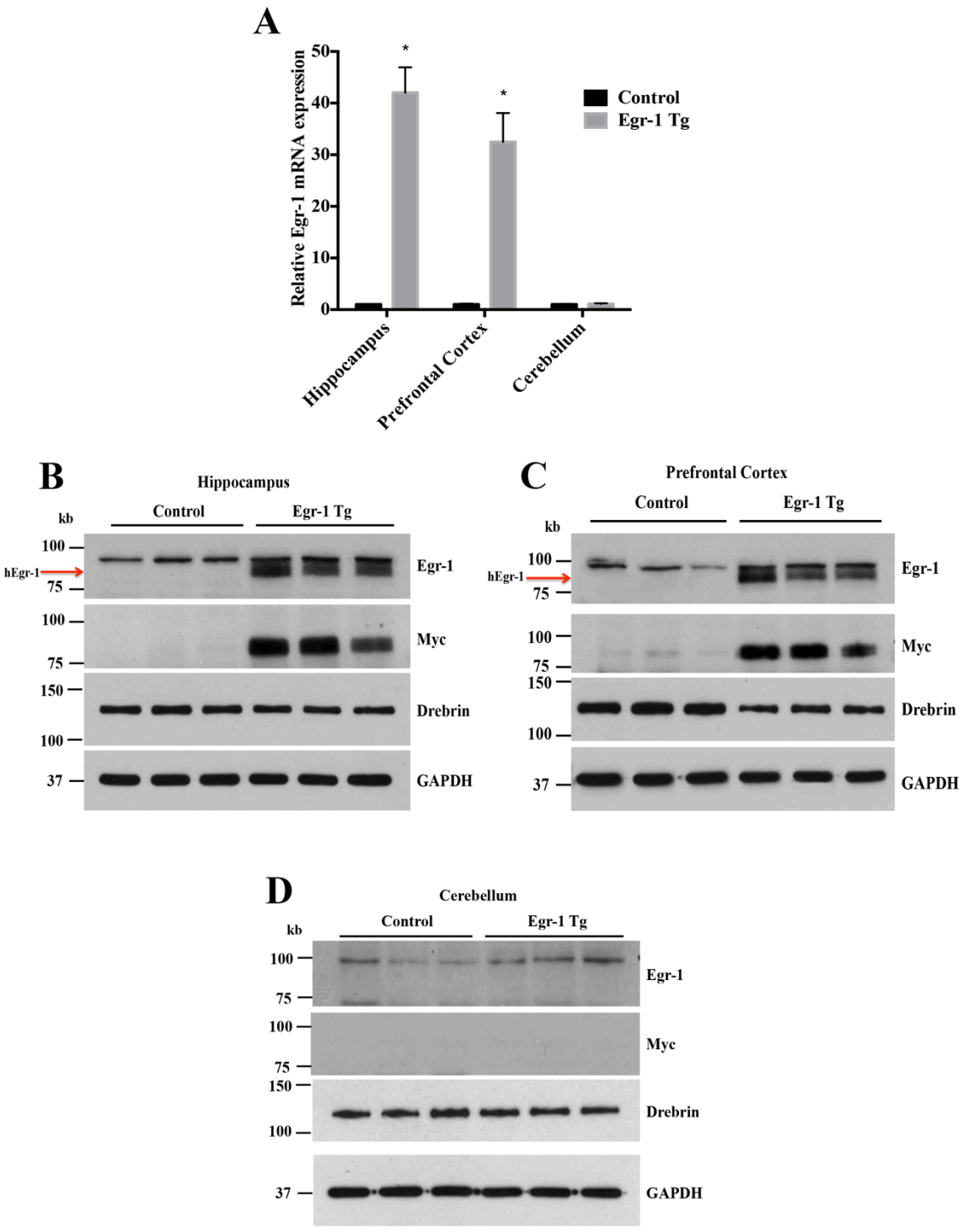
A
Relative Egr-1 mRNA expression
50
40
30
20
10
0
*
*
Control
Egr-1 Tg
Hippocampus
Prefrontal Cortex
Cerebellum
B
Hippocampus
Control
Egr-1 Tg
kb
100
hEgr-1
75
Egr-1
100
75
Myc
150
100
Drebrin
37
GAPDH
C
Prefrontal Cortex
Control
Egr-1 Tg
kb
100
hEgr-1
75
Egr-1
100
75
Myc
150
100
Drebrin
37
GAPDH
D
Cerebellum
Control
Egr-1 Tg
kb
100
75
Egr-1
100
75
Myc
150
100
Drebrin
37
GAPDH

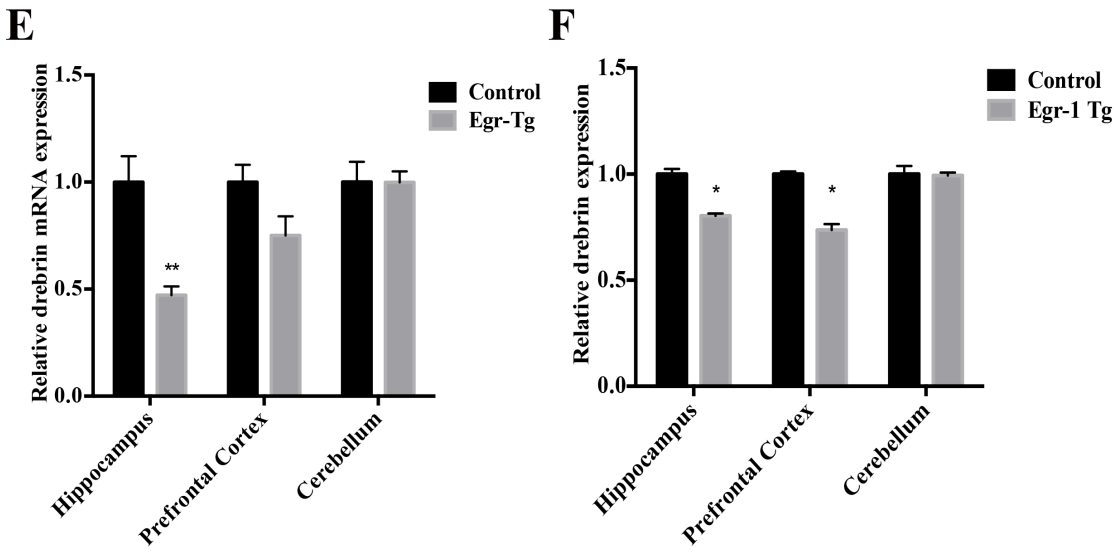

Figure 17. Changes in drebrin level in Egr-1 Tg mouse upon Egr-1 upregulation. In order to study the effect of Egr-1 upregulation on drebrin, 16-mo Egr-1 Tg mouse was allowed to upregulate Egr-1 in the forebrain for 3 months (n=3/genotype). For comparison, the control mRNA and protein levels were arbitrarily set as 1. Egr-1 upregulation was confirmed by measuring **A**, Egr-1 mRNA level. Immunoblotting was used to confirm Egr-1 induction by probing for the myc-tag and Egr-1 protein, and also was used to quantify drebrin protein levels in the **B**, hippocampus, **C**, prefrontal cortex, and **D**, cerebellum. **E**, mRNA levels of drebrin in Egr-1 Tg mice compared with the control, **F**, densitometry analysis of the immunoblots for drebrin. *$p<0.0001$, **$p<0.0005$. Error bars indicate mean ± SEM.

4.2.3 Drebrin level is increased in the absence of Egr-1 *in vivo*

Our data consistently show that Egr-1 upregulation leads to downregulation of drebrin *in vitro* and *in vivo*. To corroborate this inverse relationship between Egr-1 and drebrin, changes in drebrin level were examined in response to Egr-1 loss-of-function using 12-mo Egr-1 -/- mouse. Here, 12-mo Egr-1 -/-, Egr-1 +/- and Egr-1 +/+ control mouse were euthanized and whole brain homogenate was prepared. Immunoblot analysis for drebrin showed increase in drebrin protein level for Egr-1 -/- mouse compared to Egr-1 +/- and +/+ mouse (Figure 18A). Densitometry analysis revealed an incremental dose-dependent increase in drebrin where Egr-1 -/- and Egr-1 +/- expressed 1.9- and 1.4-fold greater levels of drebrin protein when compared with the Egr-1 +/+ mouse (Figure 18B). These data suggests Egr-1 loss-of-function leads to dose-dependent increase in drebrin protein level.

Next, we examined brain-specific regional changes in drebrin expression in 12-mo Egr-1 -/- and +/+ mice. Similar to Egr-1 Tg mice, drebrin expression was quantified in two regions, hippocampus and prefrontal cortex, that is known to be severely affected in AD. Hippocampus and prefrontal cortex are predominant regions affected by AD pathology [101,255-257]. Here, cerebellum was used as a negative control because physiological level of Egr-1 remains low in the cerebellum [211,258]. qRT-PCR and immunoblotting revealed significant increase in drebrin mRNA and protein level in Egr-1 -/- mouse compared with Egr-1 +/+ mouse in the hippocampus and prefrontal cortex, but not in cerebellum (Figure 18C). At the mRNA level, Egr-1 -/- mouse had significant 2.2- and 3.7-fold increased level of drebrin compared with Egr-1 +/+ mouse in the hippocampus and prefrontal cortex, respectively. Similarly, the protein level was

significant increased by 1.7- and 1.6-fold in the hippocampus and prefrontal cortex respectively in the Egr-1 -/- mouse (Figure 18D,E). These data indicate that in the absence of Egr-1, there is an increased level of drebrin mRNA and protein, further supporting the idea that Egr-1 is a negative regulator of drebrin expression.

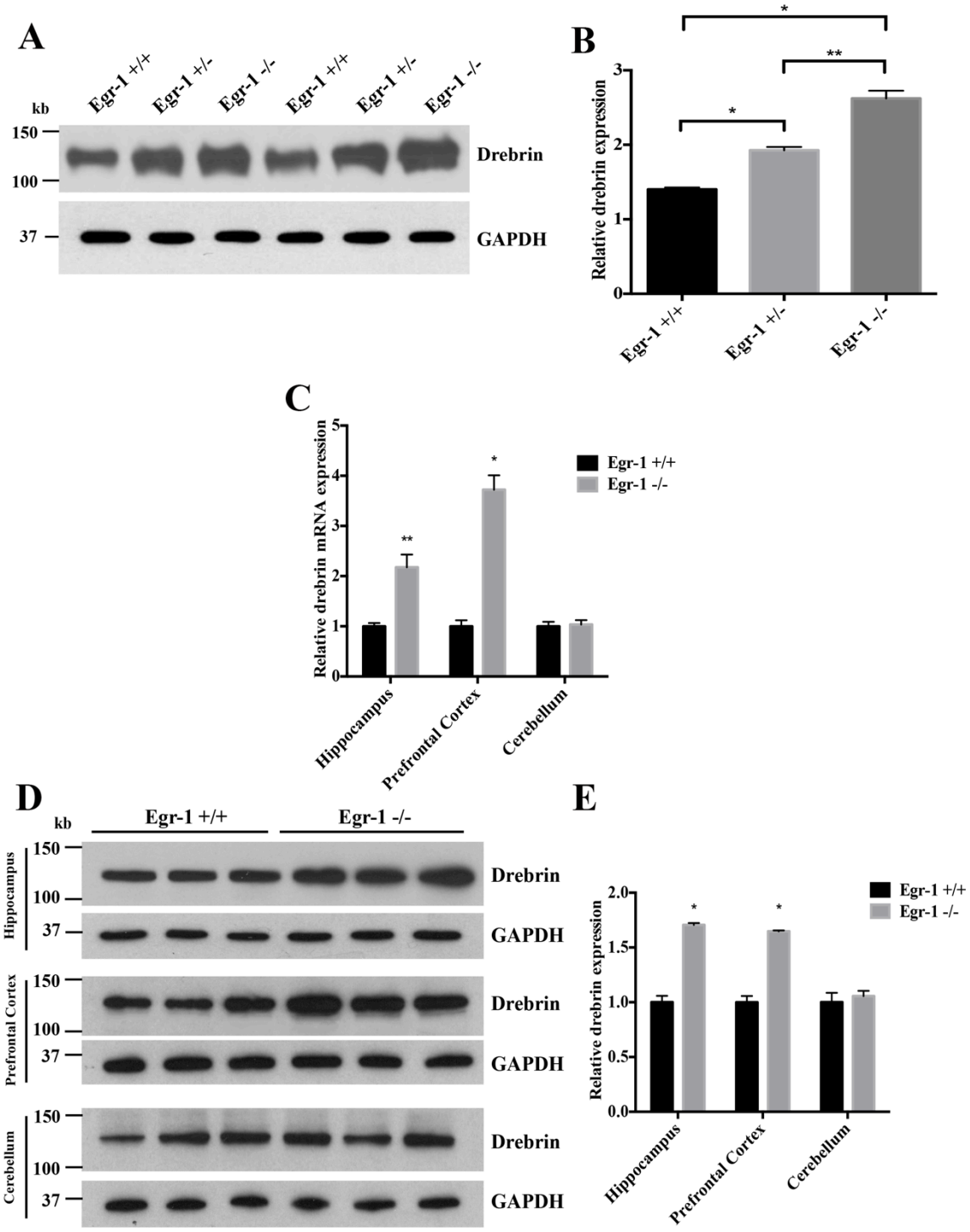
A
kb
Egr-1 +/+
Egr-1 +/-
Egr-1 -/-
Egr-1 +/+
Egr-1 +/-
Egr-1 -/-
150
100
37
Drebrin
GAPDH
B
Relative drebrin expression
0
1
2
3
*
**
*
Egr-1 +/+
Egr-1 +/-
Egr-1 -/-
C
Relative drebrin mRNA expression
0
1
2
3
4
5
**
*
Egr-1 +/+
Egr-1 -/-
Hippocampus
Prefrontal Cortex
Cerebellum
D
kb
Egr-1 +/+
Egr-1 -/-
Hippocampus
Prefrontal Cortex
Cerebellum
150
100
37
Drebrin
GAPDH
E
Relative drebrin expression
0.0
0.5
1.0
1.5
2.0
*
*
Egr-1 +/+
Egr-1 -/-
Hippocampus
Prefrontal Cortex
Cerebellum

Figure 18. Drebrin expression in Egr-1 -/- mouse. **A**, Total drebrin (both E and A isoforms) protein level was measured in 12-mo Egr-1 -/-, +/- and +/+ mouse (n=3/genotype) using immunoblotting. For comparison, the Egr-1 +/+ mRNA and protein levels were arbitrarily set as 1. **B**, Densitometry analysis of the drebrin immunoblot. Based on this result, drebrin expression was in the hippocampus, prefrontal cortex and cerebellum of 12-mo Egr-1 -/- and +/+ mouse (n=3/genotype). **C**, mRNA level of total drebrin (both E and A isoforms) was measured using qRT-PCR. **D**, Immunoblots and **E**, densitometry analysis for drebrin in in the hippocampus, prefrontal cortex and cerebellum. *$p<0.0001$; **$p<0.0005$. Error bars indicate mean ± SEM.

4.3 Loss of drebrin in response to Egr-1 upregulation correlates with loss of dendritic spines

4.3.1 Drebrin is lost in 3xTg-AD mouse model

In AD, drebrin is reduced which correlate with loss of dendritic spines and thus with synaptic pathology [12]. Drebrin loss is also apparent in AD mouse models that display dendritic spine loss [259]. Here, for the first time, we found reduced drebrin in 3xTg-AD mouse model (Figure 19). 3xTg-AD mouse displays two pathological hallmarks of AD, senile plaques and neurofibrillary tangles, throughout life [260]. 3xTg-AD mouse also show loss of dendritic spines at 13-mo [260].

To test whether loss of dendritic spines is associated with reduction in drebrin level, we quantified drebrin protein in the whole brain homogenate from 15-mo 3xTg-AD mice (n=3) using immunoblotting (Figure 19A). Densitometry of the immunoblot showed 32% reduction in drebrin protein level in 15-mo 3xTg-AD compared with control mice (Figure 19B). We then tested the reduction of drebrin with respect to age and brain region by quantifying drebrin protein level in hippocampus, prefrontal cortex and cerebellum for 3-, 9- and 15-mo 3xTg-AD mouse (Figure 19C). In the hippocampus, 15-mo 3xTg-AD mice had significant reduction of drebrin protein by 76% and 69% compared to 3-mo and 9-mo 3xTg-AD mouse respectively (Figure 19D). 3xTg-AD mice also had significant reductions in drebrin protein in the prefrontal cortex by 35% and 30% compared to 3-mo and 9-mo 3xTg-AD mouse respectively. However, drebrin protein levels in the cerebellum remained comparable. These data indicate that drebrin is significantly reduced in the forebrain of old 3xTg-AD that is known to display loss of dendritic spines.

To test whether similar reduction occurs in the presynaptic terminal and that the loss of drebrin correlates with synapse dysfunction, we quantified synaptophysin protein level in hippocampus, prefrontal cortex and cerebellum preparations from 3-, 9- and 15-mo 3xTg-AD mouse (Figure 19E). In the hippocampus of 15-mo 3xTg-AD mouse, significant reductions of 33% and 26% in synaptophysin level was observed compared with 3-mo and 9-mo 3xTg-AD mice, respectively (Figure 19F). In the prefrontal cortex, a decreasing trend in synaptophysin level was observed comparing expression of 3-mo and 9-mo 3xTg-AD mouse, but the reduction was not statistically significant (P=0.26). The synaptophysin protein in the cerebellum remained comparable. Therefore, presynaptic terminals appear to undergo degeneration similar to the postsynaptic dendritic spines. We also measured changes for Egr-1 protein level in 3-, 9- and 15-mo 3xTg-AD mice. In contrast to the increase observed in AD patients, Egr-1 level in 3xTg-AD mice were variable (data not shown). These data indicate that drebrin reduction correlate with synapse dysfunction. Also, the degree of reduction of drebrin protein suggests that drebrin is comparatively more sensitive to loss during synaptic pathology than synaptophysin.

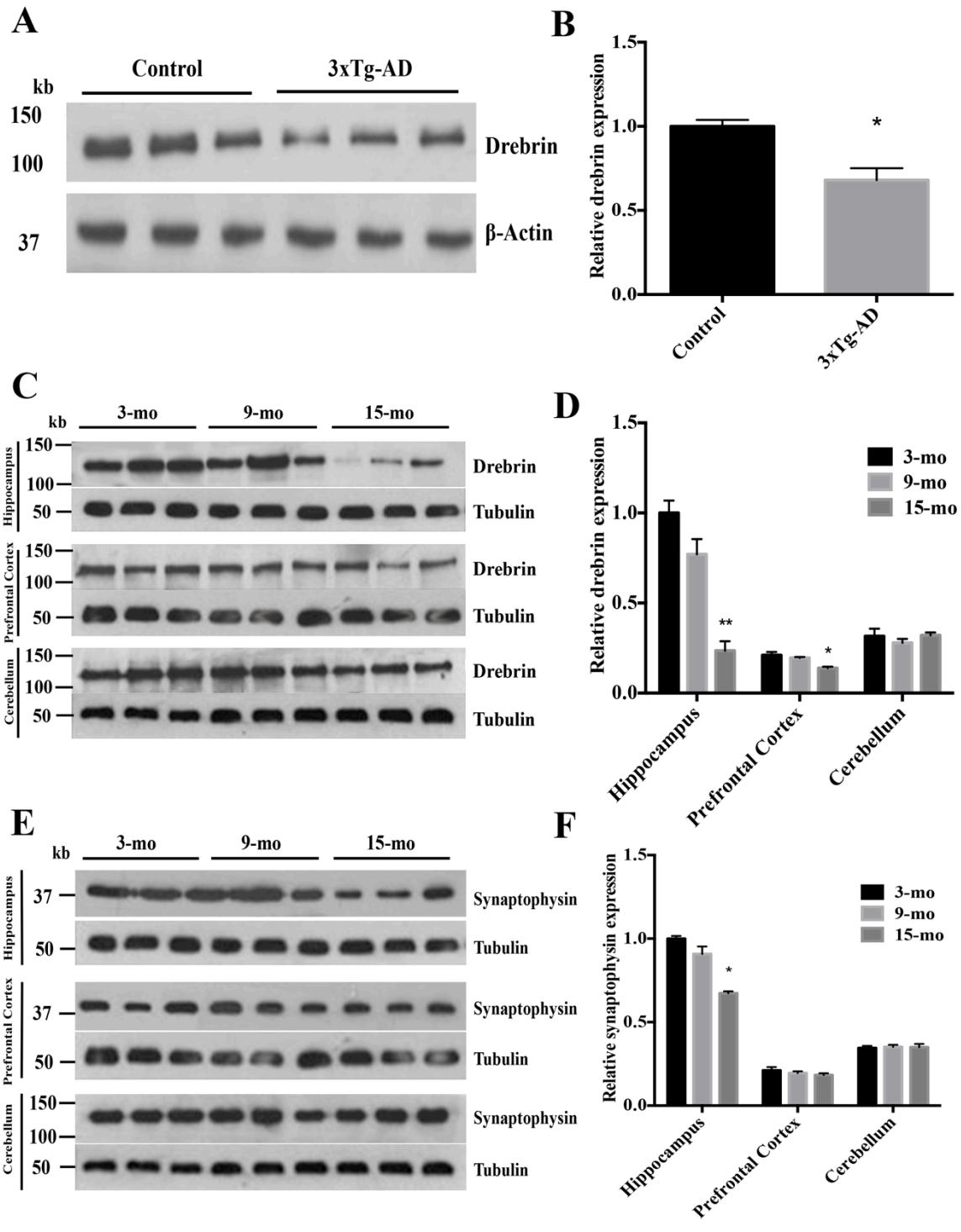
A
Control
3xTg-AD
kb
150
100
37
Drebrin
β-Actin
B
Relative drebrin expression
1.5
1.0
0.5
0.0
*
Control
3xTg-AD
C
3-mo
9-mo
15-mo
kb
Hippocampus
Prefrontal Cortex
Cerebellum
150
100
50
Drebrin
Tubulin
D
Relative drebrin expression
3-mo
9-mo
15-mo
**
*
Hippocampus
Prefrontal Cortex
Cerebellum
E
3-mo
9-mo
15-mo
kb
37
50
Synaptophysin
Tubulin
F
Relative synaptophysin expression
3-mo
9-mo
15-mo
*
Hippocampus
Prefrontal Cortex
Cerebellum

Figure 19. Loss of drebrin and synaptophysin in 15-mo 3xTg-AD mouse (n=3/genotype). For comparison, protein levels of the age-matched control mouse and 3-mo hippocampus data from 3xTg-AD mouse were arbitrarily set as 1 for their respective experiments. **A**, Immunoblotting of the whole brain homogenate from 15-mo 3xTg-AD mouse and the age-matched control to measure the level of drebrin. **B**, Densitometry analysis of the drebrin immunoblot. **C**, Immunoblotting of hippocampus, prefrontal cortex and cerebellum for drebrin. **D**, Densitometry analysis of the immunoblots from hippocampus, prefrontal cortex and cerebellum for drebrin. **E**, Immunoblotting of the hippocampus, prefrontal cortex and cerebellum for synaptophysin. **F**, Densitometry analysis of the immunoblots from hippocampus, prefrontal cortex and cerebellum for synaptophysin.*$p<0.05$; **$p<0.005$. Error bars indicate mean ± SEM.

4.3.2 Egr-1 upregulation results in loss of dendritic spines *in vitro*

In AD, drebrin is lost while Egr-1 TF is upregulated [12,28]. The loss of drebrin in AD and related disorders was found to be associated with loss of dendritic spines in patients and animal models [10,12,259] including 3xTg-AD mouse that we have demonstrated in the previous section (Figure 19). These data, together with our finding Egr-1 upregulation leads to loss of drebrin, led to the hypothesis that upregulation of Egr-1 would also lead to loss of dendritic spines by downregulating drebrin expression.

To test whether downregulation of drebrin is correlated with changes in dendritic spines, we quantified dendritic protrusion density and characterized the protrusion morphology in Egr-1 upregulated hippocampal neurons (Figure 20). Rat primary hippocampal neurons transduced with either Ln-Egr-1 or Ln-vector on the day of isolation were stained for F-actin at 16 DIV to visualize the morphology of dendritic protrusions (Figure 20A). We found a decrease in the density of dendritic protrusions in Egr-1 upregulated neurons compared with the Ln-vector control. Egr-1 transduced neurons had significantly reduced protrusion density of 2.3 ± 0.2 protrusions/10μm when compared with the vector transduced neurons (4.8 ± 0.2 protrusions/10μm) (Figure 20B). We concluded that Egr-1 upregulation leads to decreases in the density of dendritic protrusions.

The morphology of dendritic spines correlates with their maturity and function [1,44,45]. To identify whether the morphology of dendritic protrusions were altered by the downregulation of drebrin, we measured lengths and widths of the protrusions (Figure 20C). We found the dendritic protrusions of Egr-1 upregulated neuron had comparable widths and lengths as well as the length-to-width ratio (LWR) that was calculated (Figure

20D). The measured widths and lengths together with LWR were used to categorize and compare the structural difference between the dendritic protrusions of Ln-Egr-1 and Ln-vector (Figure 20E). Each protrusion was classified as one of the following: filopodia, thin, stubby or mushroom (Table 1). Filopodia, precursors for dendritic spines, was defined by a protrusion that had a length of greater than 2μm. Immature spines comprised of thin and stubby spines. Thin spines had a length and width of less than 2μm and 0.6μm respectively. Stubby spines had a length and width of less than 0.5μm and 0.6μm respectively. Mushroom spines had length of less of 2μm and width of greater than 0.6μm, and they were considered as mature spines. We found Egr-1 upregulation did not significantly alter the morphological distribution of dendritic protrusions although a decreasing and increasing trend was observed for mature and immature spines respectively in Egr-1 upregulated neurons. Majority of the protrusions was classified as mature mushroom spines (48.7% for Ln-Egr-1 and 60.3% for Ln-Vector) followed by filopodia (22.7% for Ln-Egr-1 and 23.6% for Ln-Vector) and immature thin and stubby spines (27.5% for Ln-Egr-1 and 17.1% for Ln-Vector). Therefore, we demonstrate that Egr-1 upregulation leads to loss of dendritic protrusion density without significantly altering the spine morphology.

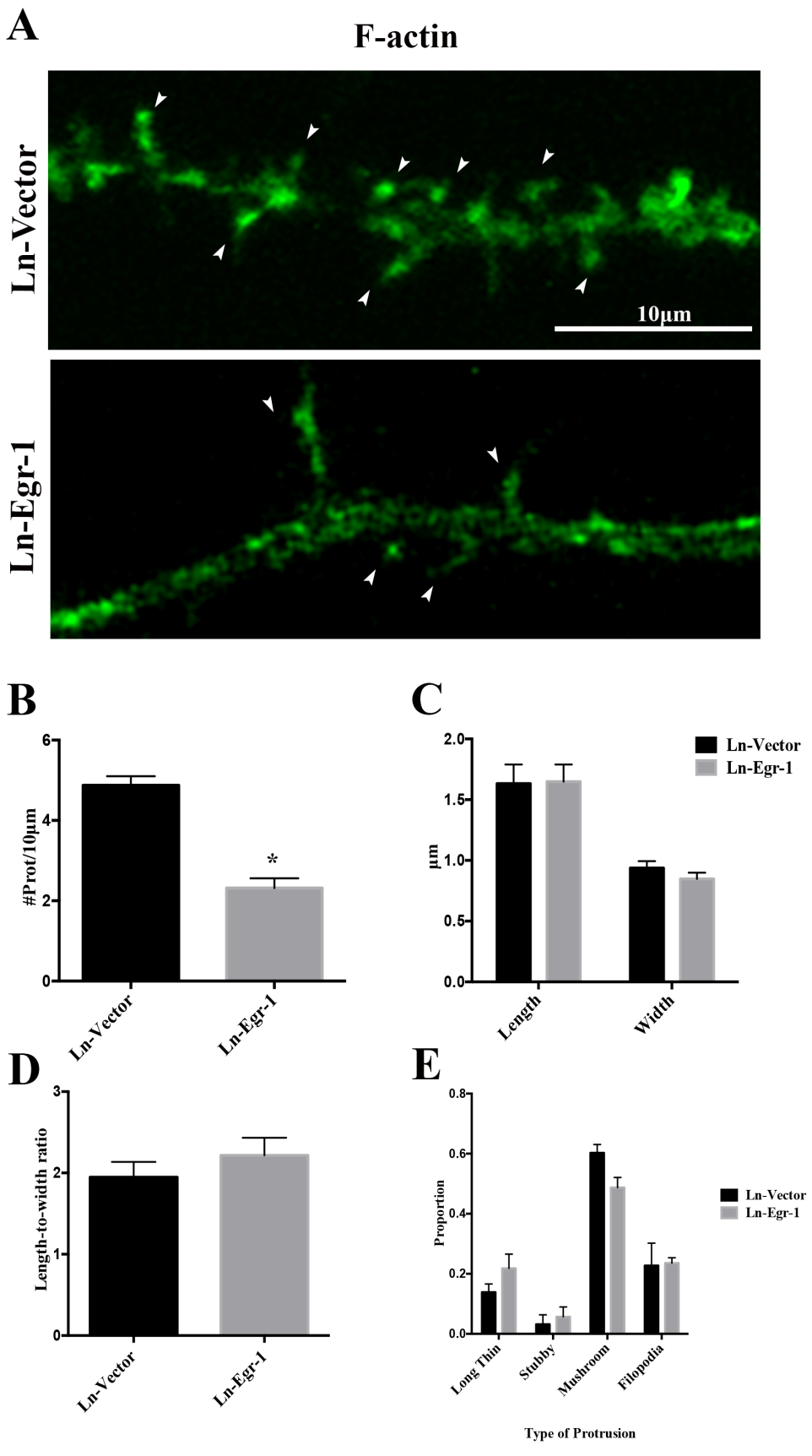
A
F-actin
Ln-Vector
10µm
Ln-Egr-1
B
#Prot/10µm
6
4
2
0
*
Ln-Vector
Ln-Egr-1
C
µm
2.0
1.5
1.0
0.5
0.0
Ln-Vector
Ln-Egr-1
Length
Width
D
Length-to-width ratio
3
2
1
0
Ln-Vector
Ln-Egr-1
E
Proportion
0.8
0.6
0.4
0.2
0.0
Ln-Vector
Ln-Egr-1
Long Thin
Stubby
Mushroom
Filopodia
Type of Protrusion

Figure 20. Changes in dendritic protrusions in response to Egr-1 upregulation. P-0 primary hippocampal neurons were transduced to upregulate Egr-1 for 16 DIV before being analyzed for spine density. **A**, Dendritic protrusions were identified by immunolabelling F-actin (examples are indicated by arrow heads). **B**, Quantification of dendritic protrusion density. **C**, Lengths and widths of the dendritic protrusions in Ln-Egr-1- and Ln-vector-transfected neurons. **D**, Length-to-width ratio of the dendritic protrusions. **E**, Morphological classification of the dendritic protrusions. *$p<0.0001$. Error bars indicate mean ± SEM.

4.3.3 Dendritic spines of CA1 region in the hippocampus are lost when Egr-1 is upregulated

Upregulation of Egr-1 in hippocampal neurons led to decrease in dendritic spine density. To corroborate this *in vitro* finding, we quantified dendritic spine density in the CA1 region of the hippocampus in Egr-1 Tg mice by Golgi staining. CA1 region of the hippocampus is prone to early onset of synaptic pathology in AD that quickly progresses in severity. Also, Egr-1 expression in the CA1 region was highest in the hippocampus [25] suggesting that Egr-1-mediated loss of spine density would be greatest in this region. Thus, the pyramidal hippocampal neurons were identified with Golgi staining that allows visualization of dendritic morphology in the brains of animals [252].

16-month old Egr-1 Tg mice (n=3) were induced to upregulate Egr-1 in the forebrain for 3 months duration as shown in 4.2.2 (Figure 17) before Golgi analysis. Dendritic spines on the stained hippocampal neuron was categorized based on their location and distance from the cell soma into basal proximal (30 to 120μm from cell soma), apical proximal (30 to 120μm from cell soma) and apical distal (>120μm from cell soma) (Figure 21A). We found significant decrease in dendritic spine density in all three regions for Egr-1 Tg mouse versus the age-matched littermate control (Figure 21B,C). Overall, Egr-1 Tg mouse had a decreased spine density of 3.7 ± 0.1 spines/10μm compared with 6.2 ± 0.2 spines/10μm for the control (Figure 21D). Therefore, Egr-1 upregulation leads to reduction in drebrin and dendritic spine density in the hippocampus.

To determine if there was also a change in spine morphology when Egr-1 was upregulated, we measured spine lengths and widths. In terms of spine length, Egr-1 Tg mice had significantly greater overall spine length compared with the control (Figure 21E). On the other hand, Egr-1 Tg mice showed comparable spine width overall with the

control (Figure 21F). Based on measured lengths and widths, LWR ratio was calculated where Egr-1 Tg mice had comparable LWR with the control (Figure 21G). The lengths, widths and LWR were used to categorize each spine according to their morphology into filopodia, immature spine (thin and stubby spine), or mature spine (mushroom and branched spine) (Table 2) (Figure 21H). In addition to the filopodia, thin, stubby and mushroom spines described in Table 1, branched spines were also found. Those with more than one spine head on a single spine neck were defined as branched spines. Branched spines where two heads share the same presynaptic bouton are thought to partake in increased synaptic plasticity in LTP although the underlying mechanism remains elusive [261]. We found that Egr-1 upregulation did not alter overall morphological distribution of the spines compared to the control. The majority of the neurons were mature spines (75.8% for Egr-1 Tg and 70.4% for the control) followed by immature spines (23.5% for Egr-1 Tg and 28.4% for the control) and filopodia (0.7% for Egr-1 Tg and 1.8% for the control). Therefore, Egr-1 upregulation leads to reduction in dendritic spine density without affecting the spine morphology.

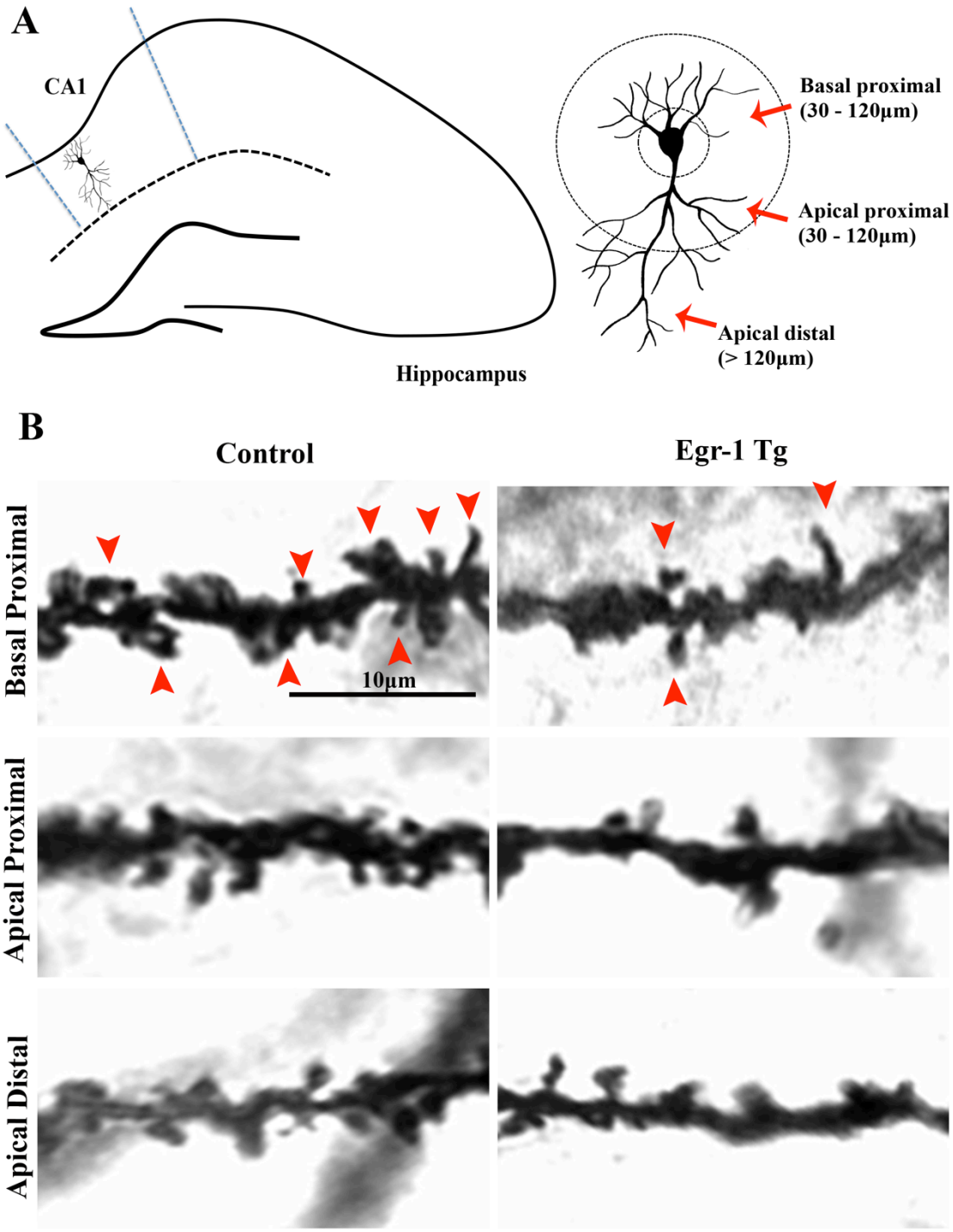
A
CA1
Hippocampus
Basal proximal
(30 - 120µm)
Apical proximal
(30 - 120µm)
Apical distal
(> 120µm)
B
Control
Egr-1 Tg
Basal Proximal
Apical Proximal
Apical Distal
10µm

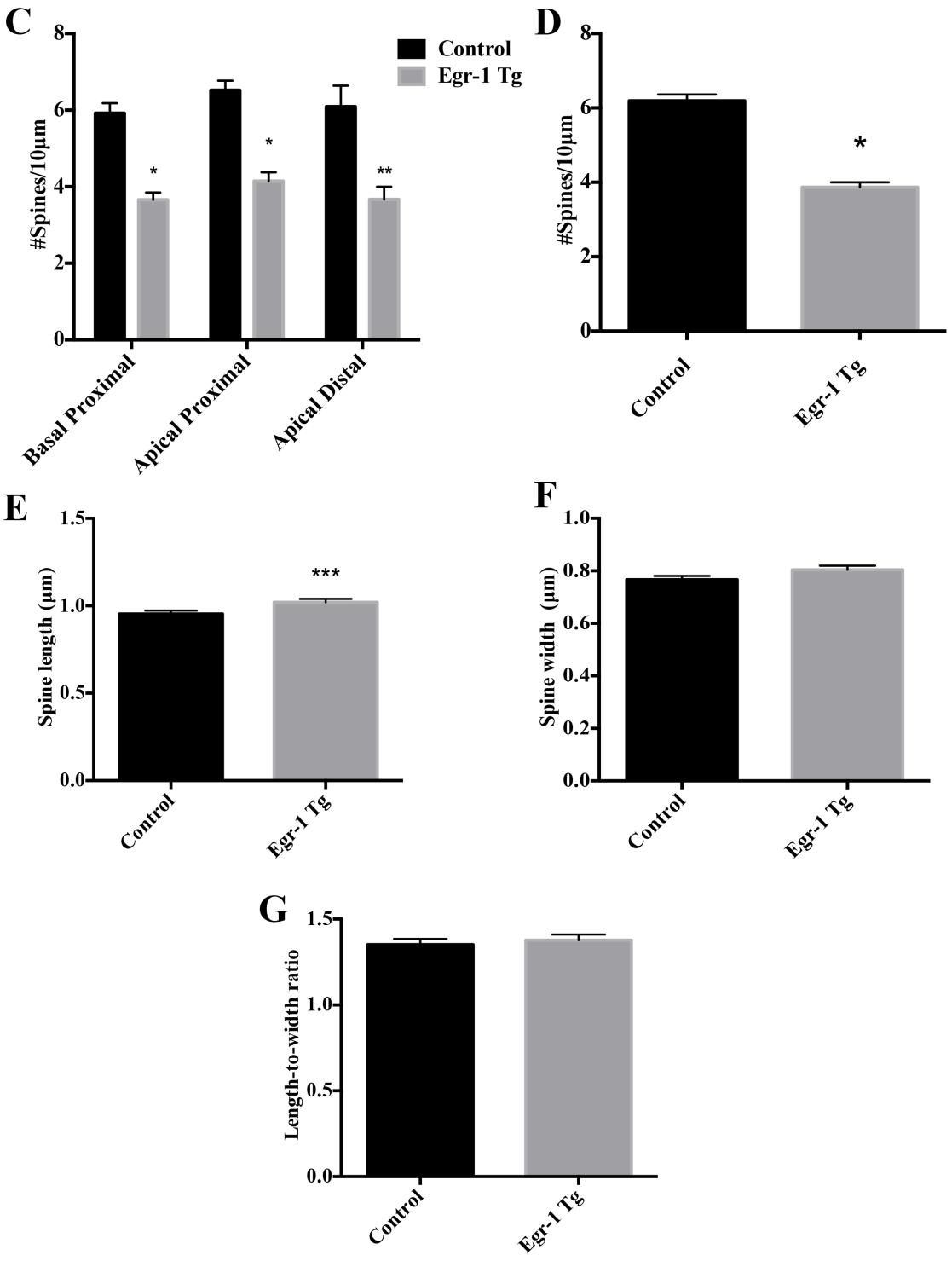
C
Control
Egr-1 Tg
#Spines/10µm
8
6
4
2
0
*
*
**
Basal Proximal
Apical Proximal
Apical Distal
D
#Spines/10µm
*
Control
Egr-1 Tg
E
Spine length (µm)
1.5
1.0
0.5
0.0
***
Control
Egr-1 Tg
F
Spine width (µm)
1.0
0.8
0.6
0.4
0.2
0.0
Control
Egr-1 Tg
G
Length-to-width ratio
1.5
1.0
0.5
0.0
Control
Egr-1 Tg

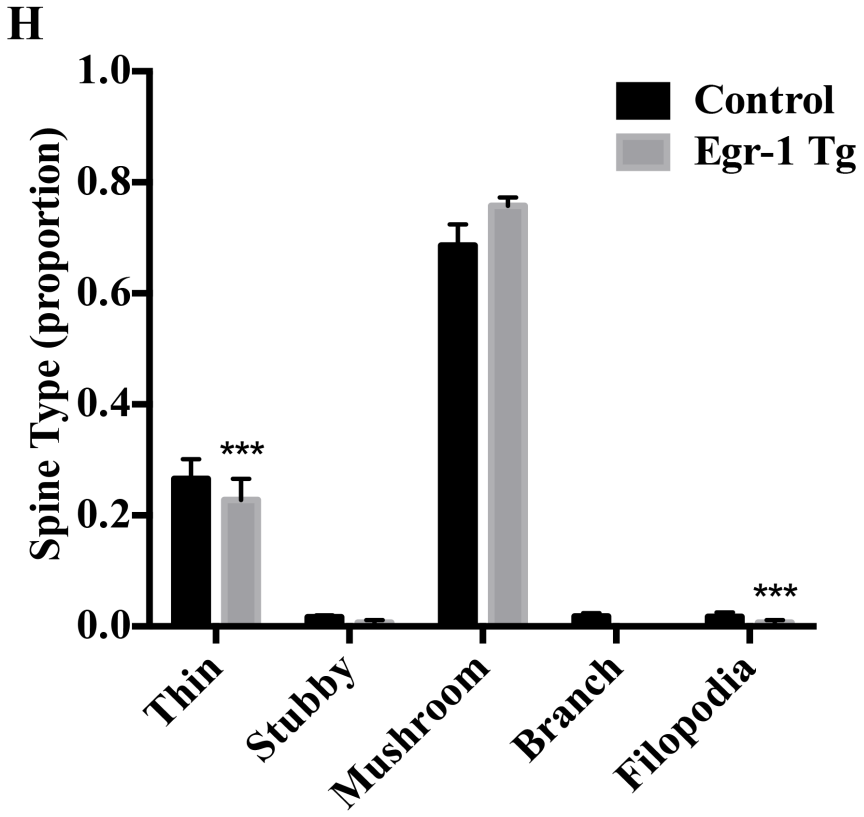
H
1.0
0.8
0.6
0.4
0.2
0.0
Spine Type (proportion)
Control
Egr-1 Tg
***
***
Thin
Stubby
Mushroom
Branch
Filopodia

Figure 21. *In vivo* dendritic spine changes in the hippocampus of Egr-1 Tg mouse. 16-mo Egr-1 Tg mouse were allowed to upregulate Egr-1 in the forebrain for three months before Golgi analysis (n=3/genotype). **A**, CA1 region of the hippocampus was analyzed where the dendritic spines were divided into three groups based on their location and distance from the cell soma. **B**, Micrographs showing golgi staining of CA1 hippocampal neurons in Egr-1 Tg mouse and the littermate control (examples of dendritic spines are indicated by red arrowheads). **C**, Analysis of spine density per 10μm in all three regions and **D**, when the spine density from all three regions combined. **E**, Spine lengths. **F**, Spine widths**. G,** length-to-width ratio of dendritic spines. **H**, Morphological classification of dendritic spines. *$p<0.0001$; **$p<0.0005$; *** $p<0.05$. Error bars indicate mean ± SEM.

4.3.4 Dendritic spine density is increased in the absence of Egr-1

Our data demonstrate that Egr-1 upregulation leads to decrease in drebrin and dendritic spine density *in vitro* and *in vivo*. We have also shown in 4.2.3 that Egr-1 loss-of-function led to increase in drebrin level (Figure 18). Based on these results, we hypothesized that Egr-1 loss-of-function would lead to increase in spine density. To test our hypothesis, 12-mo Egr-1 -/- mouse and Egr-1 +/+ control mice (n=3) were used and CA1 hippocampal neurons were golgi stained and dendritic spine density quantified as was performed for Egr-1 Tg mouse in 4.3.3 (Figure 21A). We found Egr-1 loss-of-function led to significant increases in dendritic spine density in basal proximal and apical proximal and distal regions of CA1 region of hippocampus (Figure 22A,B). Overall, Egr-1 -/- mouse had significantly increased spine density of 7.8 ± 0.2 spines/10μm compared with 4.9 ± 0.2 spines/10μm for Egr-1 +/+ mouse (Figure 22C). Therefore, this data further supports the idea that drebrin expression and dendritic spine density are correlated.

To test whether Egr-1 loss-of-function alters the spine morphology in the CA1 of the hippocampus, lengths and widths of the spines were measured. Overall dendritic spines in Egr-1 -/- mice had significantly shorter spine length (0.99 ± 0.02μm) compared with Egr-1 +/+ mouse (1.06 ± 0.02μm) (Figure 22D). For width, Egr-1 -/- mouse had comparable overall width (0.82 ± 0.01μm) with Egr-1 +/+ mouse (0.81 ± 0.01μm) (Figure 22E). The calculated LWR also significantly differed between Egr-1 -/- and +/+ mouse (Figure 22F). Egr-1 -/- mouse had significantly smaller LWR of 1.30 compared to 1.41 for Egr-1 +/+ control. Based on length, width and LWR, each dendritic spine was categorized as a filopodium, thin spine, stubby spine, mushroom spine or branched spine

(Figure 22G). We found that Egr-1 -/- and +/+ mouse had comparable distribution of mature spines (77.8% for Egr-1 -/- and 71.7% for Egr-1 +/+), immature spines (20.2% for Egr-1 -/- an 24.1% for Egr-1 +/+) and filopodia (2.1% for Egr-1 -/- and 3.3% for Egr-1 +/+). Therefore, Egr-1 loss-of-function leads to increase in spine density without altering spine morphology.

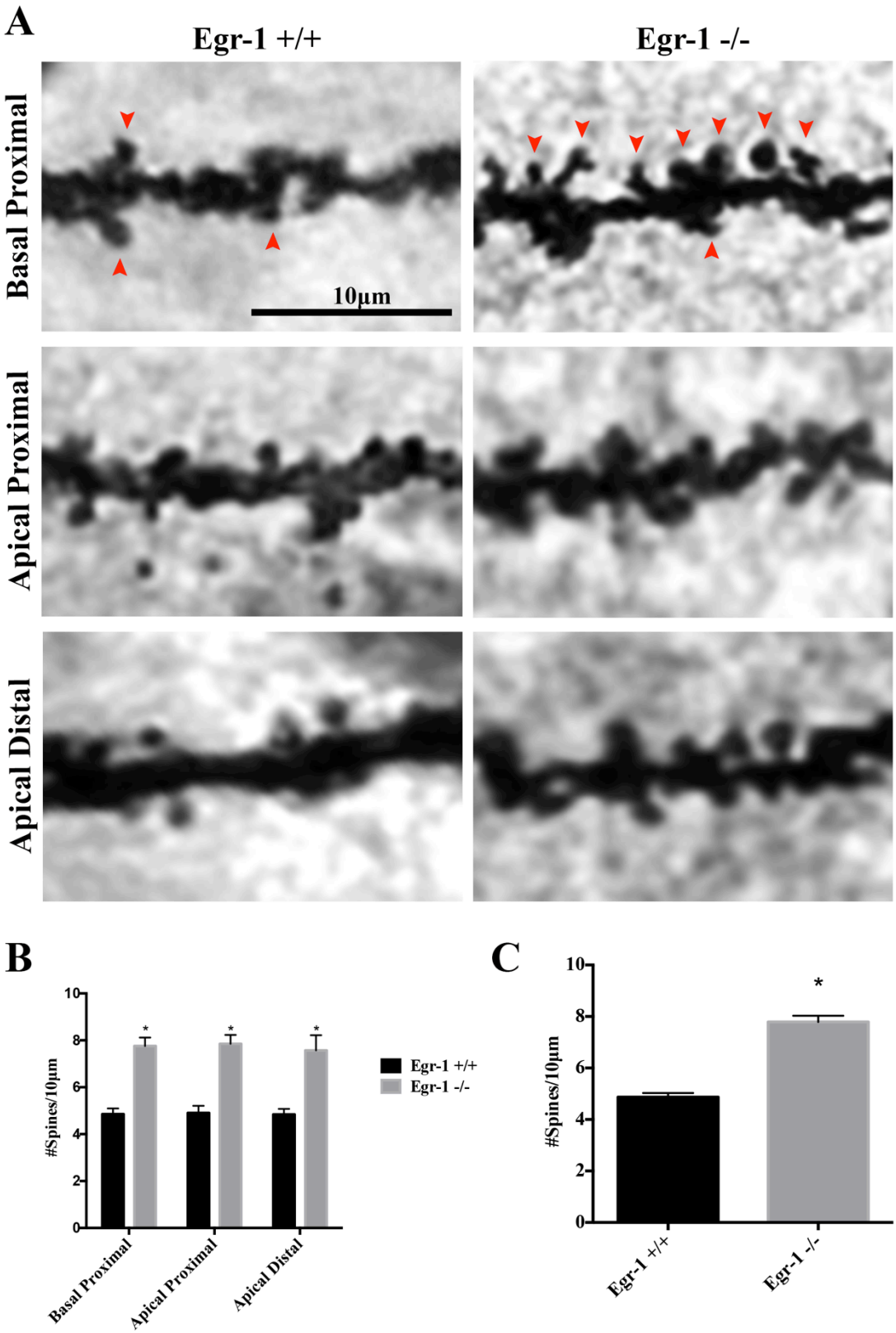
A
Egr-1 +/+
Egr-1 -/-
Basal Proximal
Apical Proximal
Apical Distal
10µm
B
#Spines/10µm
Egr-1 +/+
Egr-1 -/-
Basal Proximal
Apical Proximal
Apical Distal
C
#Spines/10µm
Egr-1 +/+
Egr-1 -/-

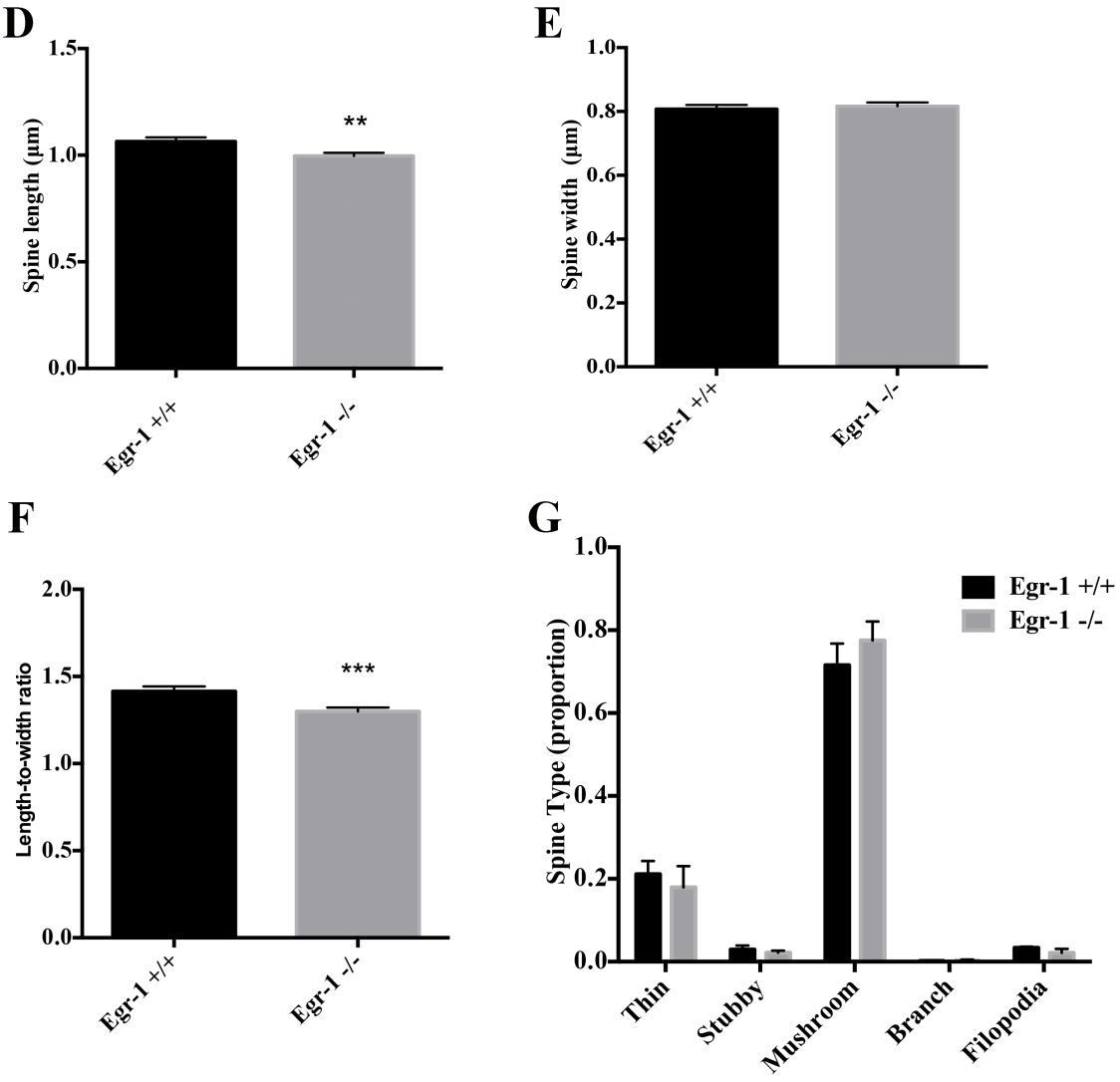
D
Spine length (µm)
1.5
1.0
0.5
0.0
**
Egr-1 +/+
Egr-1 -/-
E
Spine width (µm)
1.0
0.8
0.6
0.4
0.2
0.0
Egr-1 +/+
Egr-1 -/-
F
Length-to-width ratio
2.0
1.5
1.0
0.5
0.0
***
Egr-1 +/+
Egr-1 -/-
G
Spine Type (proportion)
1.0
0.8
0.6
0.4
0.2
0.0
Egr-1 +/+
Egr-1 -/-
Thin
Stubby
Mushroom
Branch
Filopodia

Figure 22. Comparison of dendritic spines between Egr-1 -/- and +/+ mouse. Golgi staining was performed in 12-mo Egr-1 -/- and +/+ mouse (n=3/genotype) and CA1 region of the hippocampus was analyzed. **A**, Micrographs of dendritic segments visualized using golgi staining (examples of dendritic spines are indicated by red arrowheads). **B**, Quantification of dendritic spine density per 10μm for basal proximal, apical proximal and distal spines. **C**, Quantification of combined dendritic spine density per 10μm. **D**, Lengths of dendritic spines in Egr-1 -/- and +/+ mouse. **E**, Widths of dendritic spines Egr-1 -/- and +/+ mouse. **F**, length-to-width ratio of dendritic spines in Egr-1 -/- and +/+ mouse. **G**, Morphological classification. *$p<0.0001$; **$p<0.01$; ***$p<0.005$. Errors bars indicate mean ± SEM.

4.3.5 Loss of dendritic protrusions correlate with loss of drebrin when Egr-1 is upregulated

We demonstrated that upregulation of Egr-1 leads to reduction in drebrin and dendritic spine density, indicating that they have inverse relationship. Based on our findings, we hypothesized that loss of drebrin and spine density are correlated and that Egr-1 upregulation would lead to reduction of drebrin-positive protrusions. To address our hypothesis, hippocampal neurons were isolated from P-0 rat pups and transduced with either Ln-Egr-1 or Ln-vector. After 16 DIV, hippocampal neurons were co-immunolabelled for F-actin and drebrin and analyzed for co-localization (Figure 23A).

As expected, we found a decrease in the density of dendritic protrusions identified by F-actin staining when Egr-1 was upregulated. We also found that fewer dendritic protrusions were labeled for drebrin in neurons with upregulated Egr-1 compared with the vector control. When quantified, Ln-Egr-1 neurons had significantly reduced number of drebrin-positive protrusions (1.85 out of 2.72 protrusions/10μm) compared with Ln-vector neurons (4.62 out of 4.8 protrusions/10μm) (Figure 23B). Therefore, only 68.0% of the dendritic protrusions contained drebrin puntae in response to Egr-1 upregulation compared with 96.3% for the control. These results suggest Egr-1-mediated loss of drebrin directly decrease the number of drebrin-positive dendritic protrusions leading to reduction in the protrusion density.

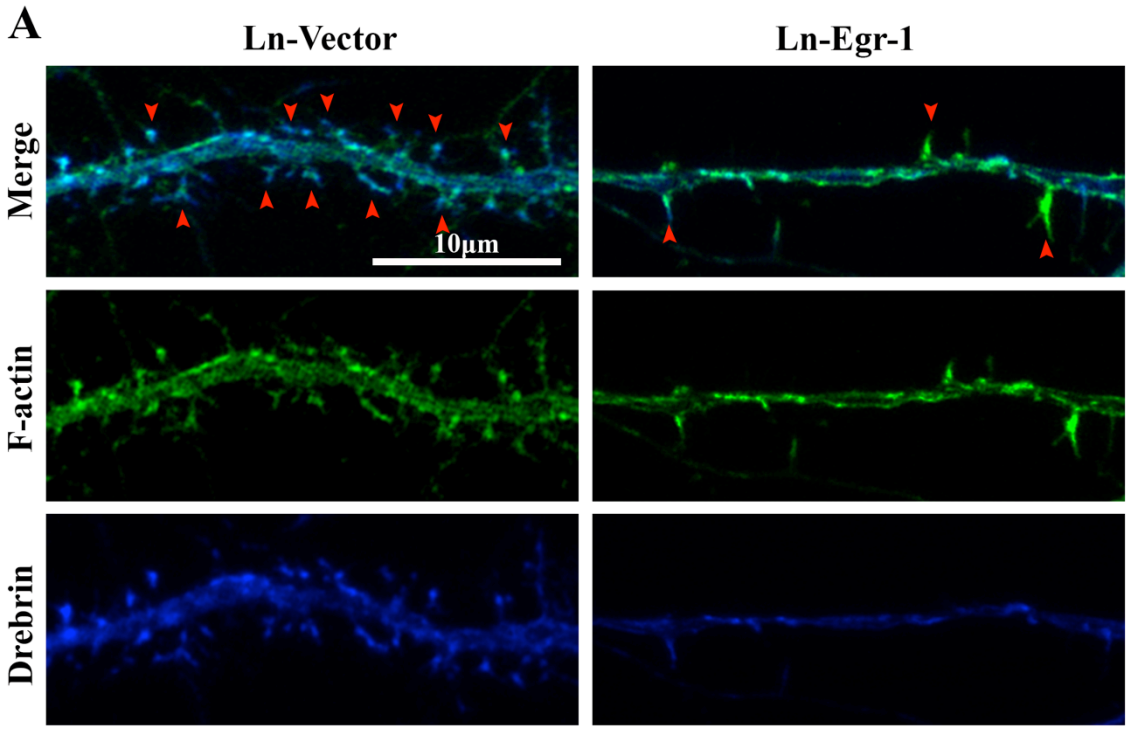
A
Ln-Vector
Ln-Egr-1
Merge
F-actin
Drebrin
10µm

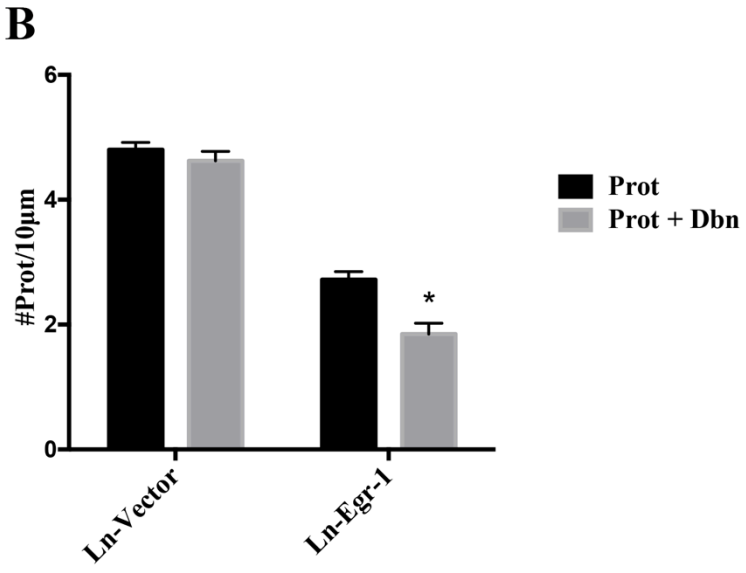
B
#Prot/10µm
6
4
2
0
*
Prot
Prot + Dbn
Ln-Vector
Ln-Egr-1

Figure 23. Changes in the distribution of drebrin-positive dendritic protrusions upon Egr-1 upregulation. Egr-1 upregulated primary hippocampal neurons were analyzed at 16DIV. **A**, Dendritic protrusions were immune-labelled for F-actin and drebrin. (examples are indicated by red arrowheads) **B**, Quantification of the densities of dendritic protrusions and drebrin-positive protrusions *$p<0.0005$. Errors bars indicate mean ± SEM.

4.3.6 Upregulation of Egr-1 leads to loss of mature dendritic spines and putative functional synaptic contacts

Our data show that upregulation of Egr-1 leads to reduction in the dendritic protrusions with drebrin puntae. To test whether loss of drebrin in dendritic protrusions also correlates with the reduction in number of functionally mature dendritic spines, we quantified the number of PSD-95-containing dendritic protrusions. PSD-95 is the major scaffolding protein in PSD recruited by drebrin and is often used as an indicator of putative mature dendritic spines [11]. Here, we immunolabelled 16 DIV hippocampal neurons transduced with Ln-Egr-1 or Ln-vector as in 4.3.5 for F-actin, drebrin and PSD-95 (Figure 24).

We found Egr-1 upregulation in hippocampal neurons led to a significant reduction in the density of dendritic protrusions that contained PSD-95 as well as PSD-95 colocalized with drebrin (Figure 24A). Very few protrusions contained PSD-95 without drebrin for Ln-Egr-1 (2.7%) and Ln-vector (1.3%) neurons and majority of the protrusions that contained PSD-95 also contained drebrin (Figure 24B). This finding supported the association between drebrin and PSD-95 and the requirement of drebrin for the recruitment of PSD-95 to dendritic spines. The Ln-vector control had the colocalization of drebrin and PSD-95 at a density of 4.56 out of 4.81 protrusions/10μm. In contrast, Egr-1 upregulation led to significant reduction in the density of protrusions with PSD-95 and drebrin colocalization (1.71 out of 2.61 protrusions/10μm). 65.5% of the dendritic protrusions had colocalized drebrin and PSD-95 in response to Egr-1 upregulation compared with 94.8% for the control. In section 4.3.5, we showed 68.0% of the dendritic protrusions contained drebrin puntae in response to Egr-1 upregulation compared with 96.3% for the control (Please refer to Figure 18B). Therefore, dendritic

protrusions with drebrin most likely also contain PSD-95. In line with this, Egr-1 upregulation-mediated reduction in dendritic protrusions with drebrin leads to loss in protrusion with PSD-95, and thus, mature spines.

Based on the finding that Egr-1 upregulation leads to loss of PSD-95-containing dendritic spines, we hypothesized that Egr-1 upregulation may also lead to overall loss of synaptic contacts. To examine this, Ln-Egr-1- and Ln-vector-transduced neurons were prepared and immunolabelled for F-actin, PSD-95 and the presynaptic marker vesicular glutamate transporter 1 (vGluT1) (Figure 25A). Colocalization of vGluT1 and PSD-95 suggest presence of putative functional glutamate synaptic contacts [262]. We found the vector control had 3.65 protrusions out of 4.7 protrusions/10μm which showed colocalization of the synaptic markers (Figure 25B). In contrast, Egr-1 upregulation led to significant reduction for co-localization of vGluT1 and PSD-95 (1.27 out of 2.82 protrusions/10μm). Thus, only 45.0% of the dendritic protrusions in Egr-1 upregulated neurons made putative functional synaptic contacts compared with 77.7% for the control. These data suggest Egr-1-mediated reduction of drebrin expression correlates with loss of mature dendritic spines and putative synaptic contacts, thereby exacerbating loss of synapses.

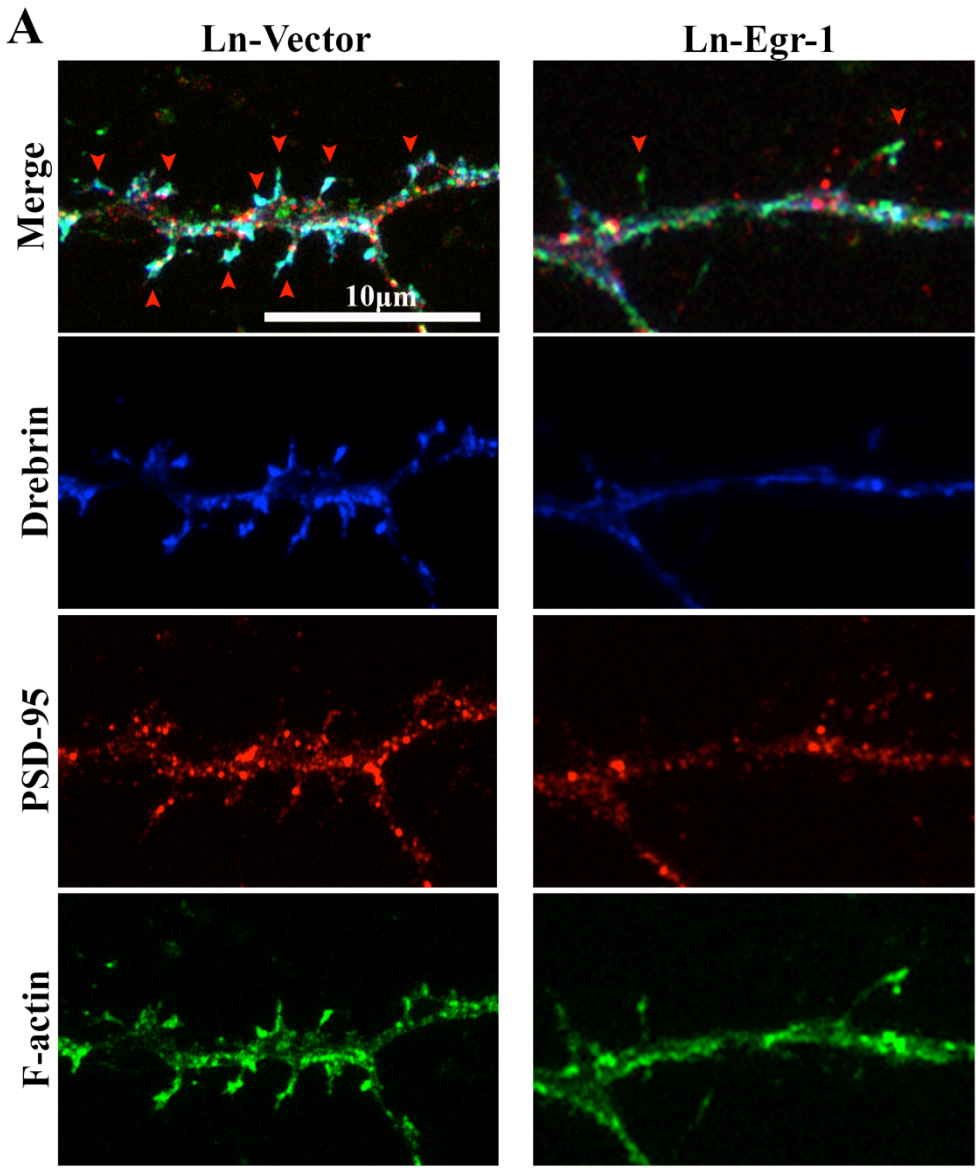
A
Ln-Vector
Ln-Egr-1
Merge
Drebrin
PSD-95
F-actin
10µm
B
#Prot/10µm
Prot
Prot + Dbn + PSD-95
Prot + PSD-95 only
Ln-Vector
Ln-Egr-1

Figure 24. Colocalization of drebrin and PSD-95 in Egr-1 upregulated primary hippocampal neurons. **A**, 16 DIV hippocampal neurons were coimmunolabelled for drebrin and PSD-95 in addition to F-actin. (examples of dendritic protrusions are indicated by red arrowheads) **B**, Quantification of drebrin and PSD-95 colocalization. *$p<0.0005$; **$p<0.0001$. Errors bars indicate mean ± SEM.

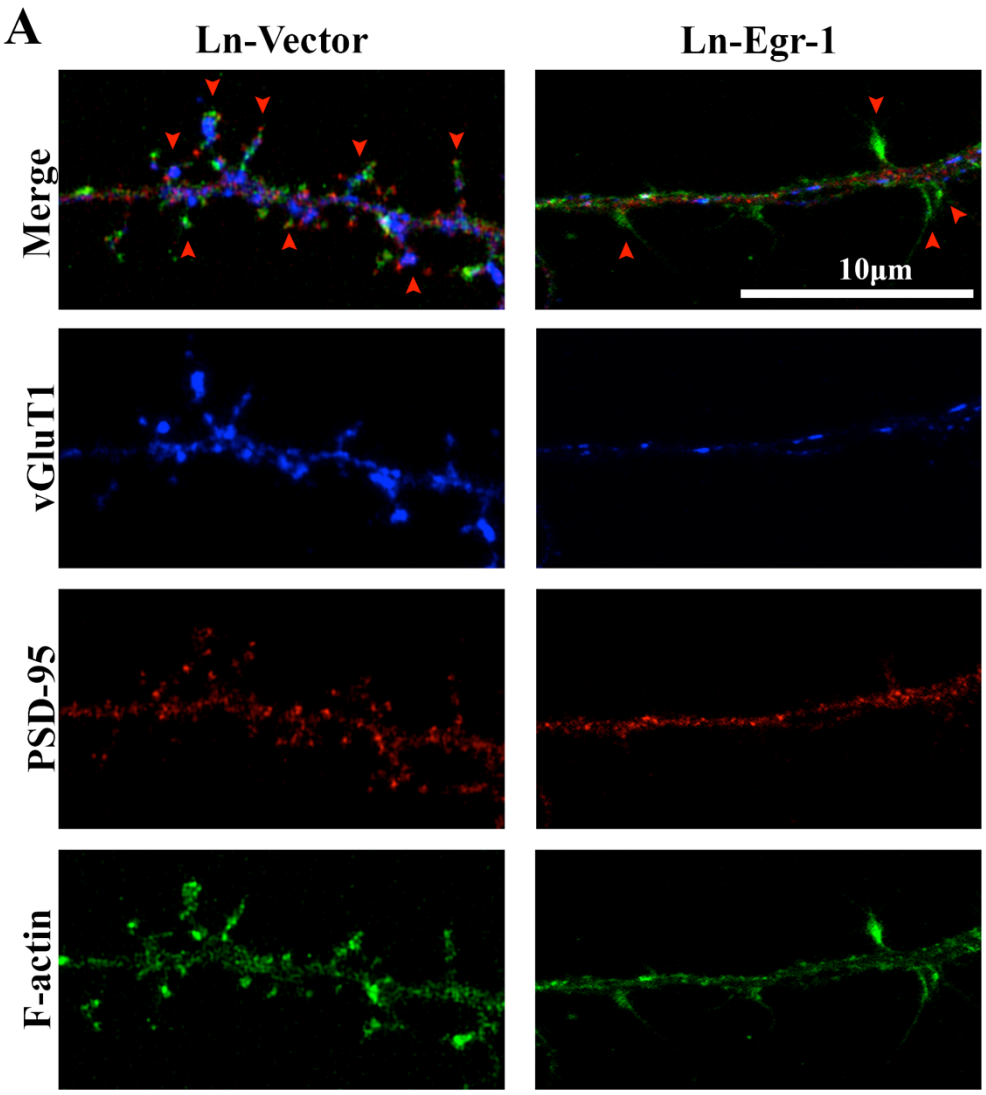
A
Ln-Vector
Ln-Egr-1
Merge
vGluT1
PSD-95
F-actin
10µm

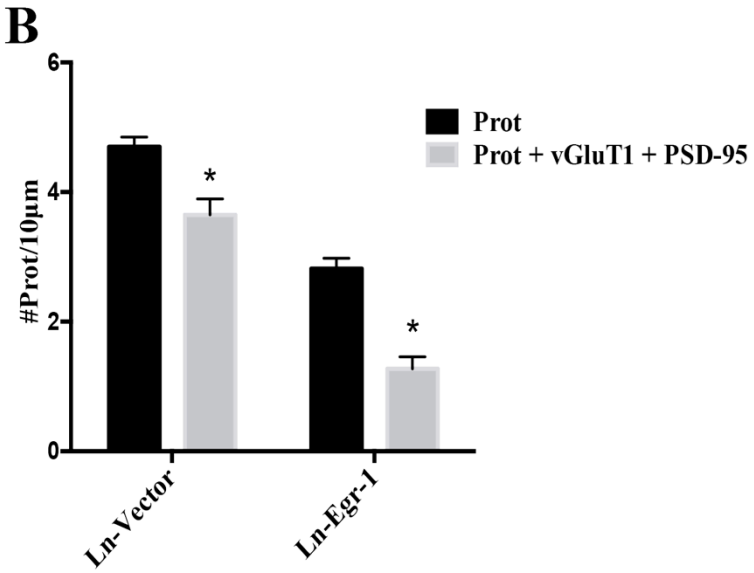
B
#Prot/10µm
6
4
2
0
Prot
Prot + vGluT1 + PSD-95
*
*
Ln-Vector
Ln-Egr-1

Figure 25. Colocalization of vGluT1 and PSD-95 in Egr-1 upregulated hippocampal neurons. **A**, 16 DIV primary hippocampal neurons were coimmunolabelled for vGluT1 and PSD-95 in addition to F-actin to quantify putative synaptic contacts. (examples of dendritic protrusions are indicated by red arrowheads) **B**, Quantification of colocalization for PSD-95 and vGluT1. *$p<0.0001$. Errors bars indicate mean ± SEM.

4.3.7 Egr-1 upregulation brings about changes in other synaptic proteins

Drebrin is downregulated in response to Egr-1 upregulation, which correlates with loss of dendritic spines. To test whether Egr-1-mediated loss of drebrin alters other synaptic proteins in the process of spine loss, we measured the levels of various synaptic proteins in Ln-Egr-1- and Ln-vector-transduced hippocampal neurons: ABPs cofilin and profilin; postsynaptic AMPAR subunit glutamate receptor 1 protein (GluA1); postsynaptic scaffolding protein PSD-95; and presynaptic vesicular glutamate transporter vGluT1 (Figure 26A). Cofilin and profilin are postsynaptic ABPs that serve different function than drebrin by directly promoting actin depolymerization and polymerization respectively. AMPARs are glutamate receptors that mediate synaptic plasticity and thus, GluA1 is a good indicator of AMPAR level. PSD-95 is the scaffolding protein that serves as the basis upon which PSD is formed. vGluT1 is the presynaptic vesicular protein that is an indicator of presynaptic activity.

We analyzed protein lysates from 9 DIV hippocampal neurons that were transduced with either Ln-Egr-1- or Ln-vector on the day of isolation (Figure 26B). According to the immunoblots, Egr-1-mediated reduction in drebrin did not alter the protein levels of the ABPs cofilin and profilin. However, postsynaptic proteins GluA1 and PSD-95 proteins were significantly reduced by 46.2% and 29.5% respectively. In contrast, presynaptic protein vGluT1 was significantly increased 1.57-fold. These data indicate that Egr-1-mediated downregulation of drebrin induces changes in other synaptic proteins and lead to loss of dendritic spines.

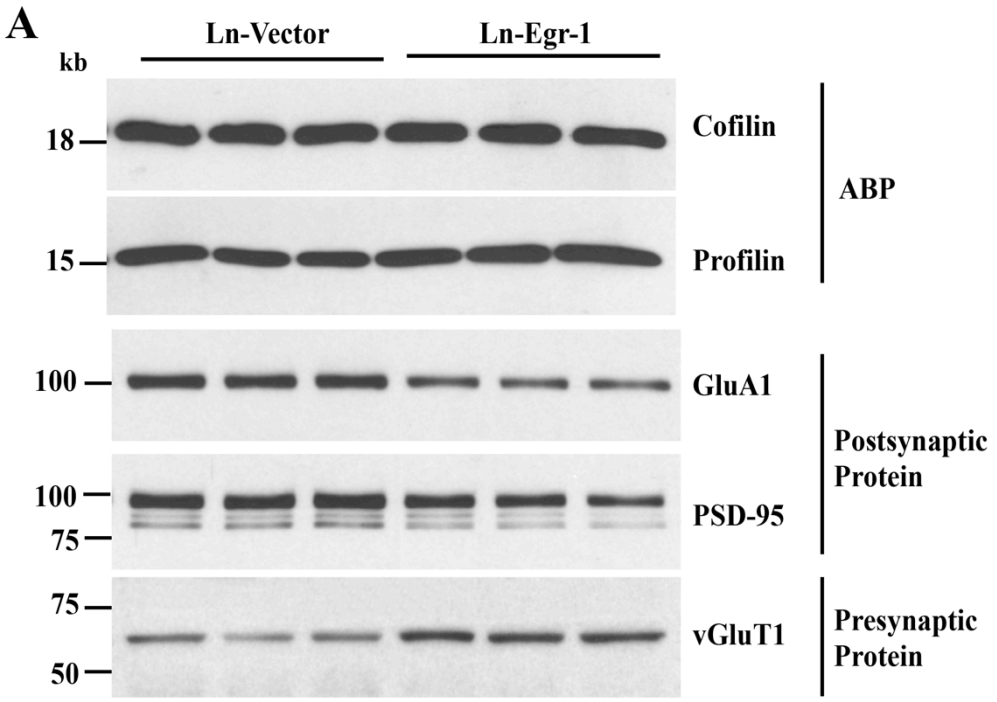
A
Ln-Vector
Ln-Egr-1
kb
18
15
100
100
75
75
50
Cofilin
Profilin
GluA1
PSD-95
vGluT1
ABP
Postsynaptic Protein
Presynaptic Protein

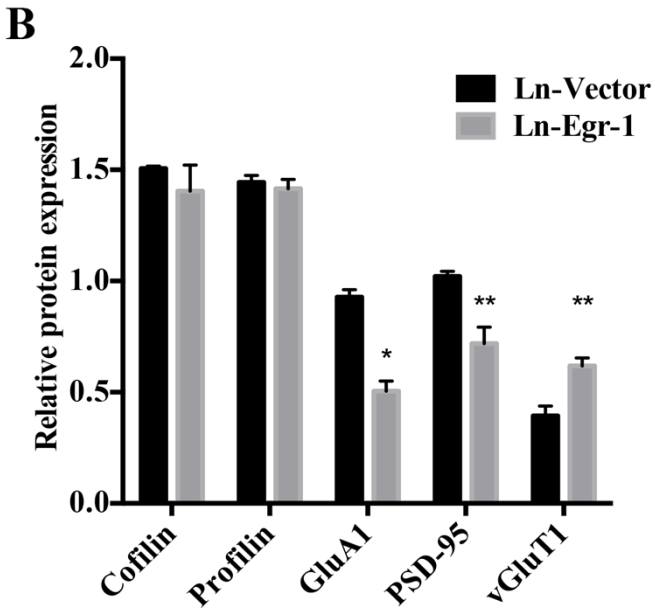
B
Relative protein expression
2.0
1.5
1.0
0.5
0.0
Ln-Vector
Ln-Egr-1
*
**
**
Cofilin
Profilin
GluA1
PSD-95
vGluT1

Figure 26. Changes in the expression of other synaptic proteins upon Egr-1 upregulation. Protein lysates from 9 DIV primary hippocampal neurons were analyzed for the protein level of various synaptic proteins using immunoblotting. **A**, Protein levels of Cofilin, profilin, GluA1, PSD-95 and vGluT1 were investigated. **B**, Densitometry analysis of the probed proteins. *$p<0.005$; **$p<0.05$. Errors bars indicate mean ± SEM.

Chapter 5. Discussion

In this thesis, we investigated the relationship between Egr-1 TF and drebrin. We hypothesized and demonstrated the following:

1) Egr-1 binds to drebrin promoter to regulate drebrin expression
2) Egr-1 negatively regulate drebrin expression
3) Egr-1-mediated loss of drebrin leads to decrease in dendritic spine density

We propose that Egr-1-mediated downregulation of drebrin as a novel mechanism of dendritic spine loss in AD pathology.

5.1 Egr-1 regulates drebrin expression

Here, we demonstrated that the drebrin promoter contains two EREs that bind Egr-1 TF (Figure 14) both *in vitro* and *in vivo* using luciferase promoter assay and ChIP assays. The promoter assay and ChIP assay indicated Egr-1 associates with drebrin promoter at regions where consensus EREs were found as well as regions that did not have EREs. Drebrin promoter is enriched with GC-rich sequences that comprise greater than 60% of the promoter. The GC-rich drebrin promoter, thus, presents Egr-1 with multiple consensus and non-consensus EREs because Egr-1 is able to associate with a 9-bp GC-rich sequences that closely matches the consensus sequence [215]. Egr-1 binding to drebrin promoter was conserved between cell lines derived from human, monkey and rat suggesting that the Egr-1-drebrin interaction is likely conserved between species. Furthermore, our data from hippocampal neurons *in vitro* and *in vivo* models of Egr-1 demonstrated that drebrin expression was synchronously altered at mRNA and protein level in response to changes in Egr-1 level, thus supporting transcriptional regulation of

drebrin by Egr-1. This is in support of high-density microarray data that showed a 23% downregulation of drebrin in Egr-1 upregulated PC12 cells [29].

Information regarding regulation of drebrin expression and drebrin promoter is largely unknown despite drebrin's importance in formation and maintenance of dendritic spines as well as its precarious loss in AD. Currently, only two TFs, NXF and Sim2, that belongs to bHLH-PAS protein family are known to bind to drebrin promoter [174]. NXF was found to upregulate drebrin expression and thus, likely does not play a role in loss of drebrin observed in AD. Sim2, on the other hand, was suggested to downregulate drebrin in the context of Down's syndrome, because Sim2 is abundantly expressed in Down's syndrome due to the Sim2 locus trisomic state [175]. However, Sim2-mediated downregulation of drebrin was only tested *in vitro* through promoter assay and *in vivo* studies to support this regulation is lacking. Furthermore, in AD, Sim2 was not significantly altered in patients with a weak positive correlation with drebrin [168,177]. Hence, the regulatory factor that leads to loss of drebrin remained undetermined. Therefore, Egr-1 TF presented here offers a regulatory mechanism by which drebrin may be regulated in AD.

Egr-1 is upregulated in AD and correlates with AD progression [27,28]. An increasing number of neurological disorders result from defective DNA-protein interactions that occur in neurons brought on by sustained changes in neuronal gene expression [263]. In line with this, sustained upregulation of Egr-1 may play a pathological role in AD by binding to drebrin promoter to downregulate drebrin expression.

Under physiological conditions, Egr-1 expression is transiently induced and has been attributed to regulating synaptic plasticity, neurite outgrowth and wound repair

[226,264,265]. Therefore, Egr-1 appears to have an emphasized role in proliferation and growth, but contradictory roles of Egr-1 were also observed. AD is characterized by three pathological hallmarks: plaques composed of aggregated β-amyloid (Aβ), neurofibrillary tangles composed of hyperphosphorylated forms of tau and loss of synapses [12]. Egr-1 was found to upregulate presenilin-2 gene expression and facilitates the γ-secretase cleavage of amyloid precursor protein (APP) that leads to accumulation of amyloid plaques in AD [266]. Furthermore, our lab has shown that Egr-1 expression correlated with hyperphosphorylated tau that leads to neurofibrillary tangle pathology in AD [195]. These observations suggest that Egr-1 plays a different role in pathology where Egr-1 remains upregulated. However, it remains unclear how Egr-1 is upregulated in AD.

There are several mechanisms by which Egr-1 could be induced constitutively in AD. First, APP was found to be a down-regulator of Egr-1 expression [267]. Using APP -/- mice, it was found that in the absence of APP, enrichment of acetylated histone H4 at the Egr-1 promoter region was observed that correlated with increased expression of Egr-1. Therefore, alterations or loss of a particular function of APP in AD may lead to constitutive Egr-1 expression by acetylation of histone H4. Second, Egr-1 is induced in response to Aβ-peptide-induced excitotoxicity in AD [268]. Accumulation of Aβ peptides triggers overactivation of NMDARs whose activity is tightly linked with Egr-1 induction [25]. Accumulation of Aβ peptides would thus exacerbate the excitotoxicity leading to sustained upregulation of Egr-1. Third, cerebral ischemia that promotes AD pathogenesis was found to upregulate Egr-1 expression [25,196]. Ischemia induces brain injury that leads to cognitive impairment by inducing neuronal loss, accumulation of Aβ peptides and tau pathology [269-272]. Thus, in conjunction with APP and Aβ peptides, cerebral ischemia may

contribute to sustain Egr-1 upregulation in AD. Lastly, Egr-1 is likely involved in P21-activated kinase (PAK)/LIM-K pathway. PAK is a downstream signaling protein of the Rho/Rac family of small GTPases whereas LIM-K is PAK's downstream kinase [273]. LIM-K pathway was initially proposed to indirectly regulate drebrin by regulating cofilin that competes with drebrin for actin binding sites. In Tg2576 mice and AD patients, PAK/LIM-K activities were downregulated. Furthermore, overexpression of PAK prevented Aβ1-42-induced drebrin loss in hippocampal neurons *in vitro*. In contrast, administration of a PAK inhibitor led to drebrin loss and memory impairment in normal mice. A link between PAK and Egr-1 was found where PAK5, which is an isoform of PAK predominantly expressed in adult neuronal tissue was found to regulate growth and migration of breast cancer cells via regulating PAK5-Egr-1 signaling pathway [274]. Treatment of cancer cells with PAK5 siRNA led to an increase in expression of Egr-1. This is in line with the fact that in AD, PAK activities are downregulated while Egr-1 is upregulated. Therefore during synaptic pathology such as AD and related disorders, loss of PAK/LIM-K activity due to stressors such as Aβ and excitotoxicity may lead to constitutive upregulation of Egr-1 which then downregulates drebrin (Figure 27). These three potential pathways of Egr-1 induction could take place simultaneously as these are not mutually exclusive, but are linked. Taken together, Egr-1 is most likely the nodal point via which drebrin is regulated in AD.

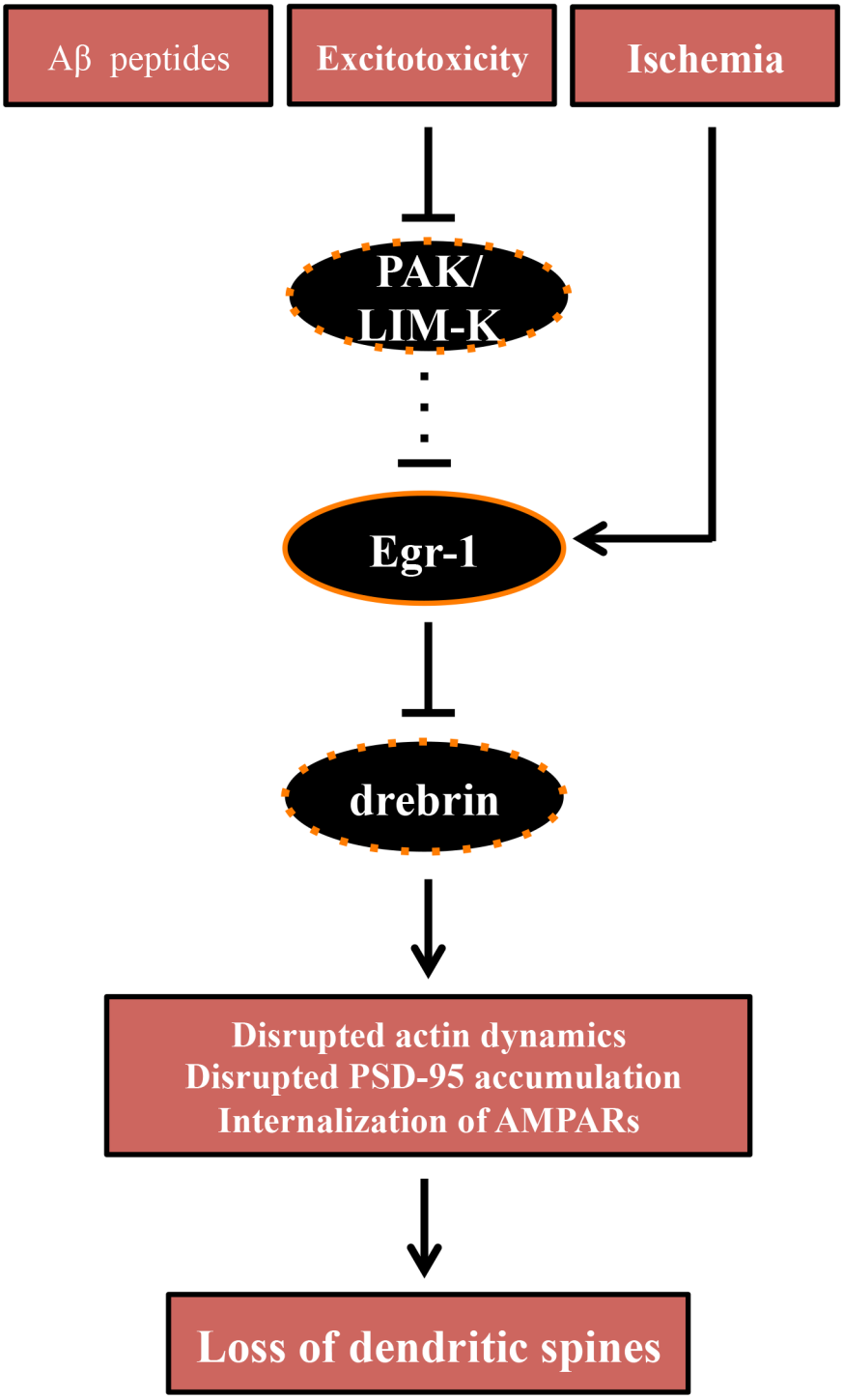
Aβ peptides
Excitotoxicity
Ischemia
PAK/
LIM-K
Egr-1
drebrin
Disrupted actin dynamics
Disrupted PSD-95 accumulation
Internalization of AMPARs
Loss of dendritic spines

Figure 27. Proposed mechanistic pathway for regulation of drebrin by Egr-1 during synaptic pathology. Pathological agents such as amyloid peptides, excitotoxicity and ischemia triggers cascade of events that lead to inhibition of PAK/KIM-K pathway. This, in turn, disinhibits Egr-1 and leads to its long-term upregulation. Subsequently, Egr-1 downregulates drebrin and disrupt actin cytoskeleton dynamics in dendritic spines leading to loss of dendritic spines and ultimately, cognitive impairment.

5.2 Drebrin is negatively regulated by Egr-1

Transcriptional regulation of drebrin led to changes in drebrin mRNA that translated into changes in protein both *in vitro* and *in vivo*. We demonstrate using hippocampal neurons transduced with Egr-1 lentivirus (Figure 15) and an inducible mouse model of Egr-1 (Figure 17) that drebrin is reduced in response to Egr-1 upregulation. On the other hand, Egr-1 loss-of-function leads to increased drebrin level (Figure 18). Taken together, these data suggests negative regulation of drebrin by Egr-1 TF.

An exception was observed in luciferase promoter assay where Egr-1 TF bound to drebrin promoter and led to activation of promoter-driven luciferase expression instead of repression (Figure 12). However, rather than contradicting our data, the luciferase promoter data highlights the limitations of the partial drebrin promoter that was inserted. The luciferase promoter assay is an invaluable and rapid tool for studying the activity of DNA fragment as the luciferase protein is available immediately upon translation [275,276]. However, the DNA fragment that was inserted is not the complete promoter sequence as it only encapsulated -624bp relative to the predominant TSS. The length of the promoter is variable amongst different genes, but in humans they are generally longer than 1kb [277]. In a separate study examining Egr-1 binding sites during monocytic differentiation, up to 7.5kb upstream of the TSS was considered as the promoter region [215]. In support, we have identified an upstream ERE located at 2.4kb from the TSS using ChIP assay that was not included in the promoter assay. Hence, the activation we observed in luciferase promoter assay was not translated into the hippocampal neurons transduced with Ln-Egr-1 or the *in vivo* animal models.

Drebrin loss occurs early in the pathogenesis of AD. Extensive 40% loss of drebrin is already evident in the hippocampus of individuals with MCI that often precedes dementia [171]. Drebrin is progressively lost with increasing severity of neurodegeneration such that in AD, a greater 80% decrease is observed [12]. No other ABPs are found to be as drastically lost as drebrin in AD. Furthermore, Egr-1 upregulation specifically targeted and downregulated drebrin without altering the levels of other ABPs, cofilin and profilin. These data suggest that the central role drebrin plays in the disruption of actin cytoskeleton precedes loss of spines and suggests that drebrin as an early marker of AD pathology. In this study, we also showed, using 3xTg-AD mice that the loss of drebrin (Figure 19A,B) also correlated with age in the forebrain (Figure 19C,D) while the presynaptic marker, synaptophysin, significant loss was observed only in the hippocampus (Figure 19E,F). In human counterparts, a similar trend was found where loss of presynaptic markers such as synaptophysin were less extensive compared to drebrin [12,13]. These indicate drebrin is more sensitive to pathology and these asymmetric changes in presynaptic and postsynaptic proteins may initiate the synaptic pathology that leads to cognitive impairment.

Drebrin is lost in the cerebral cortex of AD patients including the prefrontal cortex and hippocampus [12,13]. The loss of drebrin was recapitulated in 3xTg-AD mouse (Figure 19) [15,259]. Drebrin is also lost in animal models of AD that display synaptic pathology including Tg2576 [15], 2xKI [16] and presenilin conditional double knockout (PScDKO) mice [173]. Transgenic modeling of AD took advantage of mutations in the APP, presenilin and/or tau to reproduce senile plaques and neurofibrillary tangles pathologies. 3xTg-AD mice exhibits both amyloid and tau pathologies as well as synaptic dysfunction,

and thus, captures a broader spectrum of AD pathology compared with other AD transgenic mouse that reproduces only the amyloid pathology [244]. However, 3xTg-AD mouse model still has limitations as it is based on the expression of mutant genes that cause familial form of AD, which accounts for 5-10% of all AD cases [278]. Therefore it may not replicate the underlying pathogenesis of sporadic AD. Further, 3xTg-AD and other AD mouse models express the transgene from development, which disrupts normal development of the brain. In most cases, AD pathology occurs later in life, which calls for the need for temporal regulation of the transgenes in AD models. Additionally, 3xTg-AD (data not shown) and other mouse models do not show consistent upregulation of Egr-1, but rather shows downregulation of Egr-1 [279-282]. This is contrary to human counterparts that shows Egr-1 upregulation in AD patients [27,28]. We demonstrate here the importance of Egr-1 with regards to loss of drebrin. Taken together, Egr-1 upregulation needs to be taken into consideration for the future development of a model for AD.

Here we generated Egr-1 Tg mouse that showed reduction in drebrin level when Egr-1 was upregulated (Figure 17). Egr-1 Tg mouse addresses Egr-1 aspect of AD unlike other AD models without carrying the APP, presenilin and/or tau transgenes. Egr-1 Tg mouse model isolates and focuses on Egr-1 aspect of AD by having the advantage of being able to control Egr-1 upregulation spatiotemporally. Therefore, normal development of neurons and synapses was preserved in Egr-1 Tg mouse. Furthermore, upregulation of Egr-1 was induced once Egr-1 Tg mouse reached an old age, which addressed the association between drebrin loss in AD and aging. In addition, specific upregulation of Egr-1 in the forebrain without altering Egr-1 levels in other tissues allowed us to focus on brain regions that are severely affected in AD. In response to Egr-

1 upregulation, drebrin loss was observed in the absence of neither amyloid nor tau pathologies. This supports the idea that Egr-1 is a nodal point in AD pathogenesis whose induction leads to loss of drebrin and highlights Egr-1 as a target of therapeutic intervention in AD.

The negative regulation of drebrin was further supported using Egr-1 -/- mouse (Figure 18). Although Egr-1 loss-of-function was ubiquitous throughout the brain, the increase in drebrin was specific to brain regions involved in learning and memory where constant synaptic plasticity occurs. Under physiological conditions, Egr-1 plays a greater role in regions with high synaptic plasticity as its activation is linked to the activity of glutamate receptors, NMDARs and AMPARs [213,214]. In brain regions that display relatively less plasticity such as cerebellum the basal level of Egr-1 remains normally low [211,258], allowing drebrin to be expressed at a constant level. Whether changes in drebrin level also occurs in other regions of the forebrain remains to be determined. We predict that the increase in drebrin will be specific to regions that experience high synaptic plasticity as these regions constantly undergo dendritic spine remodeling accompanied by drebrin.

Drebrin loss is observed not only in AD but also in Down's syndrome [10] and possibly in other cognitive disorders accompanied by loss of dendritic spines. The loss of drebrin in these disorders is also likely to be regulated by Egr-1. Hence Egr-1-drebrin interaction may not be limited to AD but could be a common pathway via which dendritic spines are lost.

5.3 Dendritic spines are lost in response to Egr-1-mediated downregulation of drebrin

The correlation between loss of drebrin and dendritic spines has been studied in depth with respect to AD [10,12,283]. In line with this, we demonstrate loss of dendritic spine density correlate with Egr-1-mediated loss of drebrin in Ln-Egr-1-transduced hippocampal neurons (Figure 20) and Egr-1 Tg mouse model (Figure 21). On the other hand, increase in drebrin led to increase in spine density in response to Egr-1 loss-of-function (Figure 22). These results suggest Egr-1 negatively regulates drebrin and is inversely correlated with dendritic spine density.

Drebrin is present in 75% of the dendritic spines in the cerebral cortex [142], and could be higher in hippocampus due to the high content of glutamatergic synapses. Drebrin is essential in spine formation, maintenance and plasticity. Consequently, loss of drebrin leads to cascade of events that ultimately results in the demise of dendritic spine density. In support of our *in vitro* and *in vivo* data showing loss of drebrin and overall loss dendritic protrusion/spine density, knockdown of drebrin using antisense oligonucleotides in primary hippocampal neurons was shown to lead to loss of spine and filopodia density [8,284]. Furthermore, decrease in spine density was also observed in drebrin knockout mouse [155]. This association between drebrin and dendritic spine density was recently found to be mediated by spikar, a novel drebrin-binding protein that regulate dendritic spine density [154]. Here we demonstrated reduction in drebrin-positive dendritic protrusions and spine density in response to upregulation of Egr-1 *in vitro* and *in vivo*. These data support Egr-1 TF being the upstream regulator of drebrin whose sustained upregulation leads to downregulation of drebrin and loss of dendritic spines.

In addition to loss of dendritic spine density, we demonstrated drebrin loss correlates with impaired maturation of dendritic spines and reduction in the number of synaptic contacts (Figure 24,25). In AD and related cognitive disorders, loss of drebrin is accompanied by synaptic pathology [10,259]. These findings imply that drebrin loss in response to Egr-1 upregulation would lead to synaptic dysfunction. Drebrin is required for PSD-95 and actin clustering at dendritic spines, and thus, drebrin loss prevents PSD-95 accumulation, which hinders AMPAR and NMDAR recruitment to the postsynaptic membrane as was shown by the decrease in GluA1 subunit of AMPAR (Figure 26). The destabilization of actin cytoskeleton within dendritic spines due to loss of drebrin and the impairment in PSD-95 accumulation would promote AMPAR endocytosis [283,285]. Also, drebrin was found to directly induce synaptic targeting of NMDARs in an activity-dependent manner [8]. Consequently, the loss of PSD-95 translated into decrease in synaptic contacts [286]. The colocalization of PSD-95 and vGluT1 implies the presence of synaptic contact where in mature neurons of 14DIV, the colocalization correlated with the amplitude of the postsynaptic response AMPA-type glutamate receptor currents (uEPSCs) [286]. Based on this knowledge, we predict that decrease of synaptic contacts would correlate with the decrease of synaptic activity. In fact, downregulation of drebrin in primary hippocampal neurons impairs both glutamatergic and GABAergic synaptic activity and leads to decrease of both excitatory and inhibitory synaptic transmissions [153]. Moreover, knockout of drebrin A eliminates homeostatic synaptic plasticity that is required for maintenance of synaptic strength in order to protect the neurons from unconstrained LTP [287]. The increase in vGluT1 presynaptic protein appears to be

compensatory in order to re-establish the communication with dysfunctional postsynaptic receivers.

Knockdown of drebrin in hippocampal neurons was shown to disrupt morphological distribution of the spines by promoting formation of thin immature spines [8]. Conversely, increase of drebrin in cortical neurons was shown to elongate the dendritic spines [122] while in immature neurons, large abnormal "megapodia" was formed [288]. However, these morphological changes in response to direct manipulation of drebrin may be limited to *in vitro* studies, because drebrin knockout mice showed decrease in spine density without significant changes in morphological distribution [155]. In AD, much of drebrin loss was emphasized to be associated with loss of dendritic spines. It remains unclear to what extent morphological distribution of the spines is changed in AD although in animal models and *in vitro* models, decreases in the frequency of large spines were observed [18,289]. Here, Egr-1-mediated changes in drebrin did not induce changes in the morphological distribution of dendritic spines. Therefore, changes in the upstream regulator of drebrin appear to have more moderate effect on drebrin where Egr-1 regulates drebrin present equally in immature and mature spines. Consequently the morphological distribution was maintained while the density was reduced in Ln-Egr-1-transduced hippocampal neurons and Egr-1 Tg mouse, and increased in Egr-1 -/- mouse. These data suggest that Egr-1 upregulation in AD may contribute to synaptic dysfunction by reducing the number of dendritic spines and not by the changing of morphology.

Phenotypically, loss of dendritic spines is reflected in deterioration of cognition and information processing as synapse growth and strength represents memory formation and storage [98,100,101,104,290]. Synaptic pathology in human counterparts is associated with

neuronal degeneration and aging. In AD prominent decreases in neuronal density were observed in the CA1 and CA3 region of the hippocampus [291]. Therefore it follows that the reduction of spine density observed in the hippocampus of Egr-1 Tg would lead to memory problems and cognitive deficits. Also, based on decreased expression of drebrin observed in prefrontal cortex, we predict that there would also be decreased spine density that further adds to exacerbate the cognitive deficit.

In majority of the past studies, emphasis on Egr-1 was given for its involvement in the late-phase of LTP, which translates into memory consolidation [25]. With regards to this, an inducible mouse model of Egr-1 was used to demonstrate Egr-1's role in memory consolidation. In these mice, Egr-1 upregulation in the forebrain during the establishment of object memories led to greater capacity to form a long-term memory with regards to spatial location of objects but not of the objects themselves using object and object-place recognition memory tasks [227]. Furthermore, induction of Egr-1 in the amygdala (forebrain) of the inducible mouse model of Egr-1 from 6 days prior to experiments was shown to delay the extinction of conditioned taste aversion, which indicates Egr-1's role in memory consolidation [240]. These observations suggest short-term Egr-1 overexpression facilitates the long-term memory formation.

On the surface these data appears to contradict our hypothesis that Egr-1 upregulation leads to loss of drebrin. However, these past studies for Egr-1 only focused on the transient induction of the gene in order to elucidate the physiological role of Egr-1. Likewise, the inducible model of Egr-1 used in the recent study were younger in terms of age (between 6- to 12-mo) and most importantly, Egr-1 was transiently induced for 6-8 days prior to the experiments. Therefore, these data do not reflect the role Egr-1 plays

when its expression is sustained for a long-term as is the case in AD. Based on our data, we propose that sustained upregulation of Egr-1 which was observed in AD may exert detrimental effect on cognition due to synaptic dysfunction. Therefore, behavioral studies to measure cognitive function in our Egr-1 Tg mouse model are needed to assess whether loss of drebrin translates into cognitive impairment. It was shown that drebrin A knockout rats display disrupted synaptic function that leads to cognitive impairment as they show schizophrenia-type of impulsive behaviour including impaired pre-pulse inhibition and increased sensitivity to stimulants [163]. Egr-1 Tg mouse with sustained upregulation of Egr-1 could show similar memory deficits as in AD and other cognitive impairments as was observed in drebrin knockout rats.

Following the logic that spine density positively correlates with memory, the increased spine density observed in response to Egr-1 loss-of-function should result in enhanced LTP and memory consolidation [85]. However in Egr-1 -/- mouse, early LTP in the dentate gyrus remained intact, but late protein-synthesis dependent LTP was absent [226]. As a result, short-term working memories and retention were intact while long-term spatial memory was impaired in these mice. Also, the CA1 place cells of Egr-1 -/- mice were impaired in terms of maintaining long-term place fields, which is an essential component of the spatial memory system [239]. These learning deficits highlight the importance of transient expression Egr-1 for LTP and memory consolidation. Despite the advantages of Egr-1 -/- mouse model for elucidating the role of Egr-1 in the brain, these mice have a limitation as a knockout model. An Egr-1 loss-of-function that is present from the development stage affects the neuronal development and thus, must be different from the neuronal development of Egr-1 +/+ mouse. Consequently, the learning deficit

observed in Egr-1 -/- mouse may be the accumulated product of developmental defects and cannot be used to address Egr-1 loss-of-function with respect to aging. To address this, a need arises for a mouse model whose Egr-1 function can be turned off once maturity is reached. With relevance to AD, our data indicate that sustained upregulation of Egr-1 leads to loss of drebrin and dendritic spines. Our data, together with the current knowledge regarding physiological function of Egr-1, proposed as a future direction, to study the effect of Egr-1 downregulation in an AD model that shows increased Egr-1 expression. We predict that downregulation of Egr-1 would lead to increase in drebrin expression and may ultimately result in either prevention of spine loss or replenishment of the spines depending on the stage of AD pathology.

Chapter 6. Conclusion

The present thesis demonstrates a novel role of Egr-1 in the brain and expands the current knowledge in drebrin and dendritic spine regulation. Dendritic spine loss in AD and related disorders occurs from loss of the postsynaptic protein drebrin via an unknown mechanism. In this thesis, we proposed Egr-1 as the nodal point via which regulation of drebrin occurs during dendritic spine loss. Our combined results demonstrated by utilizing both *in vitro* and *in vivo* models, that 1) Egr-1 binds to EREs on drebrin promoter; 2) Egr-1 negatively regulates drebrin and 3) Egr-1-mediated loss of drebrin correlates with loss of dendritic spine density. These results point to a novel role and mode of action of Egr-1 during synaptic pathology in AD and possibly other cognitive impairments characterized by loss of dendritic spines and Egr-1 upregulation. While upregulation of Egr-1 leads to dendritic spine loss, physiological levels of Egr-1 are necessary for memory formation. Similarly, while loss of drebrin leads to spine loss and disrupt memory formation, overexpression of drebrin leads to formation of irregular abnormal spines. Therefore, as a therapeutic option, future research should place emphasis in re-establishing physiological levels of Egr-1, which would lead to homeostatic synaptic symmetry.

References

1 Yuste, R. & Bonhoeffer, T. Morphological changes in dendritic spines associated with long-term synaptic plasticity. *Annu Rev Neurosci* **24**, 1071-1089, doi:10.1146/annurev.neuro.24.1.1071 (2001).

2 Lang, C. *et al.* Transient expansion of synaptically connected dendritic spines upon induction of hippocampal long-term potentiation. *Proceedings of the National Academy of Sciences of the United States of America* **101**, 16665-16670, doi:10.1073/pnas.0407581101 (2004).

3 Tsai, J., Grutzendler, J., Duff, K. & Gan, W. B. Fibrillar amyloid deposition leads to local synaptic abnormalities and breakage of neuronal branches. *Nature neuroscience* **7**, 1181-1183, doi:10.1038/nn1335 (2004).

4 Selkoe, D. J. Alzheimer's disease is a synaptic failure. *Science* **298**, 789-791, doi:10.1126/science.1074069 (2002).

5 Stephan, K. E., Baldeweg, T. & Friston, K. J. Synaptic plasticity and dysconnection in schizophrenia. *Biol Psychiatry* **59**, 929-939, doi:10.1016/j.biopsych.2005.10.005 (2006).

6 Pfeiffer, B. E. & Huber, K. M. The state of synapses in fragile X syndrome. *Neuroscientist* **15**, 549-567, doi:10.1177/1073858409333075 (2009).

7 Sekino, Y., Kojima, N. & Shirao, T. Role of actin cytoskeleton in dendritic spine morphogenesis. *Neurochemistry international* **51**, 92-104, doi:10.1016/j.neuint.2007.04.029 (2007).

8 Takahashi, H., Mizui, T. & Shirao, T. Down-regulation of drebrin A expression suppresses synaptic targeting of NMDA receptors in developing hippocampal neurones. *Journal of neurochemistry* **97 Suppl 1**, 110-115, doi:10.1111/j.1471-4159.2005.03536.x (2006).

9 Mizui, T., Takahashi, H., Sekino, Y. & Shirao, T. Overexpression of drebrin A in immature neurons induces the accumulation of F-actin and PSD-95 into dendritic filopodia, and the formation of large abnormal protrusions. *Molecular and cellular neurosciences* **30**, 149-157, doi:10.1016/j.mcn.2005.06.008 (2005).

10 Shim, K. S. & Lubec, G. Drebrin, a dendritic spine protein, is manifold decreased in brains of patients with Alzheimer's disease and Down syndrome. *Neuroscience letters* **324**, 209-212 (2002).

11 Takahashi, H. *et al.* Drebrin-dependent actin clustering in dendritic filopodia governs synaptic targeting of postsynaptic density-95 and dendritic spine morphogenesis. *The Journal of neuroscience : the official journal of the Society for Neuroscience* **23**, 6586-6595 (2003).

12 Harigaya, Y., Shoji, M., Shirao, T. & Hirai, S. Disappearance of actin-binding protein, drebrin, from hippocampal synapses in Alzheimer's disease. *Journal of neuroscience research* **43**, 87-92, doi:10.1002/jnr.490430111 (1996).

13 Hatanpaa, K., Isaacs, K. R., Shirao, T., Brady, D. R. & Rapoport, S. I. Loss of proteins regulating synaptic plasticity in normal aging of the human brain and in Alzheimer disease. *J Neuropathol Exp Neurol* **58**, 637-643 (1999).

14 Counts, S. E., Nadeem, M., Lad, S. P., Wuu, J. & Mufson, E. J. Differential expression of synaptic proteins in the frontal and temporal cortex of elderly subjects with mild cognitive impairment. *J Neuropathol Exp Neurol* **65**, 592-601 (2006).
15 Calon, F. *et al.* Docosahexaenoic acid protects from dendritic pathology in an Alzheimer's disease mouse model. *Neuron* **43**, 633-645, doi:10.1016/j.neuron.2004.08.013 (2004).
16 Mahadomrongkul, V., Huerta, P. T., Shirao, T. & Aoki, C. Stability of the distribution of spines containing drebrin A in the sensory cortex layer I of mice expressing mutated APP and PS1 genes. *Brain research* **1064**, 66-74, doi:10.1016/j.brainres.2005.10.012 (2005).
17 Zhao, L. *et al.* Role of p21-activated kinase pathway defects in the cognitive deficits of Alzheimer disease. *Nature neuroscience* **9**, 234-242, doi:10.1038/nn1630 (2006).
18 Lacor, P. N. *et al.* Abeta oligomer-induced aberrations in synapse composition, shape, and density provide a molecular basis for loss of connectivity in Alzheimer's disease. *The Journal of neuroscience : the official journal of the Society for Neuroscience* **27**, 796-807, doi:10.1523/JNEUROSCI.3501-06.2007 (2007).
19 Khachigian, L. M. *et al.* Egr-1 is activated in endothelial cells exposed to fluid shear stress and interacts with a novel shear-stress-response element in the PDGF A-chain promoter. *Arterioscler Thromb Vasc Biol* **17**, 2280-2286 (1997).
20 Yan, S. F., Mackman, N., Kisiel, W., Stern, D. M. & Pinsky, D. J. Hypoxia/Hypoxemia-Induced activation of the procoagulant pathways and the pathogenesis of ischemia-associated thrombosis. *Arterioscler Thromb Vasc Biol* **19**, 2029-2035 (1999).
21 Nishi, H., Nishi, K. H. & Johnson, A. C. Early Growth Response-1 gene mediates up-regulation of epidermal growth factor receptor expression during hypoxia. *Cancer Res* **62**, 827-834 (2002).
22 Ouellette, A. J., Malt, R. A., Sukhatme, V. P. & Bonventre, J. V. Expression of two "immediate early" genes, Egr-1 and c-fos, in response to renal ischemia and during compensatory renal hypertrophy in mice. *J Clin Invest* **85**, 766-771, doi:10.1172/JCI114502 (1990).
23 Bonventre, J. V., Sukhatme, V. P., Bamberger, M., Ouellette, A. J. & Brown, D. Localization of the protein product of the immediate early growth response gene, Egr-1, in the kidney after ischemia and reperfusion. *Cell Regul* **2**, 251-260 (1991).
24 Brand, T. *et al.* Proto-oncogene expression in porcine myocardium subjected to ischemia and reperfusion. *Circ Res* **71**, 1351-1360 (1992).
25 Beckmann, A. M. & Wilce, P. A. Egr transcription factors in the nervous system. *Neurochemistry international* **31**, 477-510; discussion 517-476 (1997).
26 Baron, V., Adamson, E. D., Calogero, A., Ragona, G. & Mercola, D. The transcription factor Egr1 is a direct regulator of multiple tumor suppressors

including TGFbeta1, PTEN, p53, and fibronectin. *Cancer Gene Ther* **13**, 115-124, doi:10.1038/sj.cgt.7700896 (2006).
27 MacGibbon, G. A. *et al.* Expression of Fos, Jun, and Krox family proteins in Alzheimer's disease. *Exp Neurol* **147**, 316-332, doi:10.1006/exnr.1997.6600 (1997).
28 Gomez Ravetti, M., Rosso, O. A., Berretta, R. & Moscato, P. Uncovering molecular biomarkers that correlate cognitive decline with the changes of hippocampus' gene expression profiles in Alzheimer's disease. *PLoS One* **5**, e10153, doi:10.1371/journal.pone.0010153 (2010).
29 James, A. B., Conway, A. M. & Morris, B. J. Genomic profiling of the neuronal target genes of the plasticity-related transcription factor -- Zif268. *Journal of neurochemistry* **95**, 796-810, doi:10.1111/j.1471-4159.2005.03400.x (2005).
30 van Rossum, D. & Hanisch, U. K. Cytoskeletal dynamics in dendritic spines: direct modulation by glutamate receptors? *Trends Neurosci* **22**, 290-295 (1999).
31 Harris, K. M. & Kater, S. B. Dendritic spines: cellular specializations imparting both stability and flexibility to synaptic function. *Annu Rev Neurosci* **17**, 341-371, doi:10.1146/annurev.ne.17.030194.002013 (1994).
32 Golgi, C. Sulla struttura della sostanza grigia del cervello. *Gaz. Med. Ital. Lomb.* **33**, 244-246 (1873).
33 Cajal, S. R. *Histologie du système nerveux de l'homme & des vertébrés*. Vol. I and II (Maloine, 1911).
34 Cajal, S. R. Textura de las circunvolunciones cerebrales de los mamiferos inferiores. Nota preventiva. *Gac. Med. Catalana* **1**, 22-31 (1890).
35 Cajal, S. R. ¿Neuronismo o Reticularismo? Las Pruebas Objetivas de la Unidad Anatómica de las Células Nerviosas. *Arch. Neurobiol.* **13**, 217-291 (1933).
36 Gray, E. G. Electron microscopy of synaptic contacts on dendrite spines of the cerebral cortex. *Nature* **183**, 1592-1593 (1959).
37 Fairen, A., Peters, A. & Saldanha, J. A new procedure for examining Golgi impregnated neurons by light and electron microscopy. *J Neurocytol* **6**, 311-337 (1977).
38 Colonnier, M. Synaptic patterns on different cell types in the different laminae of the cat visual cortex. An electron microscope study. *Brain research* **9**, 268-287 (1968).
39 Korobova, F. & Svitkina, T. Molecular architecture of synaptic actin cytoskeleton in hippocampal neurons reveals a mechanism of dendritic spine morphogenesis. *Mol Biol Cell* **21**, 165-176, doi:10.1091/mbc.E09-07-0596 (2010).
40 Honkura, N., Matsuzaki, M., Noguchi, J., Ellis-Davies, G. C. & Kasai, H. The subspine organization of actin fibers regulates the structure and plasticity of dendritic spines. *Neuron* **57**, 719-729, doi:10.1016/j.neuron.2008.01.013 (2008).
41 Bellot, A. *et al.* The structure and function of actin cytoskeleton in mature glutamatergic dendritic spines. *Brain research* **1573**, 1-16, doi:10.1016/j.brainres.2014.05.024 (2014).

42 Bourne, J. N. & Harris, K. M. Balancing structure and function at hippocampal dendritic spines. *Annu Rev Neurosci* **31**, 47-67, doi:10.1146/annurev.neuro.31.060407.125646 (2008).
43 Rochefort, N. L. & Konnerth, A. Dendritic spines: from structure to in vivo function. *EMBO Rep* **13**, 699-708, doi:10.1038/embor.2012.102 (2012).
44 Kasai, H., Matsuzaki, M., Noguchi, J., Yasumatsu, N. & Nakahara, H. Structure-stability-function relationships of dendritic spines. *Trends Neurosci* **26**, 360-368, doi:10.1016/S0166-2236(03)00162-0 (2003).
45 Hayashi, Y. & Majewska, A. K. Dendritic spine geometry: functional implication and regulation. *Neuron* **46**, 529-532, doi:10.1016/j.neuron.2005.05.006 (2005).
46 Hayashi, T., Rumbaugh, G. & Huganir, R. L. Differential regulation of AMPA receptor subunit trafficking by palmitoylation of two distinct sites. *Neuron* **47**, 709-723, doi:10.1016/j.neuron.2005.06.035 (2005).
47 Bourne, J. & Harris, K. M. Do thin spines learn to be mushroom spines that remember? *Curr Opin Neurobiol* **17**, 381-386, doi:10.1016/j.conb.2007.04.009 (2007).
48 Roberts, T. F., Tschida, K. A., Klein, M. E. & Mooney, R. Rapid spine stabilization and synaptic enhancement at the onset of behavioural learning. *Nature* **463**, 948-952, doi:10.1038/nature08759 (2010).
49 Fiala, J. C., Feinberg, M., Popov, V. & Harris, K. M. Synaptogenesis via dendritic filopodia in developing hippocampal area CA1. *The Journal of neuroscience : the official journal of the Society for Neuroscience* **18**, 8900-8911 (1998).
50 Sorra, K. E. & Harris, K. M. Overview on the structure, composition, function, development, and plasticity of hippocampal dendritic spines. *Hippocampus* **10**, 501-511, doi:10.1002/1098-1063(2000)10:5<501::AID-HIPO1>3.0.CO;2-T (2000).
51 Portera-Cailliau, C., Pan, D. T. & Yuste, R. Activity-regulated dynamic behavior of early dendritic protrusions: evidence for different types of dendritic filopodia. *The Journal of neuroscience : the official journal of the Society for Neuroscience* **23**, 7129-7142 (2003).
52 Reilly, J. E., Hanson, H. H. & Phillips, G. R. Persistence of excitatory shaft synapses adjacent to newly emerged dendritic protrusions. *Molecular and cellular neurosciences* **48**, 129-136, doi:10.1016/j.mcn.2011.06.014 (2011).
53 Woolley, C. S. & McEwen, B. S. Roles of estradiol and progesterone in regulation of hippocampal dendritic spine density during the estrous cycle in the rat. *The Journal of comparative neurology* **336**, 293-306, doi:10.1002/cne.903360210 (1993).
54 Xu, T. *et al.* Rapid formation and selective stabilization of synapses for enduring motor memories. *Nature* **462**, 915-919, doi:10.1038/nature08389 (2009).
55 Yang, G., Pan, F. & Gan, W. B. Stably maintained dendritic spines are associated with lifelong memories. *Nature* **462**, 920-924, doi:10.1038/nature08577 (2009).
56 Sala, C. & Segal, M. Dendritic spines: the locus of structural and functional plasticity. *Physiol Rev* **94**, 141-188, doi:10.1152/physrev.00012.2013 (2014).

57 Hanse, E., Taira, T., Lauri, S. & Groc, L. Glutamate synapse in developing brain: an integrative perspective beyond the silent state. *Trends Neurosci* **32**, 532-537, doi:10.1016/j.tins.2009.07.003 (2009).
58 Passafaro, M., Nakagawa, T., Sala, C. & Sheng, M. Induction of dendritic spines by an extracellular domain of AMPA receptor subunit GluR2. *Nature* **424**, 677-681, doi:10.1038/nature01781 (2003).
59 Fortin, D. A. *et al.* Long-term potentiation-dependent spine enlargement requires synaptic Ca2+-permeable AMPA receptors recruited by CaM-kinase I. *The Journal of neuroscience : the official journal of the Society for Neuroscience* **30**, 11565-11575, doi:10.1523/JNEUROSCI.1746-10.2010 (2010).
60 Matsuzaki, M., Honkura, N., Ellis-Davies, G. C. & Kasai, H. Structural basis of long-term potentiation in single dendritic spines. *Nature* **429**, 761-766, doi:10.1038/nature02617 (2004).
61 Holtmaat, A., Wilbrecht, L., Knott, G. W., Welker, E. & Svoboda, K. Experience-dependent and cell-type-specific spine growth in the neocortex. *Nature* **441**, 979-983, doi:10.1038/nature04783 (2006).
62 Siekevitz, P. The postsynaptic density: a possible role in long-lasting effects in the central nervous system. *Proceedings of the National Academy of Sciences of the United States of America* **82**, 3494-3498 (1985).
63 Kennedy, M. B. Signal-processing machines at the postsynaptic density. *Science* **290**, 750-754 (2000).
64 Sheng, M. & Kim, M. J. Postsynaptic signaling and plasticity mechanisms. *Science* **298**, 776-780, doi:10.1126/science.1075333 (2002).
65 Carlin, R. K., Grab, D. J., Cohen, R. S. & Siekevitz, P. Isolation and characterization of postsynaptic densities from various brain regions: enrichment of different types of postsynaptic densities. *The Journal of cell biology* **86**, 831-845 (1980).
66 Sheng, M. & Hoogenraad, C. C. The postsynaptic architecture of excitatory synapses: a more quantitative view. *Annu Rev Biochem* **76**, 823-847, doi:10.1146/annurev.biochem.76.060805.160029 (2007).
67 Bhatt, D. H., Zhang, S. & Gan, W. B. Dendritic spine dynamics. *Annu Rev Physiol* **71**, 261-282, doi:10.1146/annurev.physiol.010908.163140 (2009).
68 Harris, K. M., Jensen, F. E. & Tsao, B. Three-dimensional structure of dendritic spines and synapses in rat hippocampus (CA1) at postnatal day 15 and adult ages: implications for the maturation of synaptic physiology and long-term potentiation. *The Journal of neuroscience : the official journal of the Society for Neuroscience* **12**, 2685-2705 (1992).
69 Harris, K. M. & Stevens, J. K. Dendritic spines of CA 1 pyramidal cells in the rat hippocampus: serial electron microscopy with reference to their biophysical characteristics. *The Journal of neuroscience : the official journal of the Society for Neuroscience* **9**, 2982-2997 (1989).
70 Papa, M., Bundman, M. C., Greenberger, V. & Segal, M. Morphological analysis of dendritic spine development in primary cultures of hippocampal neurons. *The Journal of neuroscience : the official journal of the Society for Neuroscience* **15**, 1-11 (1995).

71 Purpura, D. P. Dendritic spine "dysgenesis" and mental retardation. *Science* **186**, 1126-1128 (1974).
72 Coss, R. G. & Globus, A. Spine stems on tectal interneurons in jewel fish are shortened by social stimulation. *Science* **200**, 787-790 (1978).
73 Brandon, J. G. & Coss, R. G. Rapid dendritic spine stem shortening during one-trial learning: the honeybee's first orientation flight. *Brain research* **252**, 51-61 (1982).
74 Bradley, P. & Horn, G. Neuronal plasticity in the chick brain: morphological effects of visual experience on neurones in hyperstriatum accessorium. *Brain research* **162**, 148-153 (1979).
75 Trachtenberg, J. T. *et al.* Long-term in vivo imaging of experience-dependent synaptic plasticity in adult cortex. *Nature* **420**, 788-794, doi:10.1038/nature01273 (2002).
76 Grutzendler, J., Kasthuri, N. & Gan, W. B. Long-term dendritic spine stability in the adult cortex. *Nature* **420**, 812-816, doi:10.1038/nature01276 (2002).
77 Whitlock, J. R., Heynen, A. J., Shuler, M. G. & Bear, M. F. Learning induces long-term potentiation in the hippocampus. *Science* **313**, 1093-1097, doi:10.1126/science.1128134 (2006).
78 Gruart, A., Munoz, M. D. & Delgado-Garcia, J. M. Involvement of the CA3-CA1 synapse in the acquisition of associative learning in behaving mice. *The Journal of neuroscience : the official journal of the Society for Neuroscience* **26**, 1077-1087, doi:10.1523/JNEUROSCI.2834-05.2006 (2006).
79 Bliss, T. V. & Cooke, S. F. Long-term potentiation and long-term depression: a clinical perspective. *Clinics (Sao Paulo)* **66 Suppl 1**, 3-17 (2011).
80 Bliss, T. V. & Lomo, T. Long-lasting potentiation of synaptic transmission in the dentate area of the anaesthetized rabbit following stimulation of the perforant path. *J Physiol* **232**, 331-356 (1973).
81 Kaibara, T. & Leung, L. S. Basal versus apical dendritic long-term potentiation of commissural afferents to hippocampal CA1: a current-source density study. *The Journal of neuroscience : the official journal of the Society for Neuroscience* **13**, 2391-2404 (1993).
82 Alvarez, V. A., Ridenour, D. A. & Sabatini, B. L. Distinct structural and ionotropic roles of NMDA receptors in controlling spine and synapse stability. *The Journal of neuroscience : the official journal of the Society for Neuroscience* **27**, 7365-7376, doi:10.1523/JNEUROSCI.0956-07.2007 (2007).
83 Lee, H. K., Kameyama, K., Huganir, R. L. & Bear, M. F. NMDA induces long-term synaptic depression and dephosphorylation of the GluR1 subunit of AMPA receptors in hippocampus. *Neuron* **21**, 1151-1162 (1998).
84 Hosokawa, T., Rusakov, D. A., Bliss, T. V. & Fine, A. Repeated confocal imaging of individual dendritic spines in the living hippocampal slice: evidence for changes in length and orientation associated with chemically induced LTP. *The Journal of neuroscience : the official journal of the Society for Neuroscience* **15**, 5560-5573 (1995).
85 Lamprecht, R. The roles of the actin cytoskeleton in fear memory formation. *Front Behav Neurosci* **5**, 39, doi:10.3389/fnbeh.2011.00039 (2011).

86 Fukazawa, Y. *et al.* Hippocampal LTP is accompanied by enhanced F-actin content within the dendritic spine that is essential for late LTP maintenance in vivo. *Neuron* **38**, 447-460 (2003).
87 Kopec, C. D., Real, E., Kessels, H. W. & Malinow, R. GluR1 links structural and functional plasticity at excitatory synapses. *The Journal of neuroscience : the official journal of the Society for Neuroscience* **27**, 13706-13718, doi:10.1523/JNEUROSCI.3503-07.2007 (2007).
88 Zhou, Q., Homma, K. J. & Poo, M. M. Shrinkage of dendritic spines associated with long-term depression of hippocampal synapses. *Neuron* **44**, 749-757, doi:10.1016/j.neuron.2004.11.011 (2004).
89 Fifkova, E. & Delay, R. J. Cytoplasmic actin in neuronal processes as a possible mediator of synaptic plasticity. *The Journal of cell biology* **95**, 345-350 (1982).
90 Matus, A., Ackermann, M., Pehling, G., Byers, H. R. & Fujiwara, K. High actin concentrations in brain dendritic spines and postsynaptic densities. *Proceedings of the National Academy of Sciences of the United States of America* **79**, 7590-7594 (1982).
91 Murakoshi, H. & Yasuda, R. Postsynaptic signaling during plasticity of dendritic spines. *Trends Neurosci* **35**, 135-143, doi:10.1016/j.tins.2011.12.002 (2012).
92 Hayashi, K. *et al.* Modulatory role of drebrin on the cytoskeleton within dendritic spines in the rat cerebral cortex. *The Journal of neuroscience : the official journal of the Society for Neuroscience* **16**, 7161-7170 (1996).
93 Hotulainen, P. & Hoogenraad, C. C. Actin in dendritic spines: connecting dynamics to function. *The Journal of cell biology* **189**, 619-629, doi:10.1083/jcb.201003008 (2010).
94 Star, E. N., Kwiatkowski, D. J. & Murthy, V. N. Rapid turnover of actin in dendritic spines and its regulation by activity. *Nature neuroscience* **5**, 239-246, doi:10.1038/nn811 (2002).
95 Okamoto, K., Nagai, T., Miyawaki, A. & Hayashi, Y. Rapid and persistent modulation of actin dynamics regulates postsynaptic reorganization underlying bidirectional plasticity. *Nature neuroscience* **7**, 1104-1112, doi:10.1038/nn1311 (2004).
96 Lin, W. H. & Webb, D. J. Actin and Actin-Binding Proteins: Masters of Dendritic Spine Formation, Morphology, and Function. *Open Neurosci J* **3**, 54-66, doi:10.2174/1874082000903020054 (2009).
97 Cingolani, L. A. & Goda, Y. Actin in action: the interplay between the actin cytoskeleton and synaptic efficacy. *Nature reviews. Neuroscience* **9**, 344-356, doi:10.1038/nrn2373 (2008).
98 Tyan, S. H. *et al.* Amyloid precursor protein (APP) regulates synaptic structure and function. *Molecular and cellular neurosciences* **51**, 43-52, doi:10.1016/j.mcn.2012.07.009 (2012).
99 Kaufmann, W. E. & Moser, H. W. Dendritic anomalies in disorders associated with mental retardation. *Cerebral cortex* **10**, 981-991 (2000).
100 Selemon, L. D. & Goldman-Rakic, P. S. The reduced neuropil hypothesis: a circuit based model of schizophrenia. *Biol Psychiatry* **45**, 17-25 (1999).

101 Glantz, L. A. & Lewis, D. A. Decreased dendritic spine density on prefrontal cortical pyramidal neurons in schizophrenia. *Arch Gen Psychiatry* **57**, 65-73 (2000).
102 Gogtay, N. Cortical brain development in schizophrenia: insights from neuroimaging studies in childhood-onset schizophrenia. *Schizophr Bull* **34**, 30-36, doi:10.1093/schbul/sbm103 (2008).
103 Hutsler, J. J. & Zhang, H. Increased dendritic spine densities on cortical projection neurons in autism spectrum disorders. *Brain research* **1309**, 83-94, doi:10.1016/j.brainres.2009.09.120 (2010).
104 Tackenberg, C., Ghori, A. & Brandt, R. Thin, stubby or mushroom: spine pathology in Alzheimer's disease. *Curr Alzheimer Res* **6**, 261-268 (2009).
105 Spires-Jones, T. & Knafo, S. Spines, plasticity, and cognition in Alzheimer's model mice. *Neural Plast* **2012**, 319836, doi:10.1155/2012/319836 (2012).
106 DeKosky, S. T. & Scheff, S. W. Synapse loss in frontal cortex biopsies in Alzheimer's disease: correlation with cognitive severity. *Ann Neurol* **27**, 457-464, doi:10.1002/ana.410270502 (1990).
107 Arendt, T. Synaptic degeneration in Alzheimer's disease. *Acta Neuropathol* **118**, 167-179, doi:10.1007/s00401-009-0536-x (2009).
108 Pinto, D. *et al.* Functional impact of global rare copy number variation in autism spectrum disorders. *Nature* **466**, 368-372, doi:10.1038/nature09146 (2010).
109 Sudhof, T. C. Neuroligins and neurexins link synaptic function to cognitive disease. *Nature* **455**, 903-911, doi:10.1038/nature07456 (2008).
110 Sharma, S., Grintsevich, E. E., Phillips, M. L., Reisler, E. & Gimzewski, J. K. Atomic force microscopy reveals drebrin induced remodeling of f-actin with subnanometer resolution. *Nano letters* **11**, 825-827, doi:10.1021/nl104159v (2011).
111 Montenegro-Venegas, C. *et al.* MAP1B regulates axonal development by modulating Rho-GTPase Rac1 activity. *Mol Biol Cell* **21**, 3518-3528, doi:10.1091/mbc.E09-08-0709 (2010).
112 Nakayama, A. Y., Harms, M. B. & Luo, L. Small GTPases Rac and Rho in the maintenance of dendritic spines and branches in hippocampal pyramidal neurons. *The Journal of neuroscience : the official journal of the Society for Neuroscience* **20**, 5329-5338 (2000).
113 Murakoshi, H., Wang, H. & Yasuda, R. Local, persistent activation of Rho GTPases during plasticity of single dendritic spines. *Nature* **472**, 100-104, doi:10.1038/nature09823 (2011).
114 Gonzalez-Billault, C. *et al.* The role of small GTPases in neuronal morphogenesis and polarity. *Cytoskeleton (Hoboken)* **69**, 464-485, doi:10.1002/cm.21034 (2012).
115 Rex, C. S. *et al.* Different Rho GTPase-dependent signaling pathways initiate sequential steps in the consolidation of long-term potentiation. *The Journal of cell biology* **186**, 85-97, doi:10.1083/jcb.200901084 (2009).
116 Goldschmidt-Clermont, P. J. *et al.* The control of actin nucleotide exchange by thymosin beta 4 and profilin. A potential regulatory mechanism for actin polymerization in cells. *Mol Biol Cell* **3**, 1015-1024 (1992).

117 Kovar, D. R., Harris, E. S., Mahaffy, R., Higgs, H. N. & Pollard, T. D. Control of the assembly of ATP- and ADP-actin by formins and profilin. *Cell* **124**, 423-435, doi:10.1016/j.cell.2005.11.038 (2006).
118 Meng, Y. *et al.* Regulation of ADF/cofilin phosphorylation and synaptic function by LIM-kinase. *Neuropharmacology* **47**, 746-754, doi:10.1016/j.neuropharm.2004.06.030 (2004).
119 Mullins, R. D., Heuser, J. A. & Pollard, T. D. The interaction of Arp2/3 complex with actin: nucleation, high affinity pointed end capping, and formation of branching networks of filaments. *Proceedings of the National Academy of Sciences of the United States of America* **95**, 6181-6186 (1998).
120 Welch, M. D., Rosenblatt, J., Skoble, J., Portnoy, D. A. & Mitchison, T. J. Interaction of human Arp2/3 complex and the Listeria monocytogenes ActA protein in actin filament nucleation. *Science* **281**, 105-108 (1998).
121 Wegner, A. M. *et al.* N-wasp and the arp2/3 complex are critical regulators of actin in the development of dendritic spines and synapses. *The Journal of biological chemistry* **283**, 15912-15920, doi:10.1074/jbc.M801555200 (2008).
122 Hayashi, K. & Shirao, T. Change in the shape of dendritic spines caused by overexpression of drebrin in cultured cortical neurons. *The Journal of neuroscience : the official journal of the Society for Neuroscience* **19**, 3918-3925 (1999).
123 Shirao, T. & Obata, K. Two acidic proteins associated with brain development in chick embryo. *Journal of neurochemistry* **44**, 1210-1216 (1985).
124 Shirao, T. & Obata, K. Immunochemical homology of 3 developmentally regulated brain proteins and their developmental change in neuronal distribution. *Brain research* **394**, 233-244 (1986).
125 Shirao, T., Kojima, N., Terada, S. & Obata, K. Expression of three drebrin isoforms in the developing nervous system. *Neurosci Res Suppl* **13**, S106-111 (1990).
126 Shirao, T., Kojima, N., Nabeta, Y., and Obata, K. Two Forms of Drebrins, Developmentally Regulated Brain Proteins, in Rat. *Proc Jpn Acad* **65B**, 169 - 172 (1989).
127 Feinberg, A. P. & Vogelstein, B. A technique for radiolabeling DNA restriction endonuclease fragments to high specific activity. *Analytical biochemistry* **132**, 6-13 (1983).
128 Kojima, N., Kato, Y., Shirao, T. & Obata, K. Nucleotide sequences of two embryonic drebrins, developmentally regulated brain proteins, and developmental change in their mRNAs. *Brain research* **464**, 207-215 (1988).
129 Kojima, N., Shirao, T. & Obata, K. Molecular cloning of a developmentally regulated brain protein, chicken drebrin A and its expression by alternative splicing of the drebrin gene. *Brain research. Molecular brain research* **19**, 101-114 (1993).
130 Shirao, T., Kojima, N. & Obata, K. Cloning of drebrin A and induction of neurite-like processes in drebrin-transfected cells. *Neuroreport* **3**, 109-112 (1992).

131 Shirao, T., Kojima, N., Kato, Y. & Obata, K. Molecular cloning of a cDNA for the developmentally regulated brain protein, drebrin. *Brain research* **464**, 71-74 (1988).
132 Toda, M. *et al.* Molecular cloning of cDNA encoding human drebrin E and chromosomal mapping of its gene. *Biochemical and biophysical research communications* **196**, 468-472, doi:10.1006/bbrc.1993.2273 (1993).
133 Fisher, L. W., Mcbride, O.W., Filpula, D., Ibaraki, K., Young, M.F. Human drebrin cDNA sequence, mRNA tissue distribution and chromosomal localization. *Neurosci res comm.* **14**, 35-42 (1994).
134 Jin, M. *et al.* A novel, brain-specific mouse drebrin: cDNA cloning, chromosomal mapping, genomic structure, expression, and functional characterization. *Genomics* **79**, 686-692, doi:10.1006/geno.2002.6764 (2002).
135 Lappalainen, P., Kessels, M. M., Cope, M. J. & Drubin, D. G. The ADF homology (ADF-H) domain: a highly exploited actin-binding module. *Mol Biol Cell* **9**, 1951-1959 (1998).
136 Tu, J. C. *et al.* Homer binds a novel proline-rich motif and links group 1 metabotropic glutamate receptors with IP3 receptors. *Neuron* **21**, 717-726 (1998).
137 Worth, D. C., Daly, C. N., Geraldo, S., Oozeer, F. & Gordon-Weeks, P. R. Drebrin contains a cryptic F-actin-bundling activity regulated by Cdk5 phosphorylation. *The Journal of cell biology* **202**, 793-806, doi:10.1083/jcb.201303005 (2013).
138 Xu, W. & Stamnes, M. The actin-depolymerizing factor homology and charged/helical domains of drebrin and mAbp1 direct membrane binding and localization via distinct interactions with actin. *The Journal of biological chemistry* **281**, 11826-11833, doi:10.1074/jbc.M510141200 (2006).
139 Mammoto, A. *et al.* Interactions of drebrin and gephyrin with profilin. *Biochemical and biophysical research communications* **243**, 86-89, doi:10.1006/bbrc.1997.8068 (1998).
140 Shiraishi-Yamaguchi, Y. *et al.* Interaction of Cupidin/Homer2 with two actin cytoskeletal regulators, Cdc42 small GTPase and Drebrin, in dendritic spines. *BMC Neurosci* **10**, 25, doi:10.1186/1471-2202-10-25 (2009).
141 Shirao, T. The roles of microfilament-associated proteins, drebrins, in brain morphogenesis: a review. *J Biochem* **117**, 231-236 (1995).
142 Aoki, C. *et al.* Drebrin A is a postsynaptic protein that localizes in vivo to the submembranous surface of dendritic sites forming excitatory synapses. *The Journal of comparative neurology* **483**, 383-402, doi:10.1002/cne.20449 (2005).
143 Asada, H., Uyemura, K. & Shirao, T. Actin-binding protein, drebrin, accumulates in submembranous regions in parallel with neuronal differentiation. *Journal of neuroscience research* **38**, 149-159, doi:10.1002/jnr.490380205 (1994).
144 Ishikawa, R. *et al.* Drebrin, a development-associated brain protein from rat embryo, causes the dissociation of tropomyosin from actin filaments. *The Journal of biological chemistry* **269**, 29928-29933 (1994).

145 Grintsevich, E. E. & Reisler, E. Drebrin inhibits cofilin-induced severing of F-actin. *Cytoskeleton (Hoboken)* **71**, 472-483, doi:10.1002/cm.21184 (2014).
146 Bonder, E. M. & Mooseker, M. S. Cytochalasin B slows but does not prevent monomer addition at the barbed end of the actin filament. *The Journal of cell biology* **102**, 282-288 (1986).
147 Sampath, P. & Pollard, T. D. Effects of cytochalasin, phalloidin, and pH on the elongation of actin filaments. *Biochemistry* **30**, 1973-1980 (1991).
148 Ishikawa, R., Yamashiro, S. & Matsumura, F. Differential modulation of actin-severing activity of gelsolin by multiple isoforms of cultured rat cell tropomyosin. Potentiation of protective ability of tropomyosins by 83-kDa nonmuscle caldesmon. *The Journal of biological chemistry* **264**, 7490-7497 (1989).
149 Biedler, J. L., Helson, L. & Spengler, B. A. Morphology and growth, tumorigenicity, and cytogenetics of human neuroblastoma cells in continuous culture. *Cancer Res* **33**, 2643-2652 (1973).
150 Sasaki, Y., Hayashi, K., Shirao, T., Ishikawa, R. & Kohama, K. Inhibition by drebrin of the actin-bundling activity of brain fascin, a protein localized in filopodia of growth cones. *Journal of neurochemistry* **66**, 980-988 (1996).
151 Nwabuisi-Heath, E., LaDu, M. J. & Yu, C. Simultaneous analysis of dendritic spine density, morphology and excitatory glutamate receptors during neuron maturation in vitro by quantitative immunocytochemistry. *J Neurosci Methods* **207**, 137-147, doi:10.1016/j.jneumeth.2012.04.003 (2012).
152 Takahashi, H., Yamazaki, H., Hanamura, K., Sekino, Y. & Shirao, T. Activity of the AMPA receptor regulates drebrin stabilization in dendritic spine morphogenesis. *J Cell Sci* **122**, 1211-1219, doi:10.1242/jcs.043729 (2009).
153 Ivanov, A., Esclapez, M., Pellegrino, C., Shirao, T. & Ferhat, L. Drebrin A regulates dendritic spine plasticity and synaptic function in mature cultured hippocampal neurons. *J Cell Sci* **122**, 524-534, doi:10.1242/jcs.033464 (2009).
154 Yamazaki, H. *et al.* Spikar, a novel drebrin-binding protein, regulates the formation and stabilization of dendritic spines. *Journal of neurochemistry* **128**, 507-522, doi:10.1111/jnc.12486 (2014).
155 Jung, G. *et al.* Drebrin depletion alters neurotransmitter receptor levels in protein complexes, dendritic spine morphogenesis and memory-related synaptic plasticity in the mouse hippocampus. *Journal of neurochemistry* **134**, 327-339, doi:10.1111/jnc.13119 (2015).
156 Tu, J. C. *et al.* Coupling of mGluR/Homer and PSD-95 complexes by the Shank family of postsynaptic density proteins. *Neuron* **23**, 583-592 (1999).
157 Shiraishi, Y. *et al.* Cupidin, an isoform of Homer/Vesl, interacts with the actin cytoskeleton and activated rho family small GTPases and is expressed in developing mouse cerebellar granule cells. *The Journal of neuroscience : the official journal of the Society for Neuroscience* **19**, 8389-8400 (1999).
158 Shiraishi, Y., Mizutani, A., Mikoshiba, K. & Furuichi, T. Coincidence in dendritic clustering and synaptic targeting of homer proteins and NMDA receptor complex proteins NR2B and PSD95 during development of cultured

hippocampal neurons. *Molecular and cellular neurosciences* **22**, 188-201 (2003).
159 Shiraishi, Y., Mizutani, A., Yuasa, S., Mikoshiba, K. & Furuichi, T. Glutamate-induced declustering of post-synaptic adaptor protein Cupidin (Homer 2/vesl-2) in cultured cerebellar granule cells. *Journal of neurochemistry* **87**, 364-376 (2003).
160 Sala, C. *et al.* Regulation of dendritic spine morphology and synaptic function by Shank and Homer. *Neuron* **31**, 115-130 (2001).
161 Fregnac, Y. & Imbert, M. Development of neuronal selectivity in primary visual cortex of cat. *Physiol Rev* **64**, 325-434 (1984).
162 Imamura, K., Shirao, T., Mori, K. & Obata, K. Changes of drebrin expression in the visual cortex of the cat during development. *Neuroscience research* **13**, 33-41 (1992).
163 Kobayashi, R. *et al.* Antisense knockdown of drebrin A, a dendritic spine protein, causes stronger preference, impaired pre-pulse inhibition, and an increased sensitivity to psychostimulant. *Neuroscience research* **49**, 205-217, doi:10.1016/j.neures.2004.02.014 (2004).
164 Kojima, N. *et al.* Genetic disruption of the alternative splicing of drebrin gene impairs context-dependent fear learning in adulthood. *Neuroscience* **165**, 138-150, doi:10.1016/j.neuroscience.2009.10.016 (2010).
165 Rinaldi, A., Mandillo, S., Oliverio, A. & Mele, A. D1 and D2 receptor antagonist injections in the prefrontal cortex selectively impair spatial learning in mice. *Neuropsychopharmacology* **32**, 309-319, doi:10.1038/sj.npp.1301176 (2007).
166 Vijayraghavan, S., Wang, M., Birnbaum, S. G., Williams, G. V. & Arnsten, A. F. Inverted-U dopamine D1 receptor actions on prefrontal neurons engaged in working memory. *Nature neuroscience* **10**, 376-384, doi:10.1038/nn1846 (2007).
167 Takahashi, H., Yamada, M. & Suhara, T. Functional significance of central D1 receptors in cognition: beyond working memory. *J Cereb Blood Flow Metab* **32**, 1248-1258, doi:10.1038/jcbfm.2011.194 (2012).
168 Julien, C. *et al.* Decreased drebrin mRNA expression in Alzheimer disease: correlation with tau pathology. *Journal of neuroscience research* **86**, 2292-2302, doi:10.1002/jnr.21667 (2008).
169 Arai, H., Sato K., Uto A., Yasumoto Y. Effect of transient cerebral ischemia in mongolian gerbils on synaptic vesicle protein (SVP-38) and developmentally regulated brain protein (drebrin). *Neurosci Res Commun.* **9**, 143-150 (1991).
170 Weitzdoerfer, R., Dierssen, M., Fountoulakis, M. & Lubec, G. Fetal life in Down syndrome starts with normal neuronal density but impaired dendritic spines and synaptosomal structure. *Journal of neural transmission. Supplementum*, 59-70 (2001).
171 Counts, S. E. *et al.* Hippocampal drebrin loss in mild cognitive impairment. *Neurodegener Dis* **10**, 216-219, doi:10.1159/000333122 (2012).
172 Flood, D. G. *et al.* FAD mutant PS-1 gene-targeted mice: increased A beta 42 and A beta deposition without APP overproduction. *Neurobiol Aging* **23**, 335-348 (2002).

173 Lee, D. & Aoki, C. Presenilin conditional double knockout mice exhibit decreases in drebrin a at hippocampal CA1 synapses. *Synapse* **66**, 870-879, doi:10.1002/syn.21578 (2012).
174 Ooe, N., Saito, K., Mikami, N., Nakatuka, I. & Kaneko, H. Identification of a novel basic helix-loop-helix-PAS factor, NXF, reveals a Sim2 competitive, positive regulatory role in dendritic-cytoskeleton modulator drebrin gene expression. *Mol Cell Biol* **24**, 608-616 (2004).
175 Vialard, F. *et al.* Overexpression of mSim2 gene in the zona limitans of the diencephalon of segmental trisomy 16 Ts1Cje fetuses, a mouse model for trisomy 21: a novel whole-mount based RNA hybridization study. *Brain Res Dev Brain Res* **121**, 73-78 (2000).
176 Ema, M. *et al.* Mild impairment of learning and memory in mice overexpressing the mSim2 gene located on chromosome 16: an animal model of Down's syndrome. *Hum Mol Genet* **8**, 1409-1415 (1999).
177 Shim, K. S., Ferrando-Miguel, R. & Lubec, G. Aberrant protein expression of transcription factors BACH1 and ERG, both encoded on chromosome 21, in brains of patients with Down syndrome and Alzheimer's disease. *Journal of neural transmission. Supplementum*, 39-49 (2003).
178 Petzke TL, R. E., Goodyer CG, LeBlanc AC. Substrates of caspase-6 in human primary neurons: a proteomic study. *Society for Neuroscience* **Prgram No.80.9** (2005).
179 Guo, H. *et al.* Active caspase-6 and caspase-6-cleaved tau in neuropil threads, neuritic plaques, and neurofibrillary tangles of Alzheimer's disease. *Am J Pathol* **165**, 523-531, doi:10.1016/S0002-9440(10)63317-2 (2004).
180 Calon, F. *et al.* Dietary n-3 polyunsaturated fatty acid depletion activates caspases and decreases NMDA receptors in the brain of a transgenic mouse model of Alzheimer's disease. *Eur J Neurosci* **22**, 617-626, doi:10.1111/j.1460-9568.2005.04253.x (2005).
181 Chimura, T., Launey, T. & Yoshida, N. Calpain-Mediated Degradation of Drebrin by Excitotoxicity In vitro and In vivo. *PLoS One* **10**, e0125119, doi:10.1371/journal.pone.0125119 (2015).
182 Park, C. K., Nehls, D. G., Graham, D. I., Teasdale, G. M. & McCulloch, J. The glutamate antagonist MK-801 reduces focal ischemic brain damage in the rat. *Ann Neurol* **24**, 543-551, doi:10.1002/ana.410240411 (1988).
183 McShane, R., Areosa Sastre, A. & Minakaran, N. Memantine for dementia. *Cochrane Database Syst Rev*, CD003154, doi:10.1002/14651858.CD003154.pub5 (2006).
184 Stieg, P. E., Sathi, S., Warach, S., Le, D. A. & Lipton, S. A. Neuroprotection by the NMDA receptor-associated open-channel blocker memantine in a photothrombotic model of cerebral focal ischemia in neonatal rat. *Eur J Pharmacol* **375**, 115-120 (1999).
185 Ishizuka, Y. *et al.* Histone deacetylase mediates the decrease in drebrin cluster density induced by amyloid beta oligomers. *Neurochemistry international* **76**, 114-121, doi:10.1016/j.neuint.2014.07.005 (2014).
186 Davis, H. P. & Squire, L. R. Protein synthesis and memory: a review. *Psychol Bull* **96**, 518-559 (1984).

187 Matthies, H. In search of cellular mechanisms of memory. *Prog Neurobiol* **32**, 277-349 (1989).
188 Besse, D., Lombard, M. C., Perrot, S. & Besson, J. M. Regulation of opioid binding sites in the superficial dorsal horn of the rat spinal cord following loose ligation of the sciatic nerve: comparison with sciatic nerve section and lumbar dorsal rhizotomy. *Neuroscience* **50**, 921-933 (1992).
189 Noguchi, K., Dubner, R. & Ruda, M. A. Preproenkephalin mRNA in spinal dorsal horn neurons is induced by peripheral inflammation and is co-localized with Fos and Fos-related proteins. *Neuroscience* **46**, 561-570 (1992).
190 Pellegrini-Giampietro, D. E., Zukin, R. S., Bennett, M. V., Cho, S. & Pulsinelli, W. A. Switch in glutamate receptor subunit gene expression in CA1 subfield of hippocampus following global ischemia in rats. *Proceedings of the National Academy of Sciences of the United States of America* **89**, 10499-10503 (1992).
191 Friedman, W. J., Altiok, N., Fredholm, B. B. & Persson, H. Mechanisms of nerve growth factor mRNA regulation by interleukin-1 beta in hippocampal cultures: role of second messengers. *Journal of neuroscience research* **33**, 37-46, doi:10.1002/jnr.490330106 (1992).
192 Robertson, H. A. Immediate-early genes, neuronal plasticity, and memory. *Biochem Cell Biol* **70**, 729-737 (1992).
193 Kaczmarek, L. Molecular biology of vertebrate learning: is c-fos a new beginning? *Journal of neuroscience research* **34**, 377-381, doi:10.1002/jnr.490340402 (1993).
194 Knapska, E. & Kaczmarek, L. A gene for neuronal plasticity in the mammalian brain: Zif268/Egr-1/NGFI-A/Krox-24/TIS8/ZENK? *Prog Neurobiol* **74**, 183-211, doi:10.1016/j.pneurobio.2004.05.007 (2004).
195 Lu, Y., Li, T., Qureshi, H. Y., Han, D. & Paudel, H. K. Early growth response 1 (Egr-1) regulates phosphorylation of microtubule-associated protein tau in mammalian brain. *The Journal of biological chemistry* **286**, 20569-20581, doi:10.1074/jbc.M111.220962 (2011).
196 Milbrandt, J. A nerve growth factor-induced gene encodes a possible transcriptional regulatory factor. *Science* **238**, 797-799 (1987).
197 Pagel, J. I. & Deindl, E. Early growth response 1--a transcription factor in the crossfire of signal transduction cascades. *Indian J Biochem Biophys* **48**, 226-235 (2011).
198 Christy, B. & Nathans, D. DNA binding site of the growth factor-inducible protein Zif268. *Proceedings of the National Academy of Sciences of the United States of America* **86**, 8737-8741 (1989).
199 Pavletich, N. P. & Pabo, C. O. Zinc finger-DNA recognition: crystal structure of a Zif268-DNA complex at 2.1 A. *Science* **252**, 809-817 (1991).
200 Carman, J. A. & Monroe, J. G. The EGR1 protein contains a discrete transcriptional regulatory domain whose deletion results in a truncated protein that blocks EGR1-induced transcription. *DNA Cell Biol* **14**, 581-589 (1995).
201 Thiel, G. *et al.* The human transcriptional repressor protein NAB1: expression and biological activity. *Biochimica et biophysica acta* **1493**, 289-301 (2000).

202 Crosby, S. D., Puetz, J. J., Simburger, K. S., Fahrner, T. J. & Milbrandt, J. The early response gene NGFI-C encodes a zinc finger transcriptional activator and is a member of the GCGGGGGCG (GSG) element-binding protein family. *Mol Cell Biol* **11**, 3835-3841 (1991).
203 Chavrier, P. *et al.* A gene encoding a protein with zinc fingers is activated during G0/G1 transition in cultured cells. *EMBO J* **7**, 29-35 (1988).
204 Matheny, C., Day, M. L. & Milbrandt, J. The nuclear localization signal of NGFI-A is located within the zinc finger DNA binding domain. *The Journal of biological chemistry* **269**, 8176-8181 (1994).
205 Gashler, A. L., Swaminathan, S. & Sukhatme, V. P. A novel repression module, an extensive activation domain, and a bipartite nuclear localization signal defined in the immediate-early transcription factor Egr-1. *Mol Cell Biol* **13**, 4556-4571 (1993).
206 Burmeister, S. S. & Fernald, R. D. Evolutionary conservation of the egr-1 immediate-early gene response in a teleost. *The Journal of comparative neurology* **481**, 220-232, doi:10.1002/cne.20380 (2005).
207 Lemaire, P. *et al.* The serum-inducible mouse gene Krox-24 encodes a sequence-specific transcriptional activator. *Mol Cell Biol* **10**, 3456-3467 (1990).
208 Waters, C. M., Hancock, D. C. & Evan, G. I. Identification and characterisation of the egr-1 gene product as an inducible, short-lived, nuclear phosphoprotein. *Oncogene* **5**, 669-674 (1990).
209 Mack, K. J., Cortner, J., Mack, P. & Farnham, P. J. krox 20 messenger RNA and protein expression in the adult central nervous system. *Brain research. Molecular brain research* **14**, 117-123 (1992).
210 Mack, K., Day, M., Milbrandt, J. & Gottlieb, D. I. Localization of the NGFI-A protein in the rat brain. *Brain research. Molecular brain research* **8**, 177-180 (1990).
211 Herdegen, T. *et al.* Basal expression of the inducible transcription factors c-Jun, JunB, JunD, c-Fos, FosB, and Krox-24 in the adult rat brain. *The Journal of comparative neurology* **354**, 39-56, doi:10.1002/cne.903540105 (1995).
212 Hironishi, M., Ueyama, E. & Senba, E. Systematic expression of immediate early genes and intensive astrocyte activation induced by intrastriatal ferrous iron injection. *Brain research* **828**, 145-153 (1999).
213 Worley, P. F. *et al.* Constitutive expression of zif268 in neocortex is regulated by synaptic activity. *Proceedings of the National Academy of Sciences of the United States of America* **88**, 5106-5110 (1991).
214 Wang, J. Q., Daunais, J. B. & McGinty, J. F. Role of kainate/AMPA receptors in induction of striatal zif/268 and preprodynorphin mRNA by a single injection of amphetamine. *Brain research. Molecular brain research* **27**, 118-126 (1994).
215 Kubosaki, A. *et al.* Genome-wide investigation of in vivo EGR-1 binding sites in monocytic differentiation. *Genome Biol* **10**, R41, doi:10.1186/gb-2009-10-4-r41 (2009).

216 Thiel, G., Schoch, S. & Petersohn, D. Regulation of synapsin I gene expression by the zinc finger transcription factor zif268/egr-1. *The Journal of biological chemistry* **269**, 15294-15301 (1994).
217 Li, Y., Camp, S., Rachinsky, T. L., Bongiorno, C. & Taylor, P. Promoter elements and transcriptional control of the mouse acetylcholinesterase gene. *The Journal of biological chemistry* **268**, 3563-3572 (1993).
218 Li, L., Carter, J., Gao, X., Whitehead, J. & Tourtellotte, W. G. The neuroplasticity-associated arc gene is a direct transcriptional target of early growth response (Egr) transcription factors. *Mol Cell Biol* **25**, 10286-10300, doi:10.1128/MCB.25.23.10286-10300.2005 (2005).
219 Mo, J. *et al.* Early growth response 1 (Egr-1) directly regulates GABAA receptor alpha2, alpha4, and theta subunits in the hippocampus. *Journal of neurochemistry* **133**, 489-500, doi:10.1111/jnc.13077 (2015).
220 Beckmann, A. M., Davidson, M. S., Goodenough, S. & Wilce, P. A. Differential expression of Egr-1-like DNA-binding activities in the naive rat brain and after excitatory stimulation. *Journal of neurochemistry* **69**, 2227-2237 (1997).
221 Gass, P., Herdegen, T., Bravo, R. & Kiessling, M. Induction and suppression of immediate early genes in specific rat brain regions by the non-competitive N-methyl-D-aspartate receptor antagonist MK-801. *Neuroscience* **53**, 749-758 (1993).
222 Murphy, T. H., Worley, P. F. & Baraban, J. M. L-type voltage-sensitive calcium channels mediate synaptic activation of immediate early genes. *Neuron* **7**, 625-635 (1991).
223 Mailleux, P., Zhang, F. & Vanderhaeghen, J. J. The dopamine D1 receptor antagonist SCH-23390 decreases the mRNA levels of the transcription factor zif268 (krox-24) in adult rat intact striatum--an in situ hybridization study. *Neuroscience letters* **147**, 182-184 (1992).
224 Daunais, J. B. & McGinty, J. F. The effects of D1 or D2 dopamine receptor blockade on zif/268 and preprodynorphin gene expression in rat forebrain following a short-term cocaine binge. *Brain research. Molecular brain research* **35**, 237-248 (1996).
225 Saffen, D. W. *et al.* Convulsant-induced increase in transcription factor messenger RNAs in rat brain. *Proceedings of the National Academy of Sciences of the United States of America* **85**, 7795-7799 (1988).
226 Jones, M. W. *et al.* A requirement for the immediate early gene Zif268 in the expression of late LTP and long-term memories. *Nature neuroscience* **4**, 289-296, doi:10.1038/85138 (2001).
227 Penke, Z. *et al.* Zif268/Egr1 gain of function facilitates hippocampal synaptic plasticity and long-term spatial recognition memory. *Philos Trans R Soc Lond B Biol Sci* **369**, 20130159, doi:10.1098/rstb.2013.0159 (2014).
228 Lynch, G., Larson, J., Kelso, S., Barrionuevo, G. & Schottler, F. Intracellular injections of EGTA block induction of hippocampal long-term potentiation. *Nature* **305**, 719-721 (1983).
229 Soderling, T. R. & Derkach, V. A. Postsynaptic protein phosphorylation and LTP. *Trends Neurosci* **23**, 75-80 (2000).

230 Nguyen, P. V., Abel, T. & Kandel, E. R. Requirement of a critical period of transcription for induction of a late phase of LTP. *Science* **265**, 1104-1107 (1994).
231 Frey, U., Krug, M., Reymann, K. G. & Matthies, H. Anisomycin, an inhibitor of protein synthesis, blocks late phases of LTP phenomena in the hippocampal CA1 region in vitro. *Brain research* **452**, 57-65 (1988).
232 Otani, S. & Abraham, W. C. Inhibition of protein synthesis in the dentate gyrus, but not the entorhinal cortex, blocks maintenance of long-term potentiation in rats. *Neuroscience letters* **106**, 175-180 (1989).
233 Cole, A. J., Saffen, D. W., Baraban, J. M. & Worley, P. F. Rapid increase of an immediate early gene messenger RNA in hippocampal neurons by synaptic NMDA receptor activation. *Nature* **340**, 474-476, doi:10.1038/340474a0 (1989).
234 Wisden, W. *et al.* Differential expression of immediate early genes in the hippocampus and spinal cord. *Neuron* **4**, 603-614 (1990).
235 Richardson, C. L. *et al.* Correlation between the induction of an immediate early gene, zif/268, and long-term potentiation in the dentate gyrus. *Brain research* **580**, 147-154 (1992).
236 Abraham, W. C., Dragunow, M. & Tate, W. P. The role of immediate early genes in the stabilization of long-term potentiation. *Mol Neurobiol* **5**, 297-314 (1991).
237 Hall, J., Thomas, K. L. & Everitt, B. J. Rapid and selective induction of BDNF expression in the hippocampus during contextual learning. *Nature neuroscience* **3**, 533-535, doi:10.1038/75698 (2000).
238 Miyashita, Y., Kameyama, M., Hasegawa, I. & Fukushima, T. Consolidation of visual associative long-term memory in the temporal cortex of primates. *Neurobiol Learn Mem* **70**, 197-211, doi:10.1006/nlme.1998.3848 (1998).
239 Renaudineau, S., Poucet, B., Laroche, S., Davis, S. & Save, E. Impaired long-term stability of CA1 place cell representation in mice lacking the transcription factor zif268/egr1. *Proceedings of the National Academy of Sciences of the United States of America* **106**, 11771-11775, doi:10.1073/pnas.0900484106 (2009).
240 Baumgartel, K. *et al.* Control of the establishment of aversive memory by calcineurin and Zif268. *Nature neuroscience* **11**, 572-578, doi:10.1038/nn.2113 (2008).
241 Honkaniemi, J., Sagar, S. M., Pyykonen, I., Hicks, K. J. & Sharp, F. R. Focal brain injury induces multiple immediate early genes encoding zinc finger transcription factors. *Brain research. Molecular brain research* **28**, 157-163 (1995).
242 Abe, K., Kawagoe, J., Sato, S., Sahara, M. & Kogure, K. Induction of the 'zinc finger' gene after transient focal ischemia in rat cerebral cortex. *Neuroscience letters* **123**, 248-250 (1991).
243 Gubits, R. M., Burke, R. E., Casey-McIntosh, G., Bandele, A. & Munell, F. Immediate early gene induction after neonatal hypoxia-ischemia. *Brain research. Molecular brain research* **18**, 228-238 (1993).

244 Oddo, S. *et al.* Triple-transgenic model of Alzheimer's disease with plaques and tangles: intracellular Abeta and synaptic dysfunction. *Neuron* **39**, 409-421 (2003).
245 Sterniczuk, R., Antle, M. C., Laferla, F. M. & Dyck, R. H. Characterization of the 3xTg-AD mouse model of Alzheimer's disease: part 2. Behavioral and cognitive changes. *Brain research* **1348**, 149-155, doi:10.1016/j.brainres.2010.06.011 (2010).
246 Lee, S. L., Tourtellotte, L. C., Wesselschmidt, R. L. & Milbrandt, J. Growth and differentiation proceeds normally in cells deficient in the immediate early gene NGFI-A. *The Journal of biological chemistry* **270**, 9971-9977 (1995).
247 Lee, S. L., Wang, Y. & Milbrandt, J. Unimpaired macrophage differentiation and activation in mice lacking the zinc finger transplantation factor NGFI-A (EGR1). *Mol Cell Biol* **16**, 4566-4572 (1996).
248 Li, T., Chalifour, L. E. & Paudel, H. K. Phosphorylation of protein phosphatase 1 by cyclin-dependent protein kinase 5 during nerve growth factor-induced PC12 cell differentiation. *The Journal of biological chemistry* **282**, 6619-6628, doi:10.1074/jbc.M606347200 (2007).
249 Jones, E. V., Cook, D., Murai, K.K. A neuron-astrocyte co-culture system to investigate astrocyte-secreted factors in mouse neuronal development. *Methods in Molecular Biology* **814**, 341-352 (2011).
250 Blomer, U. *et al.* Highly efficient and sustained gene transfer in adult neurons with a lentivirus vector. *J Virol* **71**, 6641-6649 (1997).
251 Naldini, L., Blomer, U., Gage, F. H., Trono, D. & Verma, I. M. Efficient transfer, integration, and sustained long-term expression of the transgene in adult rat brains injected with a lentiviral vector. *Proceedings of the National Academy of Sciences of the United States of America* **93**, 11382-11388 (1996).
252 Risher, W. C., Ustunkaya, T., Singh Alvarado, J. & Eroglu, C. Rapid Golgi analysis method for efficient and unbiased classification of dendritic spines. *PLoS One* **9**, e107591, doi:10.1371/journal.pone.0107591 (2014).
253 Liang, F., Isackson, P. J. & Jones, E. G. Stimulus-dependent, reciprocal up- and downregulation of glutamic acid decarboxylase and Ca2+/calmodulin-dependent protein kinase II gene expression in rat cerebral cortex. *Exp Brain Res* **110**, 163-174 (1996).
254 Odeh, F. *et al.* Atlas of transgenic Tet-Off Ca2+/calmodulin-dependent protein kinase II and prion protein promoter activity in the mouse brain. *Neuroimage* **54**, 2603-2611, doi:10.1016/j.neuroimage.2010.11.032 (2011).
255 Ferrer, I., Guionnet, N., Cruz-Sanchez, F. & Tunon, T. Neuronal alterations in patients with dementia: a Golgi study on biopsy samples. *Neuroscience letters* **114**, 11-16 (1990).
256 Lanz, T. A., Carter, D. B. & Merchant, K. M. Dendritic spine loss in the hippocampus of young PDAPP and Tg2576 mice and its prevention by the ApoE2 genotype. *Neurobiol Dis* **13**, 246-253 (2003).
257 Hill, J. J., Hashimoto, T. & Lewis, D. A. Molecular mechanisms contributing to dendritic spine alterations in the prefrontal cortex of subjects with schizophrenia. *Mol Psychiatry* **11**, 557-566, doi:10.1038/sj.mp.4001792 (2006).

258 Herdegen, T., Walker, T., Leah, J. D., Bravo, R. & Zimmermann, M. The KROX-24 protein, a new transcription regulating factor: expression in the rat central nervous system following afferent somatosensory stimulation. *Neuroscience letters* **120**, 21-24 (1990).
259 Kojima, N. & Shirao, T. Synaptic dysfunction and disruption of postsynaptic drebrin-actin complex: a study of neurological disorders accompanied by cognitive deficits. *Neuroscience research* **58**, 1-5, doi:10.1016/j.neures.2007.02.003 (2007).
260 Bittner, T. *et al.* Multiple events lead to dendritic spine loss in triple transgenic Alzheimer's disease mice. *PLoS One* **5**, e15477, doi:10.1371/journal.pone.0015477 (2010).
261 Harris, K. M., Fiala, J. C. & Ostroff, L. Structural changes at dendritic spine synapses during long-term potentiation. *Philos Trans R Soc Lond B Biol Sci* **358**, 745-748, doi:10.1098/rstb.2002.1254 (2003).
262 van der Stelt, I., Ruigt, G., Timmer, N., Kuiperij, B., Verbeek, M.M. Expression of glutamate-related proteins vGlut1 and PSD-95 changed in a transgenic mouse model of Alzheimer's disease. *Alzheimer's & Dementia* **7**, S147 (2011).
263 Jiang, Y., Matevossian, A., Huang, H. S., Straubhaar, J. & Akbarian, S. Isolation of neuronal chromatin from brain tissue. *BMC Neurosci* **9**, 42, doi:10.1186/1471-2202-9-42 (2008).
264 Harada, T., Morooka, T., Ogawa, S. & Nishida, E. ERK induces p35, a neuron-specific activator of Cdk5, through induction of Egr1. *Nat Cell Biol* **3**, 453-459, doi:10.1038/35074516 (2001).
265 Khachigian, L. M., Lindner, V., Williams, A. J. & Collins, T. Egr-1-induced endothelial gene expression: a common theme in vascular injury. *Science* **271**, 1427-1431 (1996).
266 Renbaum, P. *et al.* Egr-1 upregulates the Alzheimer's disease presenilin-2 gene in neuronal cells. *Gene* **318**, 113-124 (2003).
267 Hendrickx, A. *et al.* Epigenetic induction of EGR-1 expression by the amyloid precursor protein during exposure to novelty. *PLoS One* **8**, e74305, doi:10.1371/journal.pone.0074305 (2013).
268 Killick, R. *et al.* Clusterin regulates beta-amyloid toxicity via Dickkopf-1-driven induction of the wnt-PCP-JNK pathway. *Mol Psychiatry* **19**, 88-98, doi:10.1038/mp.2012.163 (2014).
269 Kalaria, R. N. The role of cerebral ischemia in Alzheimer's disease. *Neurobiol Aging* **21**, 321-330 (2000).
270 Pennypacker, K. R. *et al.* Induction of presenilins in the rat brain after middle cerebral arterial occlusion. *Brain Res Bull* **48**, 539-543 (1999).
271 Wen, Y. *et al.* Transient cerebral ischemia induces aberrant neuronal cell cycle re-entry and Alzheimer's disease-like tauopathy in female rats. *The Journal of biological chemistry* **279**, 22684-22692, doi:10.1074/jbc.M311768200 (2004).
272 Pluta, R. *et al.* Sporadic Alzheimer's disease begins as episodes of brain ischemia and ischemically dysregulated Alzheimer's disease genes. *Mol Neurobiol* **48**, 500-515, doi:10.1007/s12035-013-8439-1 (2013).

273 Lawler, S. Regulation of actin dynamics: The LIM kinase connection. *Current biology : CB* **9**, R800-802 (1999).
274 Wang, X. X. *et al.* PAK5-Egr1-MMP2 signaling controls the migration and invasion in breast cancer cell. *Tumour Biol* **34**, 2721-2729, doi:10.1007/s13277-013-0824-x (2013).
275 Ow, D. W. *et al.* Transient and stable expression of the firefly luciferase gene in plant cells and transgenic plants. *Science* **234**, 856-859, doi:10.1126/science.234.4778.856 (1986).
276 de Wet, J. R., Wood, K. V., DeLuca, M., Helinski, D. R. & Subramani, S. Firefly luciferase gene: structure and expression in mammalian cells. *Mol Cell Biol* **7**, 725-737 (1987).
277 Kristiansson, E., Thorsen, M., Tamas, M. J. & Nerman, O. Evolutionary forces act on promoter length: identification of enriched cis-regulatory elements. *Mol Biol Evol* **26**, 1299-1307, doi:10.1093/molbev/msp040 (2009).
278 Elder, G. A., Gama Sosa, M. A. & De Gasperi, R. Transgenic mouse models of Alzheimer's disease. *Mt Sinai J Med* **77**, 69-81, doi:10.1002/msj.20159 (2010).
279 Lacoste, B., Tong, X. K., Lahjouji, K., Couture, R. & Hamel, E. Cognitive and cerebrovascular improvements following kinin B1 receptor blockade in Alzheimer's disease mice. *J Neuroinflammation* **10**, 57, doi:10.1186/1742-2094-10-57 (2013).
280 Dickey, C. A. *et al.* Selectively reduced expression of synaptic plasticity-related genes in amyloid precursor protein + presenilin-1 transgenic mice. *The Journal of neuroscience : the official journal of the Society for Neuroscience* **23**, 5219-5226 (2003).
281 Dickey, C. A., De Mesquita, D. D., Morgan, D. & Pennypacker, K. R. Induction of memory-associated immediate early genes by nerve growth factor in rat primary cortical neurons and differentiated mouse Neuro2A cells. *Neuroscience letters* **366**, 10-14, doi:10.1016/j.neulet.2004.04.089 (2004).
282 Koldamova, R. *et al.* Genome-wide approaches reveal EGR1-controlled regulatory networks associated with neurodegeneration. *Neurobiol Dis* **63**, 107-114, doi:10.1016/j.nbd.2013.11.005 (2014).
283 Ma, L., Li, Y. & Wang, R. Drebrin and cognitive impairment. *Clin Chim Acta*, doi:10.1016/j.cca.2015.06.021 (2015).
284 Biou, V., Brinkhaus, H., Malenka, R. C. & Matus, A. Interactions between drebrin and Ras regulate dendritic spine plasticity. *Eur J Neurosci* **27**, 2847-2859, doi:10.1111/j.1460-9568.2008.06269.x (2008).
285 Beique, J. C. *et al.* Synapse-specific regulation of AMPA receptor function by PSD-95. *Proceedings of the National Academy of Sciences of the United States of America* **103**, 19535-19540, doi:10.1073/pnas.0608492103 (2006).
286 Kay, L., Humphreys, L., Eickholt, B. J. & Burrone, J. Neuronal activity drives matching of pre- and postsynaptic function during synapse maturation. *Nature neuroscience* **14**, 688-690, doi:10.1038/nn.2826 (2011).
287 Aoki, C. *et al.* Drebrin a knockout eliminates the rapid form of homeostatic synaptic plasticity at excitatory synapses of intact adult cerebral cortex. *The*

Journal of comparative neurology **517**, 105-121, doi:10.1002/cne.22137 (2009).
288 Mizui, T., Takahashi, H., Sekino, Y. & Shirao, T. Overexpression of drebrin A in immature neurons induces the accumulation of F-actin and PSD-95 into dendritic filopodia, and the formation of large abnormal protrusions. *Molecular and cellular neurosciences* **30**, 630-638 (2005).
289 Knafo, S. *et al.* Widespread changes in dendritic spines in a model of Alzheimer's disease. *Cerebral cortex* **19**, 586-592, doi:10.1093/cercor/bhn111 (2009).
290 Kleim, J. A. *et al.* Synapse formation is associated with memory storage in the cerebellum. *Proceedings of the National Academy of Sciences of the United States of America* **99**, 13228-13231, doi:10.1073/pnas.202483399 (2002).
291 Padurariu, M., Ciobica, A., Mavroudis, I., Fotiou, D. & Baloyannis, S. Hippocampal neuronal loss in the CA1 and CA3 areas of Alzheimer's disease patients. *Psychiatr Danub* **24**, 152-158 (2012).